2012

Studies Directed to the Development of Long Lived Palladium Membranes for Hydrogen Purification

William Glenn Pinson
The University of Montana

STUDIES DIRECTED TO THE DEVELOPMENT OF LONG LIVED PALLADIUM MEMBRANES FOR HYDROGEN PURIFICATION

By

William Glenn Pinson

B.Sc. Chemistry, University of Montana

Dissertation

Presented in partial fulfillment of the requirements

for the degree of

Doctor of Philosophy in Chemistry, Applied Inorganic Chemistry

The University of Montana

Missoula, MT

Summer 2012

Approved by:

Dr. Sandy Ross, Associate Dean

Graduate School

Dr. Edward Rosenberg, Co-Chair

Department of Chemistry

Dr. Garon Smith, Co-Chair

Department of Chemistry

Dr. Sandy Ross

Department of Chemistry

Dr. Valeriy Smirnov

Department of Chemistry

Dr. Tony Ward

The Center for Environmental Health services

Pinson, William G. Ph.D., Summer 2012 Chemistry

Studies Directed to the Development of Long Lived Palladium Membranes for Hydrogen Purification

Dr. Edward Rosenberg, Co-Chair, Department of Chemistry

Dr. Garon Smith, Co-Chair, Department of Chemistry

The focus of this study was to systematically investigate the variables involved in electroless deposition of palladium and palladium alloy membranes on a known porous stainless steel substrate, and apply the results to a new and novel porous stainless steel substrate. Different oxide pore and surface treatments were studied. The effect of silica as a diffusion barrier, surface pore modifier, and palladium nucleation site was examined. Silica sol-gel coating treated stainless steel substrates were explored. Several different formulas of sol-gel coatings and their impact on palladium and palladium copper deposition were researched. The roles of sintering and annealing and their effect on the metal membrane deposition and metal flow were inspected.

It was observed that varying the plating conditions can alter the morphology of the deposited Pd and Pd/Cu alloy membrane. New silica sintering techniques were developed, and implemented. It was observed that the use of silica sol-gel treated , and sintered silica particles allowed Pd and Pd/Cu alloy deposition of a new and novel micro fabricated porous stainless steel support matrix. Sol-gel coating the stainless steel substrates allowed the application of a membrane that significantly decreased the migration of iron and chromium into the membrane, and in some cases totally stopping it, even after annealing at 1000^0C.

ACKNOWLEDGEMENTS

I would like to thank Dr. Smith for his kindness to me when I needed it the most. Thank you for your offer, so soon after my return from combat. Thank you for opening a space in your lab for me. Your kindness and support ultimately led to this dissertation.

I would also like to thank Dr. Rosenberg for his patience, friendship, and guidance. Thanks for answers to all of those questions I ask all of the time. I also want to thank you for your kick in the butt when I needed it. Thank you for showing me *how* to find the answers. Thank you for showing me how to become a true scientist.

I would like to personally thank Dr. Bill Gleason for his friendship and support. Thank you for giving me the opportunity to work on a project that was suited to my skills. Thanks for working all of those months without pay, so I could feed my family. Words are truly inadequate to convey my gratitude.

I would like to thank my loving friend, wife, and soul mate Rozzy. I thank you for your gentle loving heart and loving push when I needed it. Thank you for your words of belief and encouragement when I was down or in doubt. Thank you for the support and understanding during all of those late nights and weekends I had to work. Thank you for making my life so wonderful and loving.

I want to acknowledge Ayesha Sharmin and Mainul Hossain for all of the help, friendship, and smiles. I want to thank Rakesh Kumar for the laughs and support during the long days, go team go. Thanks Mom and Dad for your belief in me and that can do attitude that made this possible. Thank you to Gay Allison and Rhonda Stoddard for your hugs and help. I would like to thank Lindsay Mackensie for her invaluable assistance on the XRD. Thanks to Danette Rule for the assistance on all those admin details that no one thanks you for. I would like to thank Matt Berlin for his work and assistance on this project. I want to also acknowledge the USMC for the attitude adjustment and teaching me how not to ever give up or quit.

Table of Contents

List of figures

List of Experiment Tables

Studies Directed to the Development of Long Lived Palladium Membranes for Hydrogen Purification.

This is a multiple year collaborative project that shares data and information, funded by The Office of Naval Research through the Center for Advanced Mineral and Metallurgical Processing (CAMP) and The University of Montana-Missoula (UM). I have the full permission of the CAMP project manager of this project, to use any and all shared information to include previous published work done by the center or center sponsored research concerning this project.

Chapter 1 Introduction

1.1 Statement of the problem

Current use levels of fossil fuels are unsustainable in long term projections. Current uses of fossil fuels are inefficient and grossly wasteful. New energy technology is currently being developed to help increase the efficiency of the use of these resources, as well as to utilize the waste products of both the petrochemical and agricultural industry. One branch of this new energy technology is hydrogen fuel cell technology.

Hydrogen fuel cell technology requires a source of hydrogen that is pure. Current sources of hydrogen stem from reforming processes[1]. The reformation process uses a nickel catalyst, steam and a hydrocarbon source (like natural gas, methanol, methane, propane, gasoline, (diesel fuel or jet fuels such as JP8)) under high pressure forming carbon monoxide and hydrogen as products (see equation 1). Coal and diesel fuels have metal (Na^+, K^+, Ca^{2+}, Mg^{2+}, Hg), sulfur(SO_2, H_2S, SO_x) and nitrogen impurities (N_2, NO_2,NO_x). These impurities are present due to the nature of their source (geologically compressed

animal, algae, and plant remains). These metal, nitrogen, and sulfur impurities are present in the final products after reformation. The presence of these impurities acts on the surface of the electron exchange catalytic surface and can destroy or diminish the catalytic activity. These impurities need to be removed from the hydrogen fuel cell input stream.

Steam Reforming

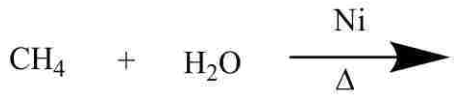

Water Gas shift Reaction

Equation 1 steam reforming and water gas shift reactions

This project focuses on the application of low signature battlefield deployable devices (such as a field portable reformer) that use a common diesel fuel labeled JP-8. JP-8 is a kerosene-based fuel that is used throughout the military in turbine and combustion powered engines. The use of JP-8 simplifies the logistics of transporting multiple fuel sources (with higher flashpoints and vapor pressures) long distances and in hardship conditions.

Palladium will allow hydrogen to dissolve into and pass through the metallic crystal structure. This ability of palladium to allow diffusion of hydrogen through the metallic crystal structure[2] makes it an excellent filter for hydrogen mixed with other gasses and impurities.

The amount of palladium required for the given substrate will depend on the surface chemistry, porosity, and roughness of the surface. Thin, defect-free membranes have been successfully produced on substrates of porous glass, alumina, and stainless steel[3;4] however, the large difference in thermal expansion coefficients between the palladium membrane and the porous glass or alumina substrates causes problems for steady operation over varying operating temperatures[5]. The advantages of stainless

steel substrates include thermal expansion coefficients similar to that of palladium, stability at the required operating temperatures and availability of raw materials.

Several methods have been used for applying palladium to the substrates, including chemical vapor deposition, electroless plating, sputter deposition, and spray pyrolysis[6,7,8]. Literature reviews show substantial efforts are being undertaken to develop this industrial process for hydrogen membranes. What is missing from these efforts is research into the basic mechanisms and properties of both the substrates used and the palladium or palladium membrane itself. Many barriers to developing these membranes, identified by entities such as the Department of Energy, have been detailed[12]. These include degradation of membrane structural integrity, degradation resulting from thermal cycling and poisoning, defects introduced during fabrication, sealing problems, difficulty operating at working temperature (300-500^{0}C) and hydrogen embrittlement. These issues can only be addressed by fundamental research into the nature of the palladium membrane itself.

1.2 Project history

A brief history of the current project and some of the personnel involved are:

2006-2008 (DOT Hydrogen Fuels Project). This project set up the initial equipment needed to do near net shape additive manufacturing on a rapid prototyping machine designated as the ExOne R2-R, using corporate staff at Ex-One, CAMP personnel (Tyler Salisbury and Stacy Davis[15,16]) and some undergraduates. The prototyping and manufacturing of the custom parts consisted of printing one layer at a time of binder on 420 stainless steel alloy metal powder to build up a three dimensional object. This object was then heated at 1100^{0}C to burn off the binder and fuse the metal powder[15] (see figure 1.2.1 a, b).

(a.) ExOne R2-R Rapid Prototyping machine

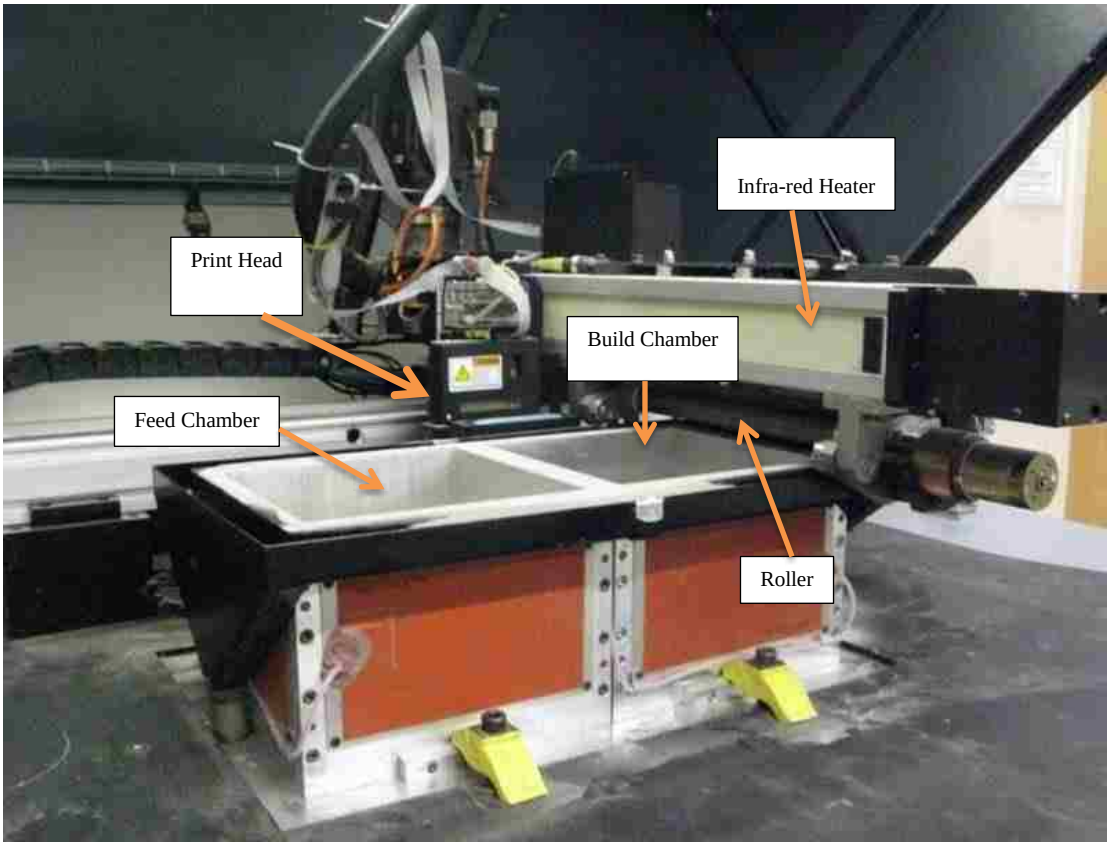

(b.) ExOne R2-R machine close up view

Figure 1.2.1 ExOne R2-R machine

Figure 1.2.1 b shows a close up view of the R2 machine. One chamber contains the feed stock (the 420 stainless steel metal powder), and the other chamber contains the part being built. The roller spreads the metal powder onto the layer of binder sprayed by the print head. The infra-red heater cures the binder, allowing part removal from the build chamber.

2007-2008 (DNR Montana Palladium Research) This project produced the initial substrate and investigated the use of palladium in hydrogen purification membranes, primarily using undergraduates.

2008-2009 (DOD Low Acoustic and Thermal Signature Battlefield Power Source) This project did the initial chemical and mechanical investigation into substrate behavior and palladium deposition mechanisms using three masters graduate students, one post-doc and various undergraduate students.

2009-2011 (DOD Low Acoustic and Thermal Signature Battlefield Power Source, Phase 2) This project did the ongoing chemical and mechanical investigation into substrate behavior and palladium deposition mechanisms using three masters graduate students, one post-doc and various undergraduate students.

2011-present (DOD Low Acoustic and Thermal Signature Battlefield Power Source, Phase 3) This project did the ongoing chemical and mechanical investigation into substrate behavior, palladium deposition mechanisms and alloy development using one masters graduate student, one PhD student and various undergraduate students.

In the fall semester of 2009 Dr. Rosenberg was asked to consult on this project. He then assigned Dr. Varadharajan Kailasam to the CAMP project (Department of Defense Low Acoustic and Thermal Signature Battlefield Power Source, Phase 2) as a post-doc from the fall semester of 2009 until the end of the fall semester 2010. He was hired to investigate the palladium deposition mechanisms, and worked closely with a master's student at Montana Tech, Stacy Davis.

Upon the departure of Dr. Kailasam in late December 2010, the project was turned over to the current research team (consisting of Dr. Rosenberg, myself, and undergraduate Matt Berlin) in early January 2011. At that time a systematic investigation into all of the variables involved in electroless palladium deposition was launched. What follows is a summary of the results of these investigations.

1.3 Background

This research is directed toward the investigation of basic science controlling palladium deposition and the application of this knowledge to coating different stainless steel substrates. This is done in order to develop a longer lived palladium membrane than that is currently being used. To date, no one has done this in a comprehensive manner. In the current literature, a limited set of parameters has been examined to improve target values [1,2, 5,19,21,23].

In this thesis we attempt to systematically investigate a larger range of variables, with an emphasis on the diffusion barrier. We will also be investigating the change in the epitaxial depositional morphologies as the plating conditions and underlying substrate change. Identifying and controlling these variables allows an atomic view into some of the inherent defects of the deposited membrane which can then be controlled and manipulated. Identifying and controlling these variables also allows a more rigorous application to different substrates in a controlled manner.

Hydrogen is highly soluble in bulk palladium and will readily pass through the metal.

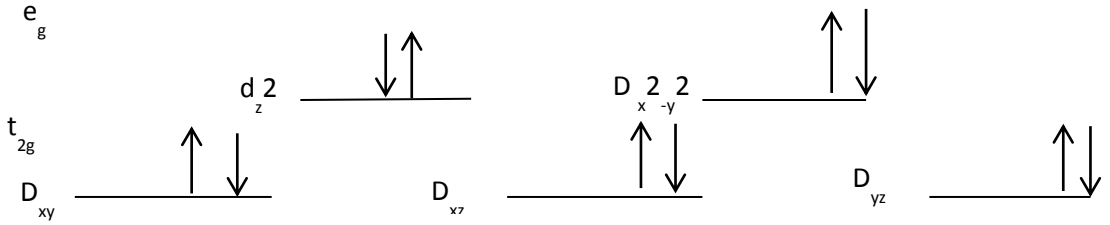

Figure 1.31 Gas phase palladium $4d^{10}$ and $5s^0$ orbitals

Figure 1.3.1 shows the gas phase palladium the electronic configuration as $4d^{10}\ 5s^{0}$. This is due to second row transition elements having larger 4d orbitals and smaller 5s orbitals. To conserve angular momentum the electrons that would normally occupy the 5s orbital are used to fill the unoccupied d_z^2 orbital to complete the d^{10} configuration

In the palladium metal, the d band of molecular orbitals are filled. The highest occupied molecular orbital (HOMO) at absolute zero is called the **Fermi**[9] level. As the temperature is raised, some of the electrons in the HOMO can occupy some of the surrounding vacant lowest unoccupied molecular orbital (LUMO) for a small amount of energy. In a metallic element, the band gap between HOMO and LUMO has been lowered to almost nonexistence by orbital overlap, creating the d-band. These accessible orbitals in the d-band allow the transfer of the electrons across the solid state metal where the atoms cannot move. This is called the conduction band.

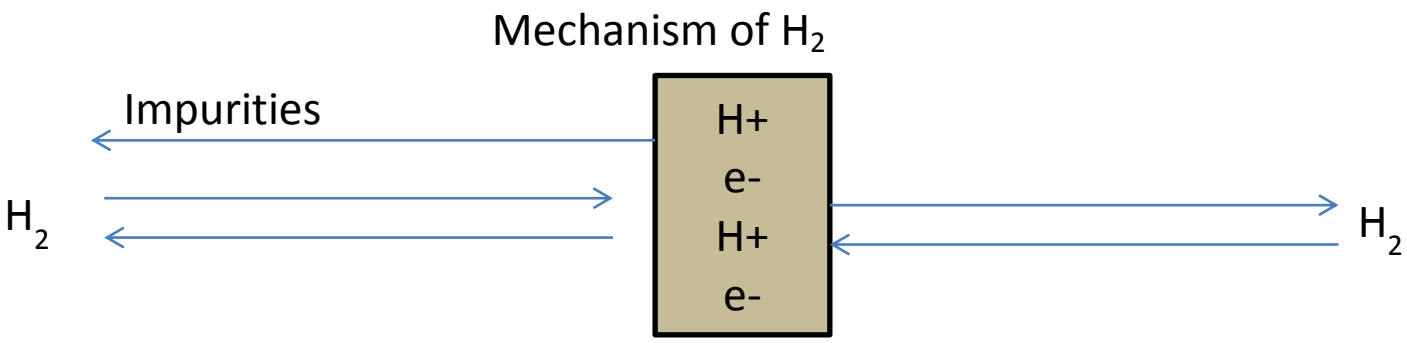

Figure 1.3.2 H_2 disassociation and electron injection into conduction band of Pd.

A structurally sound palladium-based membrane can be used to selective separate relatively pure hydrogen from other gas species and trace metal and sulfur containing contaminants. A thin palladium-based membrane can play an important role in this fuel/gas processing technology with thinner membranes allowing a greater hydrogen flux and lowering the overall cost. Many of the current research efforts are focused on improving H_2 permeation using known plating processes[10]. Investigating

the basic mechanisms and properties of both the substrates used and the palladium or palladium alloy membrane itself[11], needs to be investigated in order to increase the effectiveness of current technology in this area. The National Energy Testing Laboratory (NETL) has identified[12] a number of issues that need be addressed prior to the adoption of metallic membranes. These issues include:

- a. Degradation of membrane structural integrity.
- b. Degradation resulting from thermal cycling and poisoning.
- c. Defects introduced during fabrication.
- d. Sealing problems.
- e. Difficulty operating at temperature.
- f. Hydrogen embrittlement.

These barriers can only be addressed by fundamental research into the nature of the palladium membrane itself; little has been published in the available literature on this topic.

The NETL diffusion barriers previously investigated serve as guides to the proposed work. As stated by NETL, "membranes may be subject to atomic rearrangements, surface roughening, pitting, and formation of impurity over-layers that may adversely affect structural integrity and performance."[12] Without understanding the basic atomic structures and morphologies initially produced in palladium deposition, limiting or eliminating the problems identified above is not possible. Thermal expansion and contraction have been identified as a primary cause of failure in many thin membranes. This is due to a different coefficient of thermal expansion (CTE) for the substrate and metal membrane. While CTE data are available, specific understanding of the effect of palladium coating on substrates is limited. This is particularly true when coupled with the lack of knowledge about the form palladium takes at the interface between substrate and membrane. Poisoning in such membranes is an atomic process, just as the dissociation of the molecular hydrogen at the catalytic surface is. Understanding the mechanisms by

which contaminants enter the lattice during poisoning requires an understanding of the lattice structure as well as the nature of the contaminant binding at catalyst sites.

Neither of these is possible without knowing how the atomic structure of the Pd membrane (see figure1.3.3) differs from surface to substrate. This illustration[13] shows the structures of the body-centered-cubic (BCC) and the face-centered-cubic (FCC) structures that allow H^+ migration through the Pd layer. Pd has an equilibrium between the BCC and the FCC phases, favoring the denser FCC at lower temperatures (300^{o}C or below). Fabrication defects cannot be understood without understanding the variables affecting fabrication processes

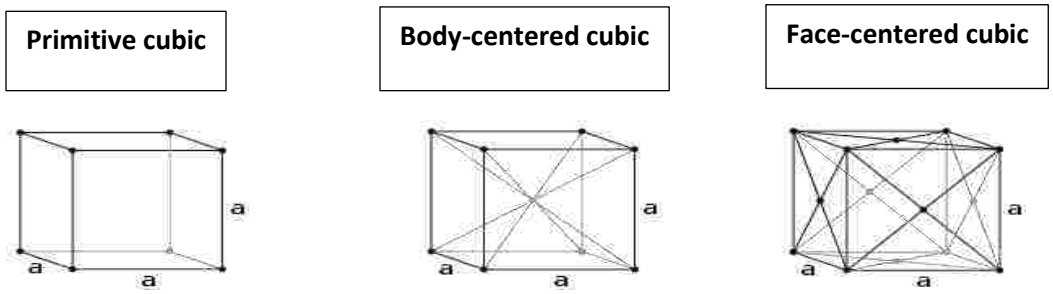

The **primitive cubic** system (CP) consists of one lattice point on each corner of the cube.
The **body-centered cubic** system (BCC) has one lattice point in the center of the unit cell in addition to the eight corner points.
The **face-centered cubic** system (FCC) has lattice points on the faces of the cube.

Figure 1.3.3 Pd crystal lattice type[13].

There are two primary objectives in this work:

- To fully develop an advanced understanding of both substrate and membrane interaction.
- To use that knowledge to design and manufacture new prototypes of longer lived hydrogen purification membranes.

Porous stainless steel (PSS) is one of the most common substrates for palladium electroless plating due to its favorable structural stability. It is also readily available and relatively cheap. Many of these

Porous stainless steel (PSS) surfaces are designed as filtering media with the interior pore structure produced in such a way that certain size particulates are blocked from passing (see figure 1.3.5 picture a MOTT disc). The MOTT Company[14] uses a hot isostatically pressed (HIP) stainless steel matrix that causes constriction of the pores and interconnecting channels. These constricted channels and pores act as an effective filter for certain particulate sizes.

The CAMP PSS design is fundamentally different because it is designed to:

a. Maximize the surface area available for the membrane.

b. Minimize the mechanical strain put on the membrane by the substrate.

c. Minimize the time-in-transit of hydrogen within the membrane.

The CAMP PSS support matrix accomplishes these characteristics by maintaining the spherical characteristics of metal powders and the existing stacking structure. . By maintaining these characteristics, a large surface area of open porosity is provided, edges where membrane meets substrate are eliminated, and available flow channels are enhanced (shown in figure 1.3.4: a side view of silica sol-gel and silica bead treated CAMP disc with a deposited Pd/Cu membrane).

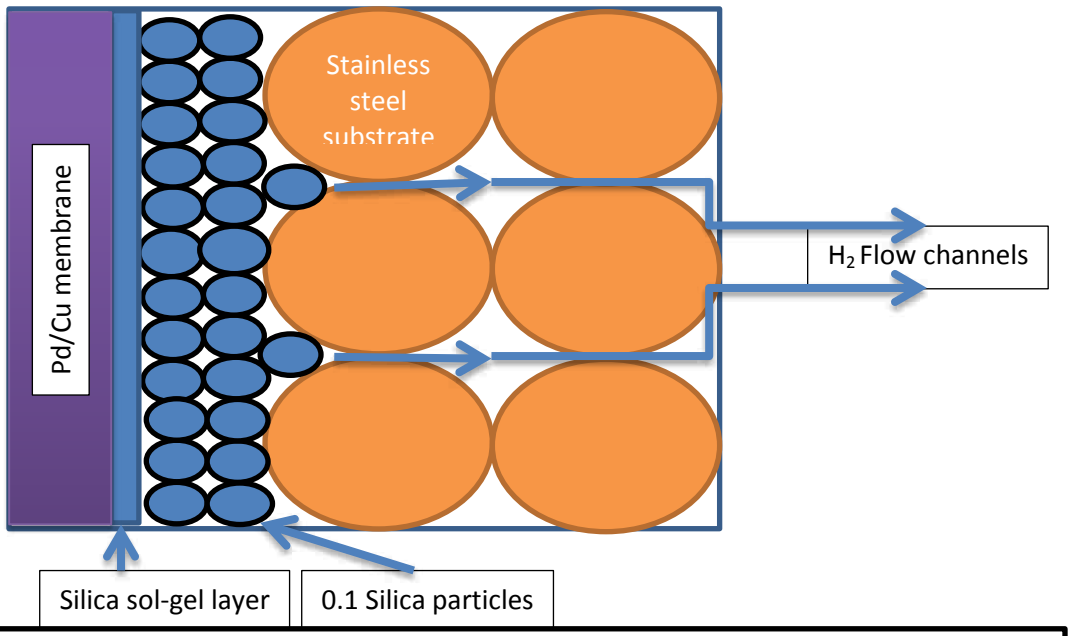

Figure 1.3.4: a side view of silica sol-gel and silica bead treated CAMP disc with a deposited Pd/Cu membrane

The CAMP PSS substrate is produced by[15] initially making a computer aided drafting (CAD) drawing of a product design and using a special software (trade named Materialise) to slice the product drawing into layers. These drawing layers are then used for a 3-D printing process using customized ExOne R2R powder printing equipment (see figure 1.2.1 a, b). The part is printed layer by layer and bound together using polymer binders, then infrared (IR) cured in situ to develop sufficient green (pre-sinter) strength to remove from the build chamber. Once printed and cured, the parts are sintered at an approximate temperature of 1525°C for 2 hours to burn off the organic binder and initiate particle to particle necking (partial metal flow from one particle to another).

420 stainless steel was chosen as the optimum substrate for hydrogen purification using a palladium membrane based on the coefficient of thermal expansion characteristics at lower temperatures of the available alloys as well as the fact that 420 does not contain appreciable amounts of nickel, suppressing any competing catalyst reactions that may occur with nickel of nickel oxide.

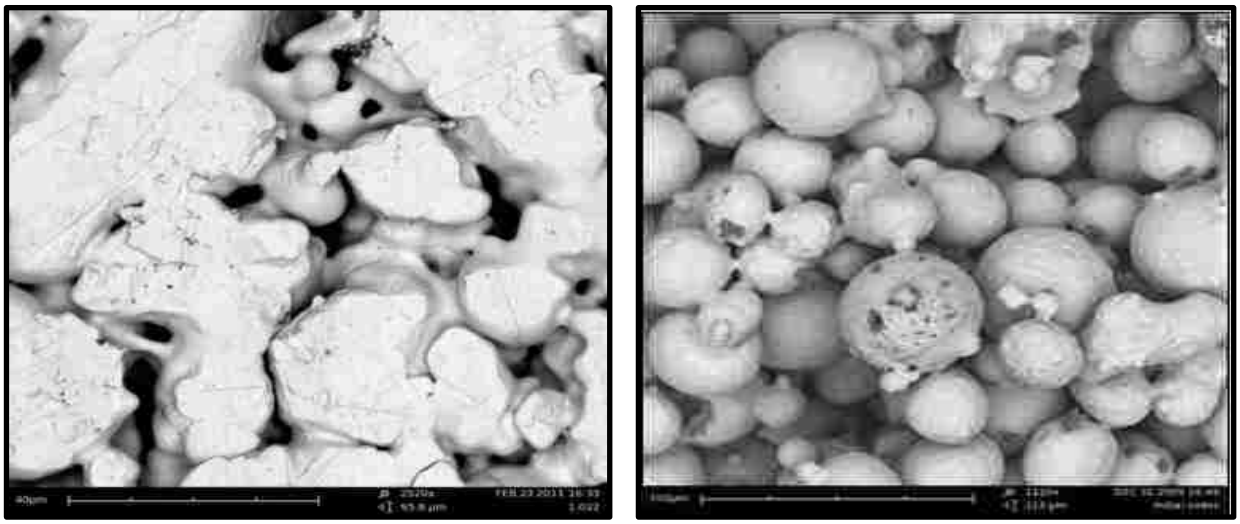

(a.) SEM of MOTT disk PSS substrate

(b.) SEM of CAMP disk PSS substrate

Figure 2.3.5: SEM of Porous stainless steel (PSS) substrates

Work done by this lab has shown that different morphologies, can be obtained through manipulation of t variables (see figure 1.3.6 SEM pictures a, b). Analysis has shown a lighter (1st) phase

forming initially on the 420 stainless steel microsphere after surface activation and sensitization, while a darker (2^{nd}) phase then nucleates and grows on existing palladium. Prior investigations[16] have revealed that these types of deposition follow three well-known deposition mechanisms, Volmer-Weber, Frank-Van Der Merwe and Stranski-Krastanov.

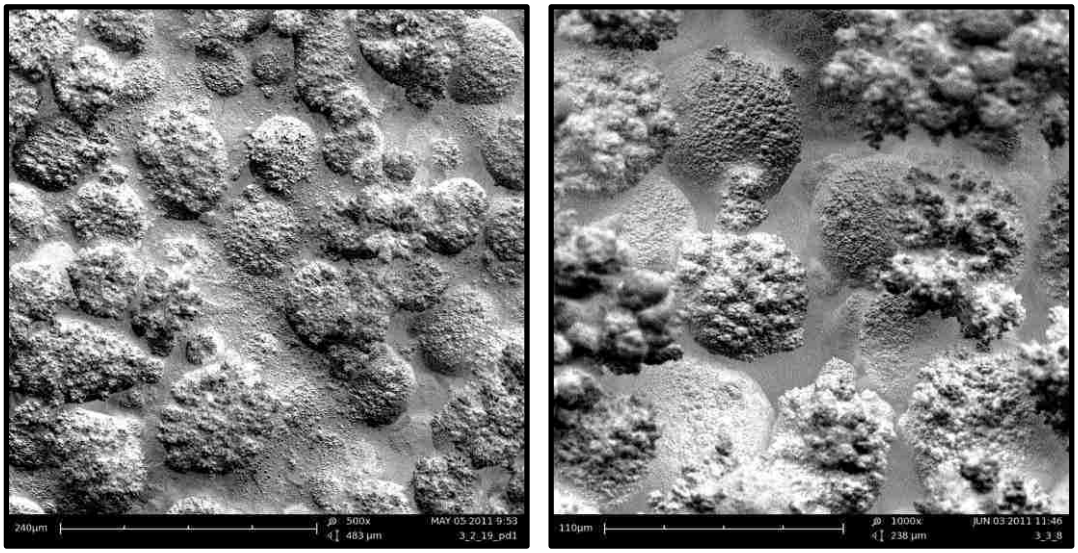

(a.) SEM at 500X of Pd/Cu treated PSS substrate disc 3-2-19

(b.) SEM at 3000X of Pd/Cu treated PSS substrate disc 3-3-8

Figure 1.3.6: Pd/Cu treated PSS substrates

The three depositional morphological mechanisms are:

- Volmer-Weber (VW)-This is the dominant growth mechanism caused when the atom to atom interaction (U_a) is greater than the atom to surface interaction (U_{as}). $U_{as} < U_a$. This mechanism results in a three dimensional rough structure full of differing sized particles and grain boundaries
- Frank-Van Der Merwe (FDM)- This is the dominant growth mechanism caused when the atom to surface interaction (U_{as})is greater than the atom to atom interaction (U_{as}). $U_{as} > U_a$ this produces a smooth two dimensional layer that covers the surface before

additional layers form. It has been suggested[17] (where h_c is the critical thickness for the misfit parameter ϵ) the critical thickness at which dislocations appear is $h_c \propto \epsilon^{-3/2}$. This was suggested to be critical thickness at which surface dislocations start to appear. The surface dislocations then start to form surface islands.

- Stranski-Krastanov (SK)- This is a combination of VK and FDM that occurs at a critical energy shift[17]. Initial deposition follows FDM ($U_{as} > U_a$)and when surface lattice strain energy creates a sign shift, where $U_{as} < U_a$. the deposition follows VK. A difference in lattice structure can also cause a depositional VK/FDM shift.

Note that all of the above mechanisms were based on a level and even surface. The CAMP substrate is not flat, but round, so these approximations will not apply without some type of surface modification.

A future collaboration is being planned between the CAMP center and the Idaho National Labs. This collaboration is designed to model surface physics of the surface lattice strain energy[17] on both the flat and the round substrate. This collaboration also seeks to model when the depositional patterns are forced to change and what forms will dominate.

Figure 1.3.6 (SEM a, b) show some of the basic forms that have been produced in a single deposition event with proper variable manipulation. The underlying layer is a coherent palladium sheet form with the second layer a palladium and copper version of this (resulting in a dendritic-type structure) while the top layer consists of nano and supra-molecular sized nodules.

After gaining a fundamental understanding of how to produce morphologies required by various applications, current work is now focused on alloy and surface preparation development to improve the mechanical and chemical stability of the membrane. Copper and silver are the two alloying elements that can be used in these membranes. Work presented in this thesis shows that the group's methods are capable of manipulating the alloying agents as well as the palladium used in the membranes. The figure

1.3.7 shows the SEM (a)of the annealed alloy morphology as well as an x-ray diffraction (XRD) scan (b) of the surface spot indicating a Pd/Cu alloy.

As alloy development continues, a suitable substrate and membrane will be produced and then tested using CAMP's planned test frame, a portion of which is shown to below (see figure 1.3.8). This frame is based on NETL designs that monitor gas flow composition, adjust temperature, and perform life-cycle testing.

a. SEM picture of Pd/Cu alloy membrane

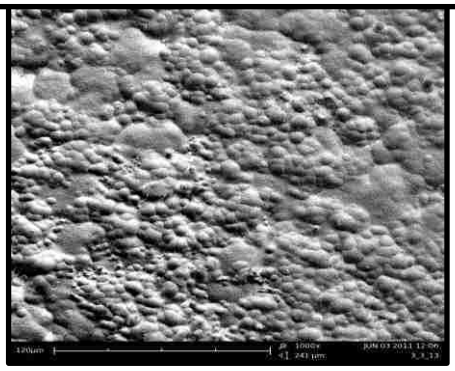

b. XRD picture of annealed Pd/Cu alloy membrane

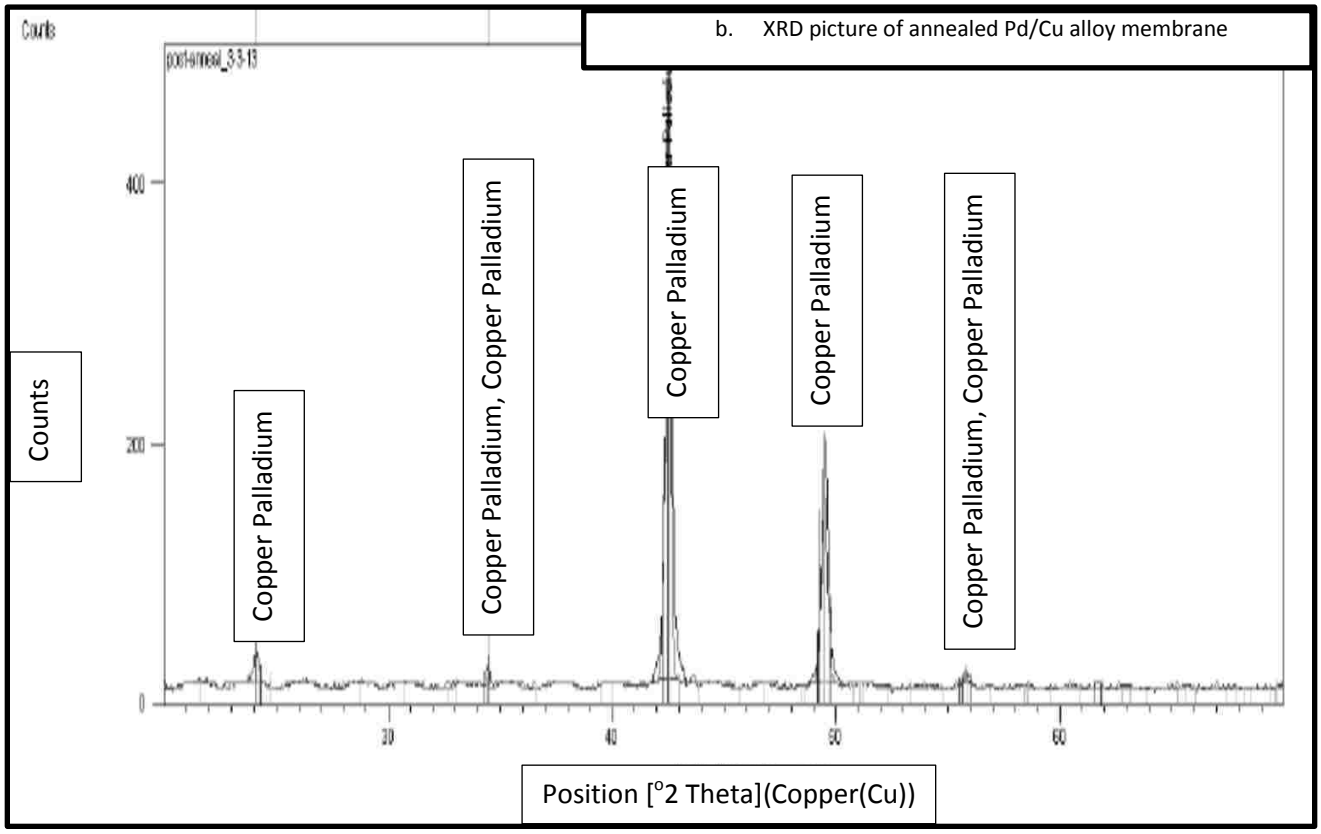

Figure 1.3.7. Sem (a) and XRD (b) of annealed palladium copper alloy MOTT disc

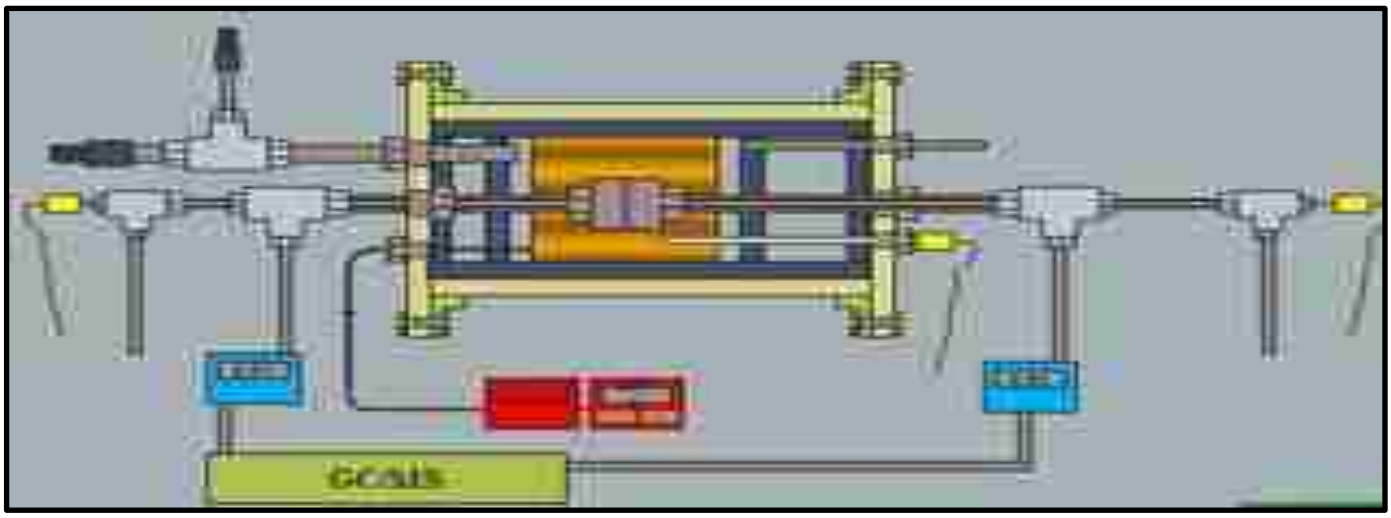

Figure 1.3.8: Schematic of permeance testing apparatus

Chapter 2 project Goals

The goals of this investigation are:

a. Create a system for systematically identifying and reproducibly controlling the variables involved in the epitaxial deposition of a palladium (or a palladium alloy) membrane on a known PSS substrate (MOTT disc).

b To apply that knowledge to a different stainless steel substrate (CAMP disc)

To achieve the project goals, the main goals were divided into smaller sub goals. These sub goals allowed a more thorough focus an in-depth investigation into these areas of inquiry. Part a of the main goals was labeled the initial goal and part b was labeled the project secondary goal.

2.1. The project initial goal

The project initial goals are:

- Compile a literature review of this area of research, in order to guide a focused and systematic approach to understanding the principle factors that affect Pd membrane deposition in a controllable and repeatable system.
- To use a studied PSS substrate (0.2µm grade PSS support matrix tube and disc manufactured by MOTT corporation)[18,34] to investigate:
    - The effects of differing oxide coatings.
    - How differing oxide coats affect palladium membrane depositional coverage.
    - How changing oxide particle sizes can affect Palladium membrane deposition.
    - The effects of sintering on the oxide coating.
    - How differing oxide treatments could mitigate chromium and iron migration from the stainless steel substrate into the palladium membrane.
    - Making palladium/copper alloy membranes.
    - The effects of annealing on multiple alloy coatings.

2.2 Project secondary goal.

The secondary goals for this project are:

- Apply the experimental knowledge gained from a known PSS substrate (MOTT disc) to a new and novel PSS substrate (CAMP disc).

- To investigate differing silica sol-gel mixtures and how well they could mitigate chromium and iron migration from the stainless steel substrate into the palladium membrane.
- To investigate the effect of oxidation on oxide particle and sol-gel treated CAMP PSS substrates.
- To examine the effect of the silica sol-gel on the efficiency of the electroless palladium alloy membrane deposition.
- To investigate the effect of alloy annealing on the coverage of the sol-gel coated silica treated CAMP PSS support matrix.

Chapter 3: EXPERIMENTAL

3.1 Materials and methods

All chemicals were reagent grade and purchased from Sigma Aldrich, Gelest, and VWR. All of the aqueous solutions were mixed with DI H_2O. All solvents used in the silica sol-gel coating were degassed with nitrogen just prior to use. The withdrawal rate for the dip coating was 140 mm per minute.

Reagents:

ammonium hydroxide from EMD CAS 1336-21-6, hydrazine hydrate 100% from Acros CAS 10217-52-4;ethanol 200 proof from VWR CAS 64-17-5.

Oxide particles: aluminum oxide, α-phase 99.9% from Alfa Aesar CAS 1344-28-1;aluminum oxide powder<10 micron 99.7% from sigma Aldrich CAS 1344-28-1; zirconium (IV) oxide from Aldrich CAS 1314-23-4; zirconium (IV) oxide 20% in H2O colloidal dispersion 0.1 micron particles from Alfa Aesar, CAS 1314-23-4; silicon (IV) oxide powder, 1.0 micron, 99.9%CAS 7631-86-9.

Palladium salts: tetraaminepalladium(II) chloride monohydrate 99.9% from Alfa Aesar CAS 13933-31-8;palladium(II) nitrate hydrate from Acros (CAS 10102-05-3); palladium (II) acetate98% from Aldrich CAS 3375-31-3; palladium (II) Chloride 99.9% from Aldrich CAS 7647-10-1.

Copper salts: cupric sulfate pentahydrate 98%from EMD CAS 7758-99-8; cupric nitrate trihydrate, from Baker CAS 3251-23-8.

Silanes: methacryloxypropyl-trimethoxy silane from Gelest CAS 2530-85-0;tetraethyl orthosilicate from Acros CAS 78-10-4.

All palladium and copper solutions were mixed just prior to plating.

3.2 Instrumentation

All dip coating was carried out in a MTI HWTL-01 Desktop Dip Coater with a temperature chamber. All annealing and sintering was carried out in a MTI GSL-1100x high temperature vacuum tube furnace in a quartz tube with vacuum and gas seals.

3.3 Spectroscopic characterization

The small desk top model scanning electron microscope (SEM) that was used at Montana Tech is an FEI Phenom. The SEM/ EDX unit at Montana Tech is a Leo 1430VP using EDAX x-ray dispersive analysis unit and software. The SEM/ EDX that was used at The University of Montana is a Hitachi S-4700 Type II cold field emission SEM which is also equipped with an energy dispersive X-ray spectroscopy (EDX) and analysis system. The XRD was performed at The University of Montana, on the PANalytical X'Pert PRO X-ray diffractometer, the data were collected using X'Pert Data Collector Software and analyzed using X'Pert HighScore Plus software.

3.4 Experiment 1

Experiment 1 was designed to investigate the effects that particle size and type of particle used to create the oxide barrier have on seeding and plating the substrate. Three sizes (10µM, 1.0µM and 0.2µM of MOTT filters were chosen to coat with oxide particles and palladium membranes. MOTT filters are graded on the particulate size that can be filtered out, not the actual pore size. Some of the pores were 30 microns or larger in diameter.

Particle sizes of 0.1, 1.0, and 10.0 micron alumina and 0.1 micron zirconia were initially chosen for use as an oxide barrier treatment. The stainless steel discs were prepared[19] by cleaning in an ultrasonic bath containing N a_2PO_3,NaOH,N_2CO_3,Detergent(triton X-100). Finally the discs were rinsed off with ethanol. The discs were then dried in an oven at 120^0C for twelve hours in air. The cleaned parts were used for a series of initial experiments.

a. MOTT disc under suction on septa b. MOTT disc under suction in zirconia solution

Figure 3.4.1: Disc holder during oxide particle application

The initial trial oxide coating experiment consisted of using 50 mL of 0.1 micron 20% colloidal dispersed zirconium (IV) that was sonicated for 30 min. A 0.2 prepped stainless steel MOTT filter disk was suspended by suction from a modified septum (See figure 3.4.1, pictures a & b). This was then placed in the solution containing suspended oxide particles (see figure 3.4.1, picture 6) under vacuum. The discs were placed in the solution for three minutes sonication, and two minutes without sonication. Three more discs were prepped the same way. The discs were then rinsed gently with DI water. This procedure was repeated once. These discs were then set aside to be later sintered in an oven for 12 hours at 500^0 C.

The sensitizing and activation[20] steps were done as follows: a disk was dipped for three seconds in a $SnCl_2$ solution, rinsed with DI water, dipped for three seconds in a $PdCl_2$ solution, then rinsed with a dilute HCl solution. After sintering and cooling down, one disk was coated three times as listed above, one disk coated six times, and one disk coated nine times with one disk left uncoated as a control. . Discs 1-14 were drilled to hold a piece of monofilament fishing line. This fishing line was used to suspend the discs during the seeding and plating steps. It was judged the MOTT discs did not need to be drilled and were set aside.

Experimental matrices 1a, 1b, and 1c were then designed and designated with a starting experiment number of 15. These experiments were formulated to investigate how altering particle size, particle type, filter pore size, seeding and multiple seeding steps, multiple oxide coats, and plating affect the palladium deposition. The matrix for each experiment was formulated to alter one variable at a time. This was done to compare the results of each individual experiment to each other and study the effects of the change.

Experiment Matrix 1a: Investigation of effects on 1.0 micron MOTT filter disc by 10 micron alumina particle coating, $Pd(Cl)_2$ seeding and Pd $(NH_3)_4Cl_2$ plating solution						
MOTT filter Size	1.0 micron					
Oxide coating	10 micron Alumina					
# times oxide coated	1			2		
Number Sensitize/Activation cycles (5 min $SnCl_2$ sensitize /5 min $PdCl_2$ activation with DI water rinse after each step)	0		1	0		1
Plate	Y	N	Y	Y	N	Y
experiment 1-01-0 (number)	15	16	17	18	19	20

Experiment Matrix 1b: Investigation of effects on 0.2 micron MOTT filter disc by 1.0 micron alumina particle coating, $Pd(Cl)_2$seeding and Pd $(NH_3)_4Cl_2$ plating solution														
MOTT filter Size	.2 micron													
Oxide coating	NA		1.0 micron Alumina											
# times oxide coated	NA		1						2					
Number Sensitize/Activation cycles (5 min $SnCl_2$ sensitize /5 min $PdCl_2$ activation with DI water rinse in after each step)	0		0		1		3		0		1		3	
Plate	Y	N	Y	N	Y	N	Y	N	Y	N	Y	N	Y	N
experiment 1-01-0 (number)	21	22	23	24	25	26	27	28	29	30	31	32	33	34

Experiment Matrix 1c: Investigation of effects on 0.2 micron MOTT filter disc by 0.1 micron alumina particle coating, $Pd(Cl)_2$seeding and Pd $(NH_3)_4Cl_2$ plating solution												
MOTT filter Size	.2 micron											
Oxide coating	0.1 micron Zirconia											
# times oxide coated	1						2					
Number Sensitize/Activation cycles (5 min $SnCl_2$ sensitize /5 min $PdCl_2$ activation with DI water rinse after each step)	0		1		3		0		1		3	
Plate	Y	N	Y	N	Y	N	Y	N	Y	N	Y	N
experiment 1-01-0 (number)	35	36	37	38	39	40	41	42	43	44	45	46

The oxide particle coating steps were as listed above. The 10 micron alumina particle size procedure was modified to a 3 hour sonication time instead of the 30 minute period used for the other particles.

The plating steps[21] use a well-established tetraamine palladium complex to coat the substrate. The net ionic equation for the reaction is:

$$2Pd\,(NH_3)_4Cl_2 + 4e^- \rightarrow 2Pd^0 + 8\,NH_3 + 4Cl^-$$

$$\underline{H_2NNH_2 + 4NH_4OH \rightarrow N_2 + 4H_2O + 4NH_4^+ + 4e^-}$$

$$2Pd(NH_3)_4Cl_2 + H_2NNH_2 + 4NH_4OH \rightarrow 2Pd^0 + N_2 + 8NH_3 + 4NH_4Cl + 4H_2O$$

Formula 1 reduction of P^{d2+} to Pd^0

To plate four MOTT discs 10 microns thick and 0.64cm in radius requires 0.5815 mmol Pd $^{2+}$. According to Ayturk et. al[4], the plating solution has a ratio of 8.2 mmol Pd to 5.4 mmol to hydrazine ratio. $Pd(NH_3)_4Cl_2 \cdot H_2O$ has a molecular weight of 263.46 g/mol. NH_2NH_2 has a molecular weight of 32.05 g/mol. For an 8.2 mmol Pd solution, mix 2.16 grams Pd $(NH_3)_4Cl_2 \cdot H_2O$ per liter of solution. For a 5.4 mmol hydrazine solution, mix 0 .49 mL of a 35% by weight solution of hydrazine per liter DI H_2O. Mix 40.1 grams per liter Na_2EDTA *$2H_2O$. Mix 198 mL (28% by weight) solution NH_4OH per liter DI H_2O. The pH was 10-11. The plating solution temperature was 60^0C. The stir rate was 400 rpm as recommended by Ayturk[21] for optimum palladium deposition.

Four discs were held in an altered septum and septum holder so only one side was plated (see Figure3.4.2). The solution (100 mL) was held at a constant temperature of 60^0 C, stirred at 400 rpm and a plating time of 50 minutes[4]. The discs were the rinsed in DI water and dried overnight at 120^0C.

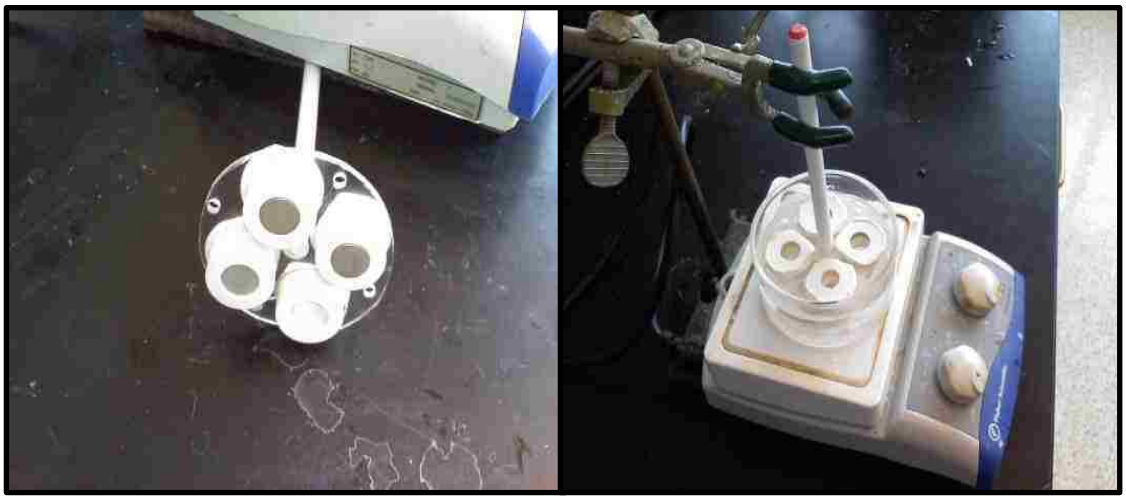

a. Multiple discs in holder

b. Multiple discs held in plating solution

Figure 3.4.2: Disc holder during Pd plating

3.5 Experiment 2

Experiment 2 (see matrix 2a, 2b, 2c) was designed to study the effects of using different palladium complexes, different substrate angles to the fluid flow, different stir speeds, multiple plating , multiple and longer seeding steps, and the role of drying after seeding. Experiment 2 consisted of over 75 different MOTT discs; each disk was treated in a different way. When looking at each matrix, scan each experiment column. X's indicate what was done to that disk.

All discs were cleaned and dried overnight at 120^0C. The discs were then oxide particle treated as described earlier and sintered at 600^0C for 12 hours. The discs were seeded and plated as called for in the experimental design matrix. Note that all palladium solutions were 9.3 µM with regards to the palladium content for each plating bath. The plating was carried out in lots of three discs per plating bath. Note that in each matrix, the row labeled 15 min/plate refers to a fifteen minute sensitizing time, rinsed in 0.01M HCL, then plated directly afterwards.

Four discs were held in an altered septum and septum holder so only one side was plated (see figure 4). The solution (100 mL) was held at a constant temperature of 60^0 C, stir at 400 RPM and the plating time of 50 minutes[4]. The discs were the rinsed in DI water and dried overnight at 120^0C.

Experiment Matrix 2a: Investigation of effects on alumina treated discs by multiple oxide coatings, seedings, changing plating speeds, and angles, amount of plating solution, and different palladium salts.

1.0 µm alumina particles

Experiment 2 disk number	1	2	19	17	18	76	5	10	13	3	8	12	6	11	4	9	7	16	14	15	20	21	25	23	24	22
1 oxide coat	x	x	x	x	x	x	x	x	x	x	x	x	x	x	x	x	x	x	x	x						
2 oxide coats																					x	x	x	x	x	x
$SnCl_2/PdCl_2$																										
1 time		x					x	x	x	x	x	x	x	x	x	x	x	x	x	x		x				x
3 times			x																				x			
15 min				x																				x		
15 min/plate					x																				x	
100 mL $Pd(NH_3)_4Cl_2$ hydrazine plating solution																										
plate parallel stir 400rpm						x	x										x	x	x	x						x
plate 30 °/stir 400 rpm								x																		
plate 90 °/stir 400 rpm									x																	
plate parallel stir 150 rpm										x																
plate 30 °/stir 150rpm											x															
plate 90 o/stir 150rpm												x														
2x plate parallel stir 400rpm													x													
2x plate 30 °/stir 400rpm														x												
2x plate parallel stir 150rpm															x											
2x plate 30 °/stir 150rpm																x										
200 mL $Pd(NH_3)_4Cl_2$ hydrazine plating solution																	x									
Alternate plating solutions																										
Pd/Cl_2 hydrazine																		x								
Pd acetate hydrazine																			x							
Pd nitrate hydrazine																				x						

Experiment Matrix 2b: Investigation of effects on silica treated discs by multiple oxide coatings, seedings, changing plating speeds, and angles, amount of plating solution, and different palladium salts.

	1.0 µm silica particles																								
Experiment 2 disk number	26	27	44	42	43	77	30	35	38	28	33	37	31	36	29	34	32	41	39	40	45	46	50	48	49	47
1 oxide coat	x	x	x	x	x	x	x	x	x	x	x	x	x	x	x	x	x	x	x	x						
2 oxide coats																					x	x	x	x	x	x
$SnCl_2/PdCl_2$																										
1 time		x					x	x	x	x	x	x	x	x	x	x	x	x	x	x		x				x
3 times			x																				x			
15 min				x																				x		
15 min/plate					x																				x	
100 mL $Pd(NH_3)_4Cl_2$ hydrazine plating solution																										
plate parallel stir 400rpm						x	x										x	x	x	x						x
plate 30 °/stir 400 rpm								x																		
plate 90 °/stir 400 rpm									x																	
plate parallel stir 150 rpm										x																
plate 30 °/stir 150rpm											x															
plate 90 o/stir 150rpm												x														
2x plate parallel stir 400rpm													x													
2x plate 30 °/stir 400rpm														x												
2x plate parallel stir 150rpm															x											
2x plate 30 °/stir 150rpm																x										
200 mL $Pd(NH_3)_4Cl_2$ hydrazine plating solution																	x									
Alternate plating solutions																										
Pd/Cl_2 hydrazine																		x								
Pd acetate hydrazine																			x							
Pd nitrate hydrazine																				x						

Experiment Matrix 2c: Investigation of effects on zirconia treated discs by multiple oxide coatings, seedings, changing plating speeds, and angles, amount of plating solution, and different palladium salts.

5.0 µm zirconia particles

Experiment 2 disk number	51	52	69	67	68	78	55	60	63	53	58	62	56	61	54	59	57	66	64	65	70	71	75	73	74	72
1 oxide coat	x	x	x	x	x	x	x	x	x	x	x	x	x	x	x	x	x	x	x	x						
2 oxide coats																					x	x	x	x	x	x
$SnCl_2/PdCl_2$																										
1 time		x					x	x	x	x	x	x	x	x	x	x	x	x	x	x		x				x
3 times			x																				x			
15 min				x																				x		
15 min/plate					x																				x	
100 mL $Pd(NH_3)_4Cl_2$ hydrazine plating solution																										
plate parallel stir 400rpm						x	x										x	x	x	x						x
plate 30 °/stir 400 rpm								x																		
plate 90 °/stir 400 rpm									x																	
plate parallel stir 150 rpm										x																
plate 30 °/stir 150rpm											x															
plate 90 o/stir 150rpm												x														
2x plate parallel stir 400rpm													x													
2x plate 30 °/stir 400rpm														x												
2x plate parallel stir 150rpm															x											
2x plate 30 °/stir 150rpm																x										
200 mL $Pd(NH_3)_4Cl_2$ hydrazine plating solution																	x									
Alternate plating solutions																										
Pd/Cl_2 hydrazine																		x								
Pd acetate hydrazine																			x							
Pd nitrate hydrazine																				x						

3.6 Experiment series 3

This matrix used the CAMP micro fabricated discs made by the method previously described. These disks were produced[22] in the CAMP facility (see picture 1.2.1), are referred to in this paper as CAMP disks. The goal of experiment series 3 was to apply the knowledge and techniques learned so far to a new and potentially better membrane substrate.

All discs (MOTT and CAMP) were washed and cleaned as per procedures previously reported (see page 19). 0.1 μm silica particles were chosen to treat discs. Two sintering temperatures of 900^0 C and 950^0 C with a time of two hours under N_2 atmosphere were chosen as a starting point.

3.6.1 Experiment 3-1

Fifteen CAMP discs were treated with silica gel particles and sintered as listed in the experiment matrix listed below. Note that a zirconia particle treatment was thought to be used as a surface preparation step, but was not executed.

Experiment matrix 3-1: Comparison of silica particle application techniques using vacuum															
experiment number 3-1	1	2	3	4	5	6	7	8	9	10	11	12	13	14	15
	CAMP disk N_2 atm 900 deg 2 hr								CAMP disk N_2 atm 950 deg 2 hr						
stainless steel prep	x	x	x	x	x	x	x	x	x	x	x	x	x	x	x
1.0μm silica particle	x	x	x	x	x	x	x	x	x	x	x	x	x	x	x
dry disk covering	x	x						x				x			x
vacuum disk covering			x	x	x	x	x		x	x	x		x	x	
vacuum disk infiltration			x	x	x	x	x		x	x	x		x	x	
0.1 μm zirconia particle prep						x	x	x					x	x	x

3.6.2 Experiment 3-2

Twenty four CAMP discs were treated with silica gel particles by variations in the matrix as listed below and a combination of solvent , vacuum and hand application. These discs were then sintered at 900^0C under N_2 for two hours .

Experiment matrix 3-2: Comparison of differing Silica particle application techniques																								
experiment number 3-2	1	2	3	4	5	6	7	8	9	10	11	12	13	14	15	16	17	18	19	20	21	22	23	24
stainless steel prep	x	x	x	x	x	x	x	x	x	x	x	x	x	x	x	x	x	x	x	x	x	x	x	x
1.0µm Silica particle	x	x	x	x	x	x	x	x	x	x	x	x	x	x	x	x	x	x	x	x	x	x	x	x
dry disk covering	x	x	x	x													x		x	x	x	x		
wet disc covering					x	x	x	x											x		x		x	
vacuum disk covering									x	x	x	x					x			x	x			x
vacuum disk infiltration													x	x	x	x			x		x	x	x	x

3.6.3.1 Experiment 3-3-1

Sensitized and plated discs numbers (19, 21) from the experiment 3-2.

3.6.3.2 Experiment 3-3-2

All discs (MOTT and CAMP) were washed according to procedures listed earlier. CAMP discs were given a silica coating by placing on an inverted septum with a hole punched in it. Suction was applied to the opposite side of the septum throughout the whole oxide coating process. Acetone was used to wet the surface of the disc. Dry silica particles were applied evenly to the surface. Solvent was applied to the surface to pack in the particles into the holes and cavities in and on the disk. The surface was then leveled off by removing excess silica from the surface with a stiff brush. The discs were examined under a microscope and more solvent/silica applied as needed. All discs were sintered at

900^0C for two hours. The copper plating[23] was done using a well-established $CuSO_4$ recipe. All discs were plated as per matrix 3-3-2

All discs from experiment 3-3-2 were tested on a membrane pressure differential manometer (See figure 3.6.3 c) . Then XRD, SEM, and EDX, were run on the disk experiments for both pre and post anneal.

The discs were annealed at 900^0 C for ½ hour and 500^0 C for 119.5 hours under a 97:3 mixture N_2/H_2 gas in an atmosphere controlled tube furnace. The discs were annealed face up, or down as listed in matrix 3-3-2a.

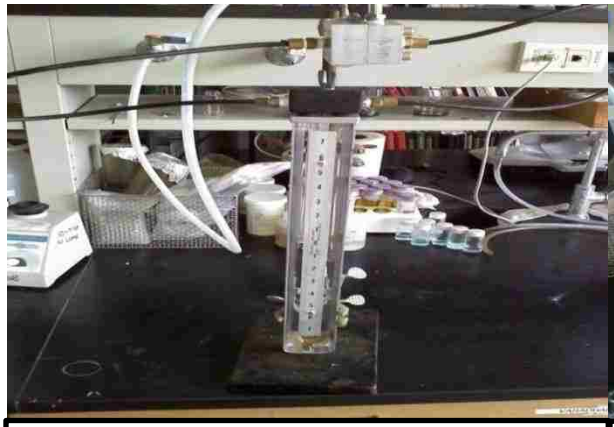

a. Test manometer and disc holder.

b. Test showing pressure differential

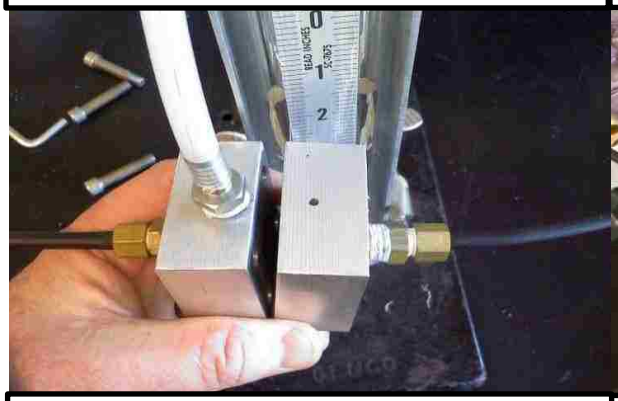

c. Disc holding block.

d. Flat gasket that secures and seals disc

Figure 3.6.3.2: Holding block and manometer leak testing device

Experimental matrix 3-3-2: Study of multiple Pd/Cu plating cycles on PSS substrate																
experiment 3-3-2 disk number	1	2	3	4	5	6	7	8	9	10	11	12	13	14	15	16
	CAMP discs												0.2 µm MOTT filter disk			
Annealing	Face up								Face down				Face down			
stainless steel prep oxide coat	x	x	x	x	x	x	x	x	x	x	x	x	x	x	x	x
sinter/900°C/2hr	x	x	x	x	x	x	x	x	x	x	x	x	x	x	x	x
0.1µm zirconia prep																
15 min Sn_2Cl_2-$PdCl_2$ seeding then plate	x	x	x	x	x	x	x	x	x	x	x	x	x	x	x	x
DI H2O rinse	x	x	x	x	x	x	x	x	x	x	x	x	x	x	x	x
coat with 100 mL $Pd(NH_3)_4Cl_2$ hydrazine plating solution 60 deg offset 60deg temp 150 rpm	1	1	1	1	1	1	1	1	1	1	1	1	1	1	1	1
DI H_2O rinse	x	x	x	x	x	x	x	x	x	x	x	x	x	x	x	x
coat with 100 mL $CuSO_4$ plating solution	1		1	1	1		1	1	1		1	1	1		1	1
DI H_2O rinse	x	x	x	x	x	x	x	x	x	x	x	x	x	x	x	x
120 deg dry 12 hrs.	x	x	x	x	x	x	x	x	x	x	x	x	x	x	x	x
coat with 100 mL $Pd(NH_3)_4Cl_2$ hydrazine plating solution 60 deg offset 60°C temp 150 rpm				1				1				1				1
DI H_2O rinse		x	x	x		x	x	x		x	x	x		x	x	x
120 deg dry 12 hrs.		x	x	x		x	x	x		x	x	x		x	x	x
coat with 100 mL $CuSO_4$ plating solution				1				1				1				1
DI H_2O rinse		x	x	x		x	x	x		x	x	x		x	x	x
coat with 100 mL Pd acetate/ hydrazine plating solution		1	1	1		1	1	1		1	1	1		1	1	1
DI H_2O rinse		x	x	x		x	x	x		x	x	x		x	x	x
experiment platings Pd	1	2	2	3	1	2	2	3	1	2	2	3	1	2	2	3
experiment platings Cu	1	0	1	2	1	0	1	2	1	0	1	2	1	0	1	2

3.7 Experiment series 4

CAMP micro fabricated discs were used in silica sol-gel coating experiments. The CAMP discs were cleaned and prepped in a sonicated alkaline solution, rinsed in deionized water five times, and dried at 120^0 C for 12 hours. A series of discs were treated with 0.1µm silica particles and sintered at 900^0C for two hours under N_2 atmosphere. A series of discs that were not silica particle treated were used as controls for the sol-gel dipping experiments.

The discs were seeded the same as in experiment 1 (see pages 19) then electroless plated using a $Pd(NH_3)_4Cl_2$/hydrazine mixture of 8.8 mmol Pd to 5.2 mmol hydrazine at 60^o C and a stir rate of 150 rpm. Select discs were then sequentially plated with a copper nitrate ($Cu(NO_3)_2$) solution to create multiple layers of copper and palladium. The multiple layers forming the alloy were then annealed at 500^0C for 120 hours under a 96 nitrogen/ 4 hydrogen ratio atmosphere.

3.7.1 Experiment 4-1

Ten CAMP discs were prepped and sintered with 0.1µm silica beads as per the procedure described on page 28. Six discs were covered with packing tape on one side and then Pd seeded as per established procedures. Discs were plated as per experimental matrix 4-1, but no anneal was performed.

3.7.2 Experiment 4-2

Experiment 4-2 used four discs left over from experiment 4-1. A matrix comparing the effects of drying versus annealing (see experimental matrix 4-2) was constructed. The discs were seeded and plated as described in experiment 4-1.

Experiment matrix 4-1: Discs (1-6)a comparison of multiple platings of Pd/Cu layers.			
experiment 4-1 number	1,4	3,5	2,6
Annealing	face down		
stainless steel prep			
oxide coat	x	x	x
sinter/900^{o}C/2hr	x	x	x
15 min Sn_2Cl_2-$PdCl_2$ seeding then plate	x	x	x
coat with 100 mL $Pd(NH_3)_4Cl_2$ hydrazine plating solution 60 deg offset 60 deg temp 150 rpm	1	1	1
0.1M HCL rinse	x	x	x
coat with 100 mL $Cu(NO_3)_2$ plating solution	1	1	1
DI H_2O rinse	x	x	x
120 deg dry 12 hrs.	x	x	x
coat with 100 mL $Pd(NH_3)_4Cl_2$ hydrazine plating solution 60 deg offset 60 ^{o}C temp 150 rpm		1	1
DI H_2O rinse		x	x
coat with 100 mL $Cu(NO_3)_2$ plating solution		1	1
coat with 100 mL $Pd(NH_3)_4Cl_2$ hydrazine plating solution 60 deg offset 60 ^{o}C temp 150 rpm			1
DI H_2O rinse		x	x
120 deg dry 12 hrs.		x	x
coat with 100 mL $Cu(NO_3)_2$ plating solution			1
DI H_2O rinse		x	x
coat with 100 mL Pd acetate/ hydrazine plating solution	1	1	1
DI H_2O rinse	x	x	x
experiment platings Pd	2	3	4
experiment platings Cu	1	2	3

Experiment matrix 4-2: Discs (1-4) establish a comparison of different anneal temperatures and multiple platings of Pd/Cu layers.				
CAMP Disk	Anneal (900°C- 5hrs)		Bake (120°C- 12hrs)	
	1	2	3	4
Sn Activation	X	X	X	X
Pd Seeding	X	X	X	X
Pd Plating 1°	X	X	X	X
Cu Plating 1°	X	X	X	X
Pd Plating 2°		X		X
Cu Plating 2°		X		X

3.8 Experiment series 5

Experiments in series 5 were developed to initially study stainless steel coating by a sol-gel technique and the effect the coating has on the surface of the CAMP disc plus membrane that is plated on top of that coating. Experiment series 5 introduces silica sol-gel coating of PSS parts. Experiment series 5 also refines and applies the initial findings of series 4. Experiments in series 5 were designed to apply everything learned thus far to the plating of a palladium or a palladium copper[23]alloy membrane on: CAMP PSS substrate, silica sol-gel coated CAMP PSS substrate. These experiments were to establish a repeatable and controllable system for deposition of a silica sol-gel coating onto a PSS substrate and a Pd or Pd/Cu alloy membrane that can be applied to that coated substrate.

3.8.1 Experiment 5-1

Experiment 5-1 was designed to study the effects of H_2O_2/H_2SO_4 oxidation surface preparation and the application of a silica sol-gel coating to the silica bead treated CAMP discs. The experiments were to asses if the H_2O_2/H_2SO_4 oxidation of the PSS is needed at all, how H_2O_2/H_2SO_4 oxidation interacts with the PSS and the sintered silica beads, how H_2O_2/H_2SO_4 oxidation affects the dip coat of the

PSS substrate (see experimental matrix 5-1), and how H_2O_2/H_2SO_4 oxidation PSS prep and sol-gel coating affects seeding and plating of the substrate.

Initial stainless steel substrate preparation was done with a modified procedure [24,28]. The substrate was immersed for 30 min in a solution of 90^0C 30% hydrogen peroxide (H_2O_2) and 70% concentrated sulfuric acid (H_2SO_4) solution. Excess solution was washed off with DI water and discs stored in DI water. The discs were dried off after an ethanol rinse under vacuum. The discs were then dip coated with an immersion time of one minute in a solution with a temperature of 60^0C and a withdrawal rate of 140mm/min. All dip coating was carried out in a MTI HWTL-01 Desktop Dip Coater, with temperature controlled chamber The coated discs were air dried for one minute. They were then placed in a tube furnace and annealed at 300^0C for 30 minutes using a ramp rate of 5^0C/min to gel the silica sol without fracturing due to different thermal expansion coefficients of silica and stainless steel.

A silica solution was prepared by an acid catalyzed, two-step hydrolysis-condensation process[24]. An initial stock solution of tetraethylorthosilicate (TEOS)(see scheme 3.8.1), ethanol, deionized water, and 1N hydrochloric acid (HCL) in molar ratio of $1:3.8:5:4.8*10^{-3}$ was prepared. The solution was stirred at 500 RPM for 90 min at 60^0C. An additional 3.6 mL 1N HCL and 1.2 mL DI water was then added to the solution and stirred at 500 rpm at 60^0C for 60 minutes. Ethanol was added to dilute the sol to obtain the volume ratio of 2parts ethanol to 1 part solution. A dip coater was used to coat the discs with a withdrawal rate of 140 mm/ minute. SEM and EDX were taken at the end of the experiment.

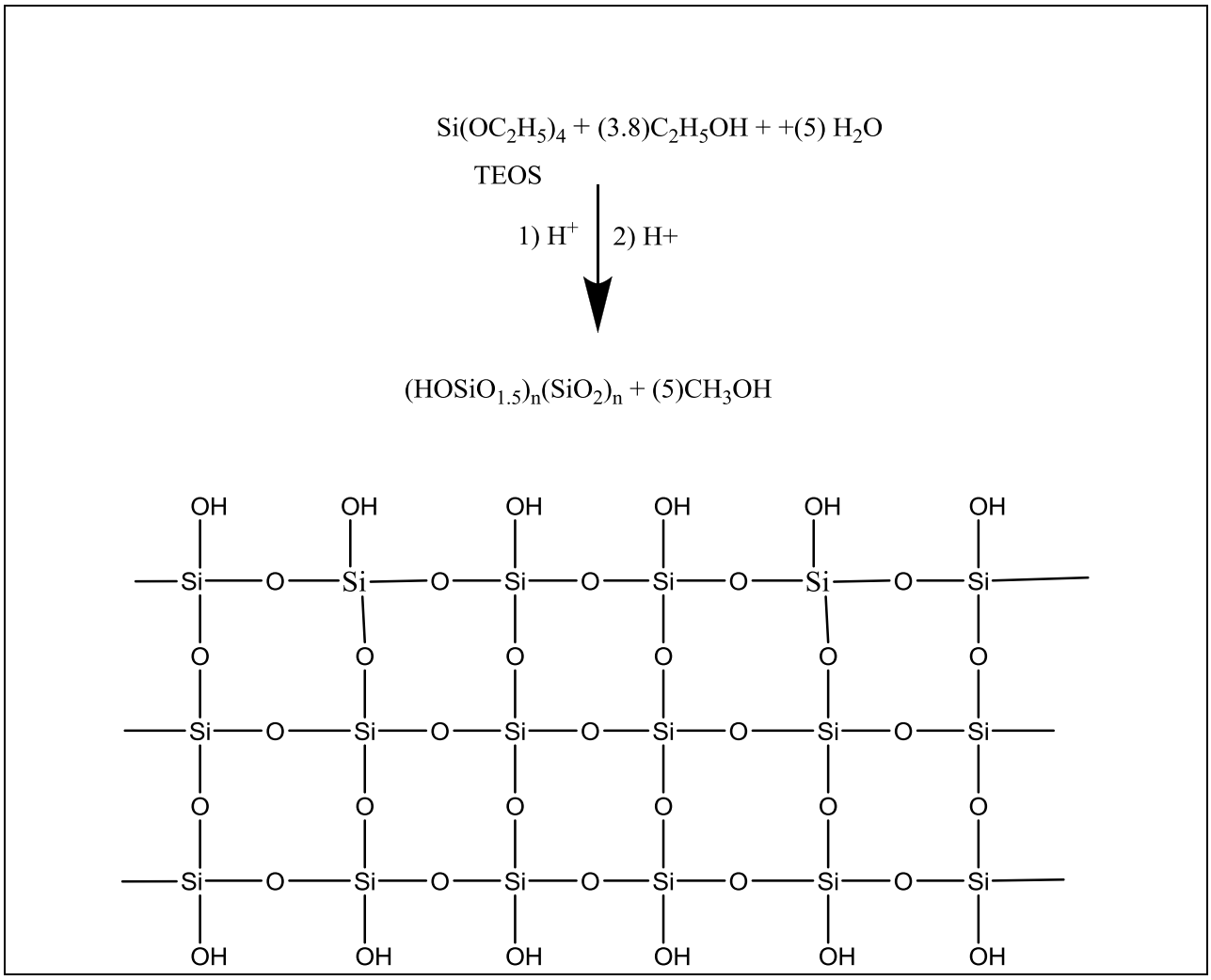

Scheme 3.8.1 Chemical structures of silica precursors used in sol-gel experiments

Experimental matrix 5-1: A study of the role that H_2O_2/H_2SO_4 oxidation plays in 100% TEOS sol-gel coating and silica bead prepping CAMP substrate.

Experiment 5-1 (Sol-gel coating)	No Activation, Seeding, or Plating	Activated + Seeded	Activated + Seeded + Pd Plated	Activated + Seeded + Pd/Cu Plated
CAMP discs/Sol-gel Coated				
Silica Sol/Sinter + Oxidize	Disk 5-1-1	Disk 5-1-2	Disk 5-1-3	Disk 5-1-4
Oxidized with NO Silica Sol	Disk 5-1-5	Disk 5-1-6	Disk 5-1-7	Disk 5-1-8
Oxidized + Silica Sol + sinter	Disk 5-1-9	Disk 5-1-10	Disk 5-1-11	Disk 5-1-12
Silica Sol + Sinter	Disk 5-1-13	Disk 5-1-14	Disk 5-1-15	Disk 5-1-16

3.8.2 Experiment 5-2

Twelve CAMP discs were cleaned as per procedures listed earlier on page 19. Eight discs were silica particle coated and sintered, four were not. All of the cleaned and particle treated discs were then treated as per experimental matrix 5-2. The sol-gel treatment used was the same as listed above.

Experimental matrix 5-2: A study of pure TEOS sol-gel coating and Pd/Cu plating on CAMP substrate.														
experiment 5-2 disk number	1	2	3	4		5	6	7	8		9	10	11	12
	CAMP discs													
Annealing	Face down													
stainless steel prep	0.1 µm Silica particle					0.1 µm Silica particle/ silica sol-gel					silica sol-gel			
oxide coat	x	x	x	x		x	x	x	x					
sinter/900deg c/2hr	x	x	x	x		x	x	x	x					
DI H2O rinse						x	x	x	x					
Sol-gel coating						x	x	x	x		x	x	x	x
30 min anneal 300 ^{o} C						x	x	x	x		x	x	x	x
15 min Sn_2Cl_2-$PdCl_2$ seeding then plate	x	x	x	x		x	x	x	x		x	x	x	x
coat with 100 mL $Pd(NH_3)_4Cl_2$ hydrazine plating solution 60 deg offset 60deg temp 400 rpm	1	1	1	1		1	1	1	1		1	1	1	1
DI H_2O rinse	x	x	x	x		x	x	x	x		x	x	x	x
coat with 100 mL $Cu(NO_3)_2$ plating solution		1	1	1			1	1	1			1	1	1
DI H2O rinse		x	x	x			x	x	x			x	x	x
120 deg dry 12 hrs.	x	x	x	x		x	x	x	x		x	x	x	x
coat with 100 mL $Pd(NH_3)_4Cl_2$ hydrazine plating solution 60 deg offset 60deg temp 400 rpm			1	1				1	1				1	1
DI H_2O rinse			x	x				x	x				x	x
coat with 100 mL $Cu(NO_3)_2$ plating solution			1	1				1	1				1	1
coat with 100 mL $Pd(NH_3)_4Cl_2$ hydrazine plating solution 60 deg offset 60^{o}C temp 400 rpm				1					1					1
DI H_2O rinse			x	x				x	x				x	x
120 deg dry 12 hrs.			x	x				x	x				x	x
coat with 100 mL $Cu(NO_3)_2$ plating solution				1					1					1
DI H_2O rinse			x	x				x	x				x	x
coat with 100 mL Pd acetate/ hydrazine plating solution		1	1	1			1	1	1			1	1	1
DI H_2O rinse		x	x	x			x	x	x			x	x	x
experiment platings Pd	1	2	3	4	0	1	2	3	4	0	1	2	3	4
experiment platings Cu	0	1	2	3	0	0	1	2	3	0	0	1	2	3

3.8.3 Experiment 5-3

Experiment 5-3 is a redo of experiment 5-2 using a different disc holder for the sol-gel coating step.

3.8.4 Experiment 5-4

Experiment 5-4 was designed to investigate the new methods of Pd seeding applied to the hydrophobic sol-gel coating. Palladium acetate and chloroform[25] seeding techniques and alternative reducing strategies[26] were conducted (see experimental matrix 5-4 below). Eight discs were cleaned and prepped as per experiment 5-1. Four discs were sol-gel coated without silica bead prep, and four were sol-gel coated with the silica bead prep. The resulting prepped discs were seeded, reduced, and plated as called for in experimental matrix 5-4.

Experimental matrix 5-4: A study of alternative seeding strategies on 100% pure TEOS sol-gel coated substrate.

Experiment 5-4 (Sol-gel coating) and different Pd(OAC)2 seeding procedures		(Gade 2008) 3.3 g $Pd(OAC)_2$ per 100 ml Chloroform, dip, evaporate,3% wt. H2O2 solution for 30 min, (340ml/L)28-30% NH_4OH plus 10 ml/L) 3M N_2H_2 for 20 min at 50 deg C	modified (Paglieri1999) (.05-0.3M) $Pd(OAC)_2$ in Chloroform Seeding,200 deg C argon purge 100 PSI 200 deg H_2 reduction in pressure vessel 2 hrs.	Seeded +coat with 100 mL $Pd(NH_3)_4Cl_2$ hydrazine plating solution 60 deg offset 60deg temp 150 rpm	
CAMP discs/Sol-gel Coated	exp 5-4-1	x			broken
CAMP discs/Sol-gel Coated	exp 5-4-2	x		x	
CAMP discs/Sol-gel Coated	exp 5-4-5		x		
CAMP discs/Sol-gel Coated	exp 5-4-6		x	x	
CAMP discs plus 0.1µm silica beads/Sol-gel Coated	exp 5-4-3	x			
CAMP discs plus 0.1µm silica beads/Sol-gel Coated	exp 5-4-4	x		x	
CAMP discs plus 0.1µm silica beads/Sol-gel Coated	exp 5-4-7		x		
CAMP discs plus 0.1µm silica beads/Sol-gel Coated	exp 5-4-8		x	x	

3.8.5 Experiment 5-5

It was decided to use the original silica sol-gel recipe[25] (10% 3-methacryloxy propyl trimethoxy silane 90% tetraethyl orthosilicate sol-gel) and a Cu $(NO_3)_2$ copper recipe[27] instead of the $CuSO_4$ used previously. It was thought that SO_4^{2-} could be reduced to H_2S and introduced into the crystal lattice. This would shorten the lifetime of the alloy membrane by sulfur poisoning. The recipe was altered to use hydrazine instead of formaldehyde. This was done because hydrazine (N_2H_4) yields $4e^-$ and N_2 versus formaldehyde HCHO yielding $2e^-$ and H_2 (see $Cu(NO_3)_2$ formaldehyde reduction formula below). The reduction goes faster and is still controllable. As seen in earlier research[34] H_2 introduction into membrane can cause pinholes, surface defects , hydrogen embrittlement and premature Pd membrane cracking.

$Cu(No_3)_2 + 2e^- \rightarrow 2\ NO_3^- + Cu^0$ $2HCHO + 4OH^- \rightarrow 2HCOO^- + H_2 + 2H_2O + 2e^-$
Formula 2: Reduction of Cu2+ to Cu0 using formaldehyde

The original procedure for sol-gel coating stainless steel[28] is as follows: tetraethylorthosilicate (TEOS, $Si(OC_2H_5)_4$) and an organic component, 3-methacryloxypropyltrimethoxysilane (MPS), ($H_2CC\ (CH_3)CO_2(CH_2)_3Si(OCH_3)_3$), used to control the flexibility and density of the sol-gel network. A silica (SiO_2) sol containing 10 mol% MPS with a TEOS :MPS ratio of 90 : 10 was used. An initial stock solution was made by combining amounts of TEOS and MPS in a mixture of ethanol (C_2H_5OH), deionized water (DI H_2O), and 1N hydrochloric acid (HCl), resulting in a TEOS :MPS:C2H5 : DI-H2O: HCl nominal molar ratio of 0.90 : 0.10 : 3.8 : 5 : 4.8×10−3. The mixture was vigorously stirred at a rate of 500rpmfor 90 min at a temperature of 60 °C, and further processing of the sol required an additional 3.6 mL 1N HCl and 1.2 mL DI H_2O to 30

mL of the stock solution. The sol was stirred again at a rate of 500 rpm for 60 min at a temperature of 60 ˚C. Ethanol was added to dilute the sol to a volume ratio of 2 : 1 ethanol to total reactants.

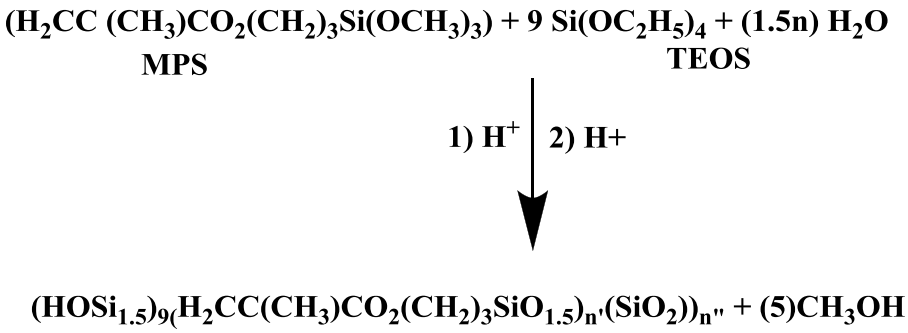

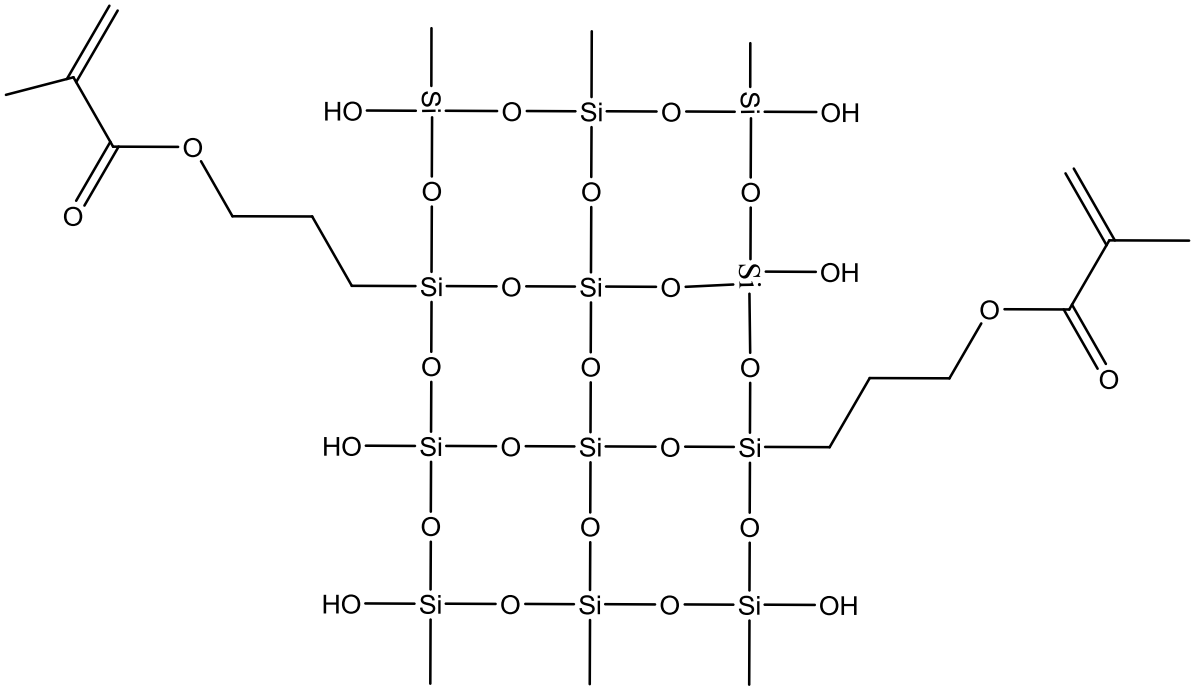

Scheme 3.8.5.1 MPS and TEOS sol-gel solution

12 CAMP discs were cleaned and silica bead prepped as per experiment 5-2, with six discs sol-gel coated once and six discs coated three times. Experimental matrix 5-5 details what was done to each disc. Two disks that were sol-gel treated once were set aside as a control. Two disks that were sol-gel treated 3 times were set aside as a control. A new annealing thermal profile 1000^{0}C for 8 hours then

step down of 2 hours to 800^{0}C hold for 16 hours then step down of 2 hours to 600^{0}C hold for 44 hours was instituted to reduce the time needed for the multiple anneals in future experiments.

3.8.6 Experiment 5-6

Experiment 5-6 was designed (see matrix 5-6) to test the repeatability of the surface prep and deposition of the palladium and copper and to study the effects of the new anneal profile. Experiment 5-6 was also formulated to produce annealed and partially annealed discs for the CAMP center to use in calorimetry experiments. These would determine the temperature and time required to form the alloy from single or multiple plating steps. Disc prep and sol-gel coating were performed as per procedures established in experiment 5-5.

Experimental matrix 5-5: A study of 90% TEOS:10% MPS sol-gel coating , Pd/Cu plating and anneal.								
experiment 5-5 number	1	2	3	4	5	6	7	8
	CAMP discs				CAMP discs			
Annealing	Face down							
stainless steel prep	0.1 μm Silica particle							
oxide coat	x	x	x	x	x	x	x	x
sinter/900° c/2hr	x	x	x	x	x	x	x	x
ETOH H_2O rinse	x	x	x	x	x	x	x	x
Sol-gel coating	x	x	x	x				
3 Sol-gel coats					x	x	x	x
30 min anneal 300°C	x	x	x	x	x	x	x	x
(Gade 2008) 3.3 g$Pd(OAC)_2$ per 100 ml Chloroform, dip, evaporate,3% wt. H_2O_2 solution for 30 min, (340ml/L) 28-30% NH_4OH plus 10 ml/L 3M N_2H_2 for 20 min at 50 deg C	x	x	x	x	x	x	x	x
coat with 100 mL $Pd(NH_3)_4Cl_2$ hydrazine plating solution 60 deg offset 60°C temp 400 rpm	1	1	1	1	1	1	1	1
DI H_2O rinse	x	x	x	x	x	x	x	x
coat with 100 mL $Cu(NO_3)_2$ plating solution		1	1	1		1	1	1
DI H_2O rinse		x	x	x		x	x	x
120 deg dry 12 hrs.	x	x	x	x	x	x	x	x
coat with 100 mL Pd(NH3)4Cl2 hydrazine plating solution 60 deg offset 60°C temp 400 rpm			1	1			1	1
DI H_2O rinse			x	x			x	x
coat with 100 mL $Cu(NO_3)_2$ plating solution			1	1			1	1
coat with 100 mL $Pd(NH_3)_4Cl_2$ hydrazine plating solution 60 deg offset 60°C temp 400 rpm				1				1
DI H_2O rinse			x	x			x	x
120 deg dry 12 hrs.			x	x			x	x
coat with 100 mL $Cu(NO_3)_2$ plating solution				1				1
DI H_2O rinse				x				x
coat with 100 mL $Pd(NH_3)_4Cl_2$ hydrazine plating solution 60 deg offset 60°C temp 400 rpm		1	1	1		1	1	1
DI H_2O rinse		x	x	x		x	x	x

Experimental matrix 5-6: A study using results from experiment 5-5 investigating the role of annealing and multiple Pd/Cu plating steps.								
experiment 5-6-(number)	1	2	3	4	5	6	7	8
Annealing								
stainless steel prep								
0.1 μm Silica particle/ silica sol-gel once	yes		yes	yes	yes	yes	yes	yes
0.1 μm Silica particle/ silica sol-gel three times		yes						
Pd acetate/chloroform dip, air dry, then NH_3OH and N_2H_4 reduction			yes	yes	yes	yes	yes	yes
coat with 100 mL $Pd(NH_3)_4Cl_2$ hydrazine plating solution 90 deg offset 60°C temp 400 rpm			1	1	1	1	1	1
DI H_2O rinse			yes	yes	yes	yes	yes	yes
coat with 100 mL $Cu(NO_3)_2$ plating solution reduction with hydrazine			1	1	1	1	1	1
1000^0 C/8 hours 2 hr cool down 800^0 C 16 hours 2 hr cool down 600^0 C 44 hours 3%/97% H2/N2 mixture			no	yes	yes	yes	yes	yes
coat with 100 mL $Pd(NH_3)_4Cl_2$ hydrazine plating solution 90 deg offset 60°C temp 400 rpm					1	1	1	1
DI H_2O rinse					yes	yes	yes	yes
coat with 100 mL $Cu(NO_3)_2$ plating solution reduction with hydrazine					1	1	1	1
1000^0 C/8 hours 2 hr cool down 800^0 C 16 hours 2 hr cool down 600^0 C 44 hours 3%/97% H2/N2 mixture					no	yes	yes	yes
coat with 100 mL Pd(NH3)4Cl2 hydrazine plating solution 60 deg offset 60°C temp 400 rpm							1	1
DI H_2O rinse							yes	yes
coat with 100 mL $Cu(NO_3)_2$ plating solution reduction with hydrazine							1	1
1000^0 C/8 hours 2 hr cool down 800^0 C 16 hours 2 hr cool down 600^0 C 44 hours 3%/97% H2/N2 mixture							no	yes
experiment platings Pd	0	0	1	1	2	2	3	3
experiment platings Cu	0	0	1	1	2	2	3	3
number of disks treated	5	5	5	7	1	5	1	5
total number of disks treated	34							

Chapter 4 Results and discussion

4.1. Project initial goals

This project is a continuation of work done by Dr. Vaharajan Kalishaam who left CAMP/UM to pursue other job interests. The plating technique used at that time was to infiltrate via zirconium oxide into a stainless steel matrix and then sensitize with $SnCl_2$ (stannous chloride) and plate with a $PdCl_2/Na_2EDTA$ mixture using NH_4OH and $NaPH_2O_2$ or N_2H_4 as a reducing agent. This was not successful and led to a product that had an inferior palladium coating that flaked and spalled at random intervals (see figure 4.1 below). This palladium-coated micro-fabricated part could not stop liquid transfer through the barrier, much less selectively filter gasses.

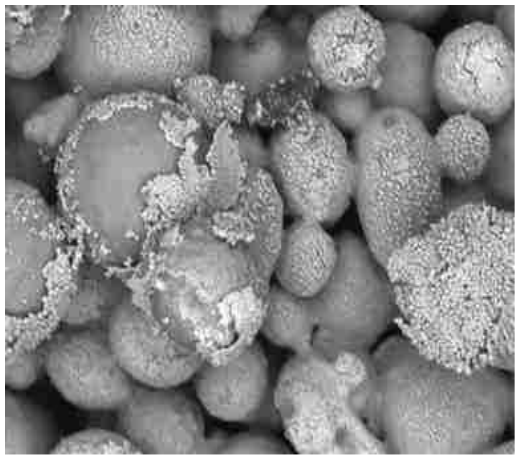

a. SEM of palladium coated starting material

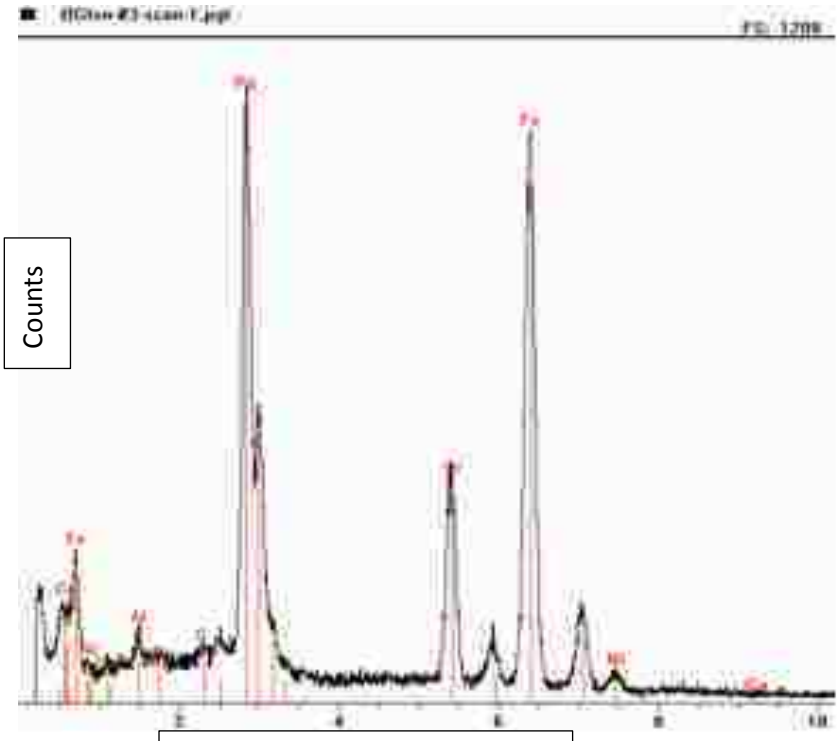

b. EDX of palladium coated staring material

Figure 4.1: SEM and EDX of initial Pd plating attempt on starting material.

As seen in figure 4.1a, the SEM shows that the deposited palladium membrane falls off and does not cover the gaps and holes on the stainless steel substrate. Note in figure 4.1 that the EDX shows palladium on the surface and the SEM shows palladium on the surface. The SEM gives an indication that the palladium is not chemically anchored to the surface, and is breaking off. Note, too that the amount of palladium needed to create a viable hydrogen selective membrane that fills all of the gaps, channels and holes in this substrate would be cost prohibitive.

At the start of this project at UM, a large group of reference articles was suggested by CAMP, along with excellent summaries by Professor Emeritus Larry Twidwell[29,30]. This body of research allowed a much more thorough and in-depth investigation to be performed, saved the UM research team countless hours, and greatly added to the effectiveness of this investigation. A great and humble thank you to Professor Twidwell is offered in this Thesis by this author.

Since the current substrate was deemed unfit to modify, another substrate was identified for investigation by the previous investigator, Dr. Kalishaam. This substrate was an isostatically heated and pressed 316 porous stainless steel (PSS) filter. These filters are available as sheets, tubes and discs. These filters come in multiple (1.0 μm, 0.5 μm, and 0.2μm) grades and the grade designates the size of the particle that it will filter out, not the pore size.

In the current literature, there are some well-done studies that shed light on key factors such as kinetics [4,7,8,9] and reducing agents [10], and differing oxide coats on PSS parts. As of 2/14/2012 there was no comprehensive study done to correlate all of these variables into a working, functioning Pd deposition process, able to handle different kinds of PSS substrates.

4.1.1 Experiment series 1.

In the initial literature search, some key parameters were[4,31,32,33,34] suggested for optimizing electroless palladium membrane deposition on stainless steel parts:

1. Part cleaning and preparation.

2. Optimized plating bath: $Pd(NH_3)_4Cl_2$/hydrazine
3. 8.8:5.2 mmol ratio Pd to hydrazine
4. 60^o C
5. 400 rpm
6. 100 mL solution per four discs

In reviewing the literature, it was noted that pore modification and installation of a diffusion barrier needed further investigation with regard to the PSS substrate. It was also noted that treating a substrate on both sides was redundant, a waste of time and resources. It was also postulated that the design of the experiments needed to account for the direction of gas flow. It was observed[35] that pore sizes for the MOTT PSS discs (0.2µm grade) ranged from 10 to 20 µm with 30 µm being the largest observed. The internal pore sizes ranged from 0.75 to 3.25µm as determined by the bubble point method. It was postulated that the required minimum membrane thickness should be approximately three times the diameter of the largest pore size on the substrate. After consideration of the substrate (see figure 1.2.1 a-b), we determined that multiple sizes and types of oxide particles were to be investigated for best results.

The differing oxide treatments, plating angles and stir speeds revealed some interesting trends (see figure 4.1.2.6).

- Plating twice, stirring at 400 rpm and plating parallel to the direction of flow allowed some secondary fill, but forced the formation of large palladium nodules in mostly primary coverage. These nodules are a waste of palladium as some areas were not subjected to the secondary fill needed for complete membrane coverage. These nodules also seem to be weakly anchored.
- Plating twice, stirring at 400 rpm and plating at 60 deg to the direction of flow allowed a more controlled deposition, limiting the presence of palladium nodules, allowing secondary palladium

fill over and around the oxide particle treatment in a branching coral-like formation with palladium fill.

- Plating twice, stirring at 150 rpm and plating parallel to the direction of flow allowed some secondary fill and sharply decreased the nodule formation.
- Plating twice, stirring at 150 rpm and plating 60 deg to the direction of flow allowed more secondary fill and optimized the primary branching seen earlier between the particle to substrate and particle to particle interactions.
- The silica particle seemed to have the better palladium fill in and around the particles creating a more complete coverage.
- Slowing down the stir rate stimulated the palladium secondary fill and limited the primary substrate to palladium deposits.

4.1.1.1 Experiment 1-01

Initially two sizes of the MOTT PSS discs (1.0 and 0.2µm) were chosen. Then alumina (particle sizes 1.0 and 0.1 µm) and zirconia (particle size 0.01µm) were used to treat the PSS substrates. The treated PSS substrates were sensitized and plated (see matrix 1a-1c page **Error! Bookmark not defined.**) in a systematic attempt to control one variable at a time. This was done in order to identify any trends by comparing the results of individual experiments to each other and studying the effects of the change.

Particle size and type can cause a big difference in pore coverage and substrate binding (see figure 4.1.1.1 .1a-d). Bigger particles tended to fill in bigger pores by mechanical wedging and small sized particles flow through filter without collecting. Note the oxidation of the surface of the PSS substrate (figure 4.1.1.1 .2a-c below) which seems to aid in the mechanical wedging of the particles.

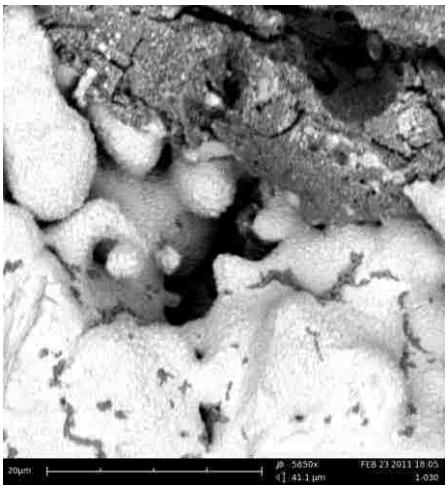

a. Experiment 1-19
1.0 µm MOTT filter disc
10 µm alumina particle
treated twice

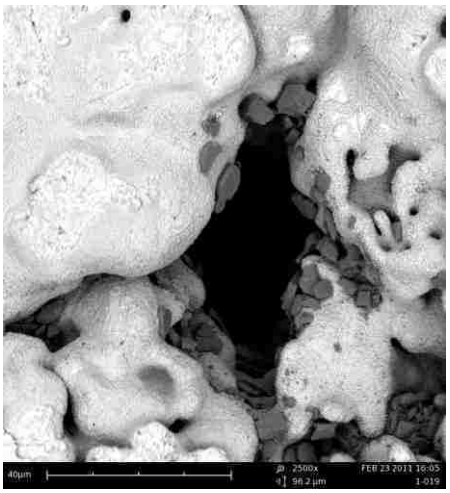

b. Experiment 1-30
0.2 µm MOTT filter disc
10 µm alumina particle
treated twice

c. Experiment 1-42
0.2 µm MOTT filter disc
0.1 µm zirconia particle
treated twice

Figure 4.1.1.1.2: Experiment 1 multiple coatings of different oxide particles on MOTT discs.

When multiple oxide particle coats were applied, the results were pretty much the same as the single coat, with one exception: that of the dual 0.1µm zirconium oxide coats (see Figure 4.1.1.1.2 c experiment 1-42).The results suggest the particles were either too small or too big to fill the pores in the substrate.

The next step was to look at the effects of seeding on the different oxide treated MOTT discs and the epitaxial layers produced. An epitaxial layer is a film grown from a liquid or gas phase. It has two forms, homoepitaxy and heteroepitaxy. Homoepitaxy is where the crystal structure of the depositing material matches that of the substrate. Heteroepitaxy is where the substrate and the depositing material are different. Heteroepitaxy has a large effect on film morphology due to the differing crystal lattice and surface area strains[16,17].

For the purposes of this paper *1^0 formations* will refer to the heteroepitaxial film characterized by Pd/PSS interactions and *2^0 formations* will refer to the homoepitaxial film characterized by the filling or bridging Pd/Pd interactions.

The next experiments in this series study the effects that oxide particle treatment and one seeding cycle has on the PSS substrate. Some trends were uncovered.

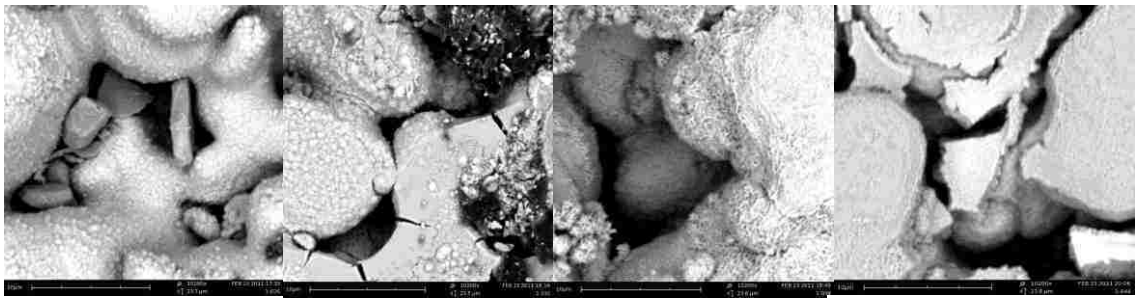

a. Experiment 1-26 0.2 µm MOTT filter disc 10 µm alumina particle treated once $SnCl_2$/ $PdCl_2$ seeded once	b. Experiment 1-32 0.2 µm MOTT filter disc 10 µm alumina particle treated once $SnCl_2$/ $PdCl_2$ seeded twice	c. Experiment 1-38 0.2 µm MOTT filter disc 0.1 µm zirconia particle treated once $SnCl_2$/ $PdCl_2$ seeded once	d. Experiment 1-44 0.2 µm MOTT filter disc 0.1 µm zirconia particle treated once $SnCl_2$/ $PdCl_2$ seeded twice

Figure 4.1.1.1.3: Experiment 1 different Pd seeding epitaxial formations.

Listed earlier (see pages 22, and 23) are three epitaxial depositional terms: See Figure 4.1.1.1.3 a-d which shows 1^0 epitaxial film formations. Only experiment 1-32 (b) shows 2^0 Pd epitaxial film formations and some Pd fill. Experiments 1-38 (c)and 1-44(d) show some interesting coral-like 1^0 epitaxial film formation. This coral-like Pd formation was postulated to be caused by a localized Pd-starved solution induced by local fluid flow dynamics[16]. Experiments 1-26, and 1-32 show nodular 1^0 epitaxial film formations. These nodular formations were postulated to be caused by a localized Pd-rich solution governed by local fluid flow dynamics. The nodular formations were theorized to take their form due to an abundance of palladium deposited in such a way as to minimize surface area. Note that all of the substrates in figure 4.1.1.1.3 have only been seeded once with no plating.

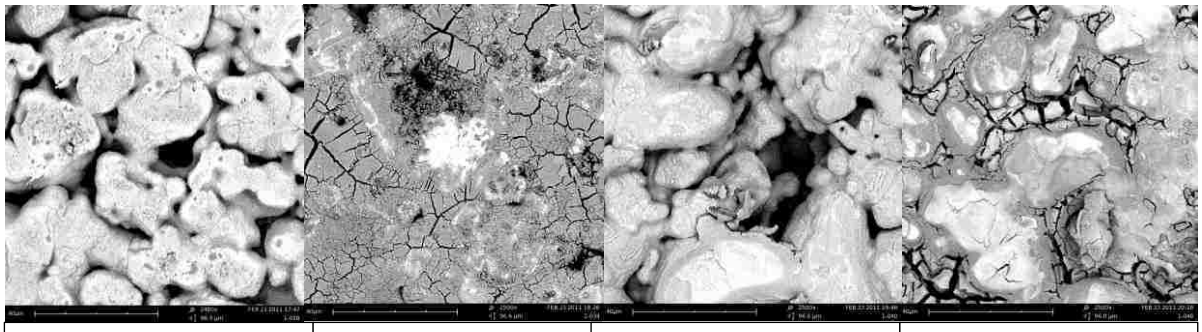

a. Experiment 1-28 0.2 µm MOTT filter disc 10 µm alumina particle Treated once $SnCl_2$/ $PdCl_2$ seeded 3 times	b. Experiment 1-34 0.2 µm MOTT filter disc 10µm alumina particle Treated twice $SnCl_2$/ $PdCl_2$ seeded 3 times	c. Experiment 1-40 0.2 µm MOTT filter disc 0.1 µm zirconia particle Treated once $SnCl_2$/ $PdCl_2$ seeded 3 times	d. Experiment 1-460.2 µm MOTT filter disc 0.1 µm zirconia particle Treated once $SnCl_2$/ $PdCl_2$ seeded 3 times

Figure 4.1.1.1.4: Experiment 1 the effect of multiple seeding steps on MOTT discs.

Examining the effect of multiple seeding steps continued the trends observed earlier (see Figure 4.1.1.1.4, relating to experiments 28, 34, 40, 46). Experiments 28, 40 and 46 showed 1^0 epitaxial film formation, and experiment 34 showed all three epitaxial film formations, plus good secondary fill.

a.. Experiment 1-34 2 µm MOTT filter disc
10µm alumina particle
Treated twice
$SnCl_2$/ $PdCl_2$ seeded 3 times

Figure 4.1.1.1.5: Close up of experiment 34 showing coral like formations with secondary fill on select edges.

Looking closer at experiment 1-34 (Figure 4.1.1.1.5) shows a trend of coral like formational deposition with secondary fill on select edges. The secondary filling has been suggested to be a function of flow direction. The flow direction was parallel to the PSS surface (see figure 3.4.2 a-b) for the disk holding apparatus.

Some observations noted from activation step(s) with no plating.

- When multiple $PdCl_2$ seeding is used, mostly primary deposition occurs with limited secondary filling.

- $PdCl_2$ seeding seems to form S primarily an epitaxial film first, then the film forms outward from the particle in three dimensions .
- When seeded multiple times, the primary coating can create a membrane by itself.

The next phase of the project looked at how plating, seeding, and the surface prep affected the palladium coating. Figures 4.1.1.1.6 a-c and 4.1.1.1.7 a-d show the differences between experiments where the MOTT discs are oxide coated one or two times, seeded once or three times and plated once.

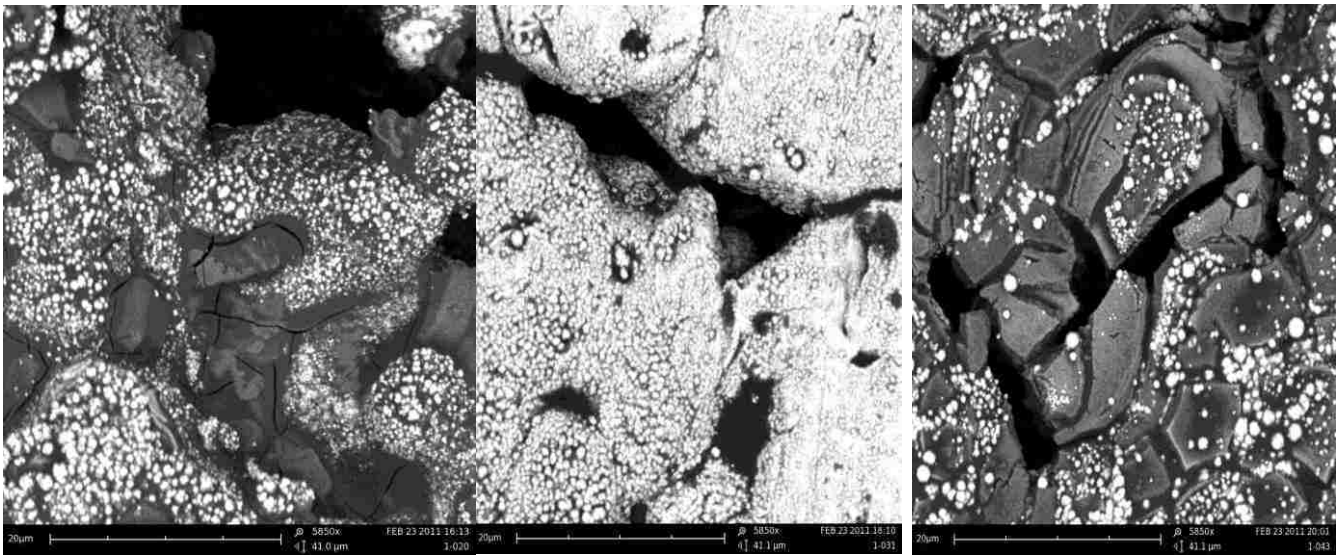

a. Experiment 1-20
1.0 µm MOTT filter disc
10µm alumina particle
Treated twice
$SnCl_2$/ $PdCl_2$ seeded once
Pd plated once

b. Experiment 1-31
0.2 µm MOTT filter disc
10µm alumina particle
Treated twice
$SnCl_2$/ $PdCl_2$ seeded once
Pd plated once

c. Experiment 1-43
0.2 µm MOTT filter disc
1.0µm zirconia particle
Treated twice
$SnCl_2$/ $PdCl_2$ seeded once
Pd plated once

Figure 4.1.1.1.6: Experiment 1 discs 20,37,43 show twice oxide coated, once seeded and once plated experiments.

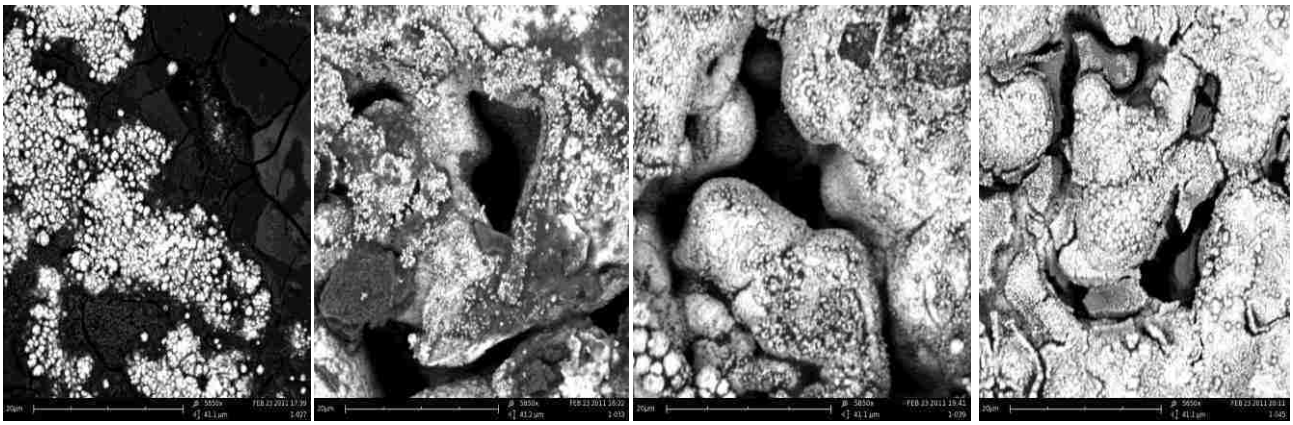

a. Experiment 1-27
0.2 µm MOTT filter disc
10 µm alumina particle
Treated once
$SnCl_2$/ $PdCl_2$ seeded 3 times
Pd plated once

b. Experiment 1-33
0.2 µm MOTT filter disc
10 µm alumina particle
Treated twice
$SnCl_2$/ $PdCl_2$ seeded 3 times
Pd plated once

c. Experiment 1-39
0.2 µm MOTT filter disc
0.1 µm zirconia particle
Treated once
$SnCl_2$/ $PdCl_2$ seeded 3 times
Pd plated once

d. Experiment 1-45
0.2 µm MOTT filter disc
0.1 µm zirconia particle
Treated once
$SnCl_2$/ $PdCl_2$ seeded 3 times
Pd plated once

Figure 4.1.1.1.7: Experiment 1 discs 27, 33, 39, 45 show once oxide coated, seeded three times and once plated experiments.

Note the shell-like epitaxial film formations in figure 4.1.1.1.7 b-d. See the extensive three dimensional SK epitaxial film formations seen in experiment 27 (figure 4.1.1.1.7 a) producing what appears to be a Pd membrane coating.

As a control to see if the seeding step is needed, a series of experiments were run using MOTT discs that were oxide prepped, not seeded and then plated (Figure 4.1.1.1.8 a-d below).

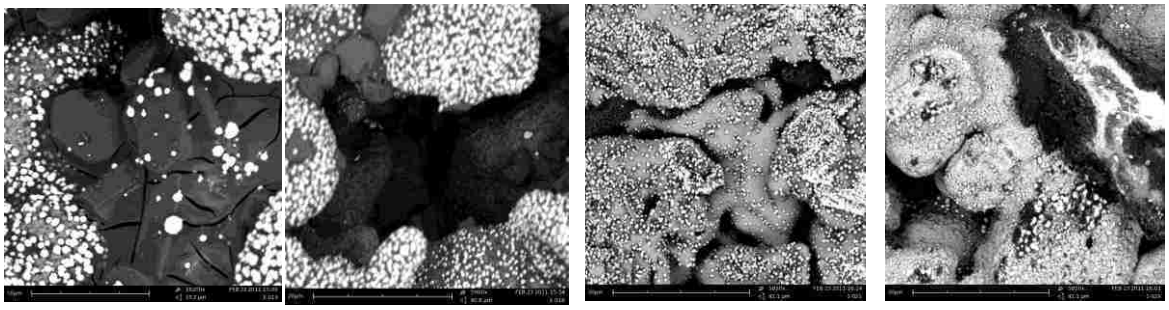

a. Experiment 1-15
1.0 µm MOTT filter disc
10 µm alumina particle
Treated once
$SnCl_2$/ $PdCl_2$ seeded 0 times
Pd plated once

b. Experiment 1-18
1.0 µm MOTT filter disc
10 µm alumina particle
Treated twice
$SnCl_2$/ $PdCl_2$ seeded 0 times
Pd plated once

c. Experiment 1-21
0.2 µm MOTT filter disc
No oxide particle treatment
No $SnCl_2$/ $PdCl_2$ seeding
Pd plated once

d. Experiment 1-29
0.2 µm MOTT filter disc
0.1 µm zirconia particle
Treated twice
$SnCl_2$/ $PdCl_2$ seeded 0 times
Pd plated once

Figure 4.1.1.1.8: Experiments 15, 18, 21, 29 show once oxide coated ,not seeded and once plated.

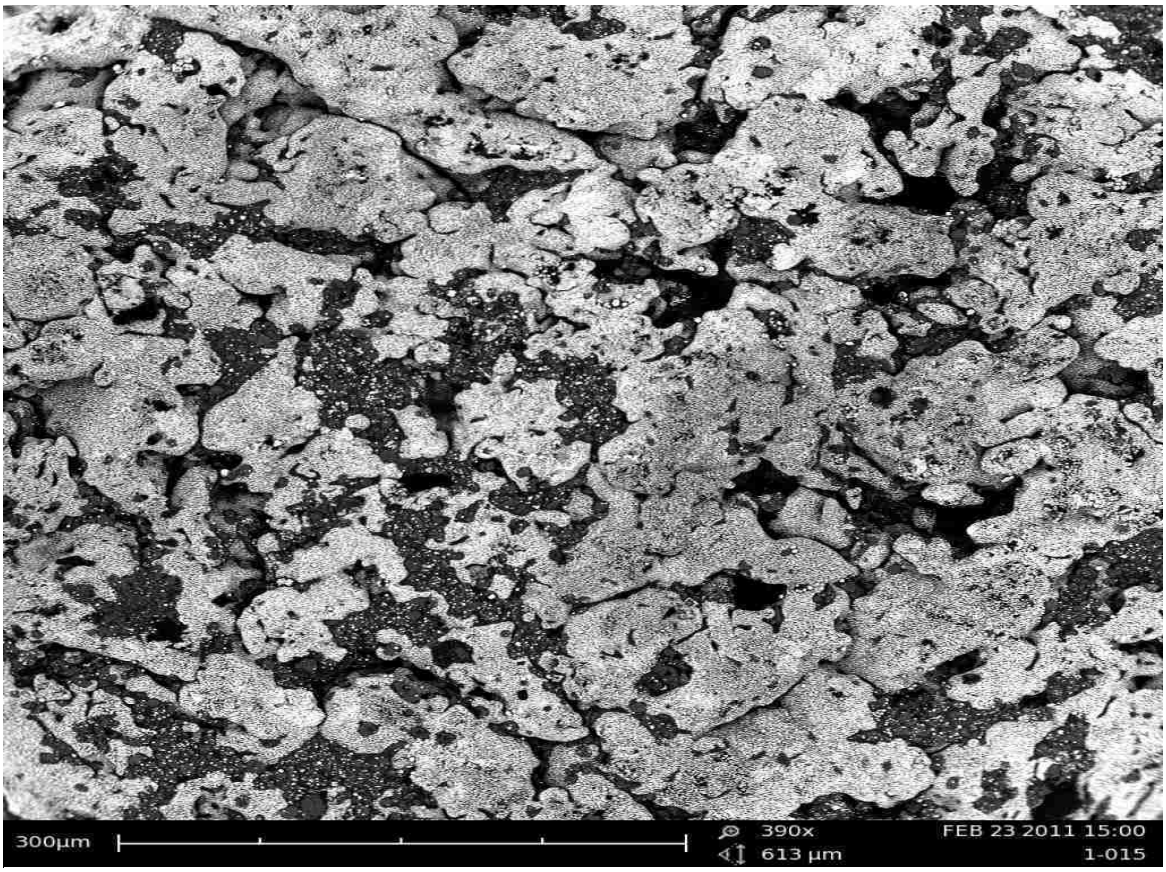

a. Experiment 1-15

Figure 4.1.1.1.9: Experiment 1 disc 15 larger image.

Examining experiment 1-15 in a larger view shows incomplete coverage (Figure 4.1.1.1.9).Note the extensive primary coverage of the PSS substrate demonstrating the best fill and membrane yet. It appears that if the oxide particle fill in the pores is sufficient and the conditions are correct, a membrane could be deposited without the need for seeding.

4.1.1.1.1 Summary of experimental results in experiment 1

When multiple $PdCl_2$ seeding occurs, only primary deposition occurs. $PdCl_2$ seeding seems to form a coating that forms upward and outward from the particle. This primary coating can start to form coral like deposits, which then fill in the pores as the seeding continues. When seeded multiple times, the primary coating can start to create a membrane by itself. Membrane deposition may be a function of directional fluid flow and needs to be investigated. 1^0 Pd particles form a covering layer first, then the

2^0 Pd particles fill in the remaining voids. 2^0 Pd particles fill and cover the smaller open spaces left by the Pd covered oxide particles. Seeding once and then plating on a substrate that has a large particle and pore size produces almost exclusively 1^0 with limited 2^0 Pd deposits. Seeding once and then plating on substrate that has the pore size reduced by an oxide coating tends to produce 1^0 with a filling layer of 2^0 Pd deposits. Seeding multiple times and then plating produces almost exclusively 1^0 Pd covering with almost no filling layer of 2^0 Pd deposits.

4.1.2 Experiment series 2

Taking into account the things learned in Experiment 1, a new series of experiments was designed. These new experiments consisted of 78 combinations of different oxide particle types, sizes, number of treatments, palladium salts, plating angles, stir speeds, single and multiple platings (see experimental Matrixes 2a-2c pages 13-15).

Experiment 2 used only the 0.2µm MOTT filter discs. This allowed a comparison to the established procedures and published results[Error! Bookmark not defined.].This purpose of this investigation was to systematically determine the role of each variable and to determine the effect on the deposited membrane. The goal was to take these results and apply them to another microfabricated PSS disc substrate produced by the CAMP center.

The first five series of experiments in each matrix (see experiments 1-5 and 21-24 Matrixes 2a, 26-30 and 45-49 Matrixes 2b, 51-55 and 70-74 Matrix 2c) were a series of controls for each oxide coating and seeding step. This showed some interesting results (see figure 4.1.2.1 a-c).

It appears as if the silica coated disc provides better oxide coverage (see figure 4.1.2.1 a-c)). The zirconia treated disc (experiment 2-51) seem consistent with previous observations (see figure 4.1.2.1 c) that it does not work well at all as a filler, but seems to prep the PSS surface in some way.

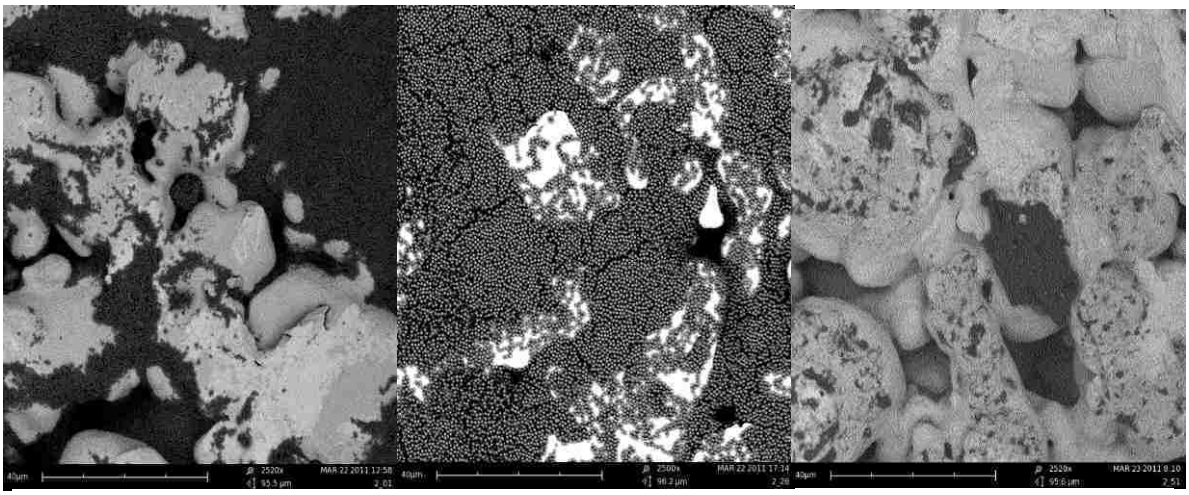

a. Experiment 2-1
1.0µm alumina particle
Treated once

b. Experiment 2-26
1.0µm silica particle
Treated once

c. Experiment 2-51
1.0µm zirconia particle
Treated once

Figure 4.1.2.1: Experiment 2 a series of controls for each oxide coating and seeding step

Seeding once, followed the same the observed trends, with an observed decrease of the oxide filler in the case of both alumina and zirconia, almost exclusive 1^0 Pd formations. Cross particle contamination was observed on discs that were simultaneously seeded multiple times (see figure 4.1.2.2). This leads to the conclusion that there needs to be a sintering process to crosslink the silica, alumina, or zirconia particles and lock them into the pore structure of the PSS part. This also supports the earlier observation of gaps in the particle coverage.

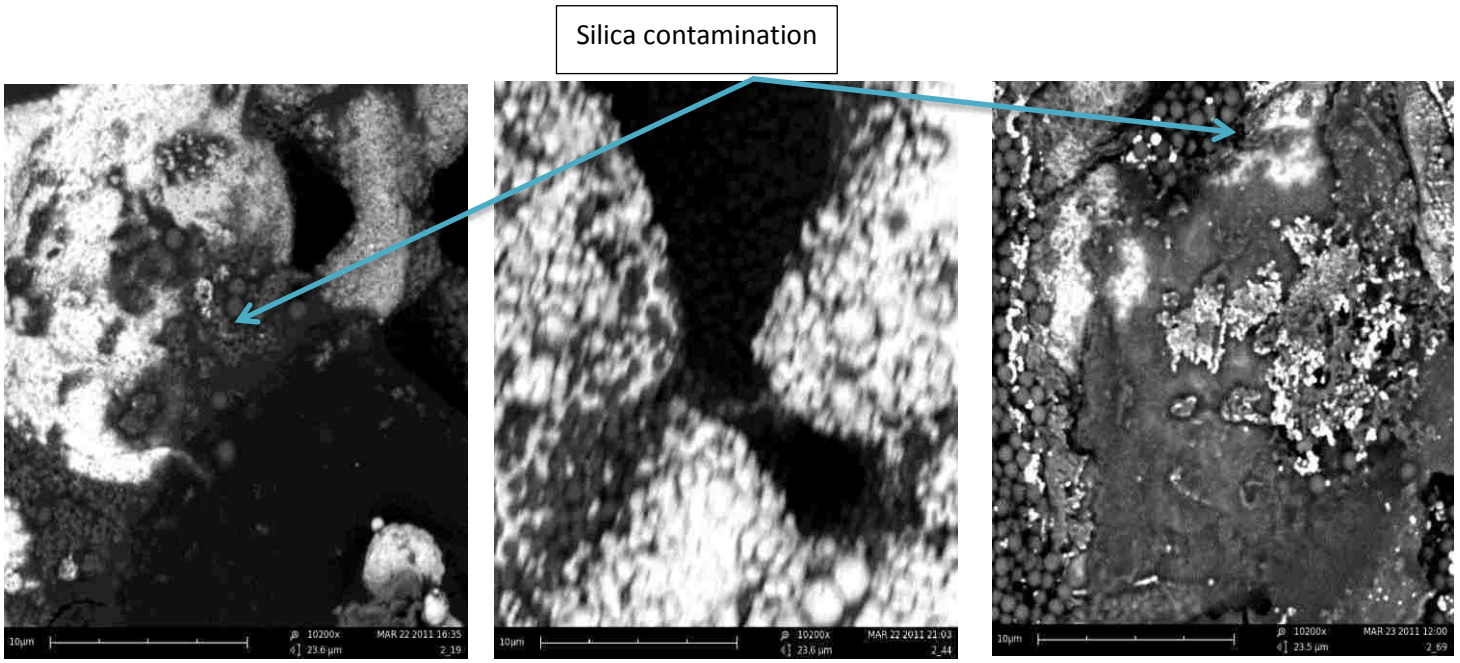

a. Alumina, Seeded three times

b. Silica, Seeded three times

c. Zirconia, Seeded three times

Figure 4.1.2.2: Experiment 2 showing silica bead contamination.

The seeding worked best when the PSS parts were seeded then immediately plated, especially 1.0 µm silica particles. Note that the oxygen-silicon bond is stronger than the oxygen zirconium or the oxygen aluminum bonds. This offers a potentially longer lived substrate at working temperatures (300-750^{o}C) and reducing atmosphere (H_2 and other gasses).

The effects of the different plating solution stir speeds and plating angle are shown in figures 4.1.2.3-5. Figure 4.1.2.3 illustrates are the alumina treated MOTT discs. Notice the absence of consistent oxide coverage in the pores. It has been suggested that the particles are being dislodged during the plating process and need to be anchored in place. Figures 4.1.2.3-5 show the trend of plating angle affecting the Pd epitaxial formation. As the angle between the substrate and the fluid flow approaches perpendicular increased formation and size of Pd nodules was noticed. As the stir speed is increased so does the size and amount of the nodular formation; the secondary branching and fill decreases. Figures 4.1.2.3-5 show more consistent palladium coverage at lower plating angles and stir speeds. 60^{0} and 150 rpm gave the best secondary branching and fill.

Alumina treated MOTT discs

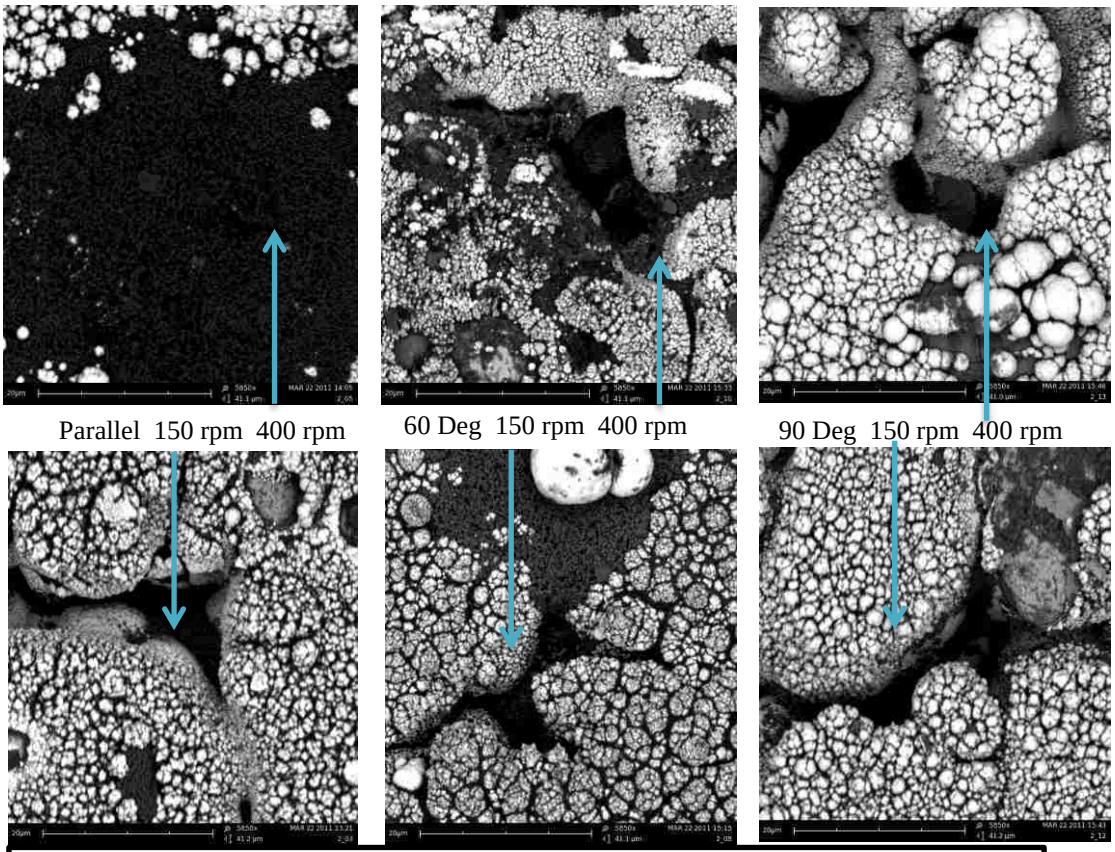

Figure 4.1.2.3: Effects of the different plating solution stir speeds and plating angle.

The effects of the plating solution stir speeds and plating angle are shown (in figure 4.1.2.4) for the silica treated MOTT discs. Notice the continued absence of complete oxide particle coverage in some of the pores, but good palladium coating and coverage overall. Also note the trend that slower stir speeds give better depositional branching and secondary fill. Finally observe that the silica particles acted as good nucleation points and allowed good particle to particle secondary branching and fill

Silica treated MOTT discs

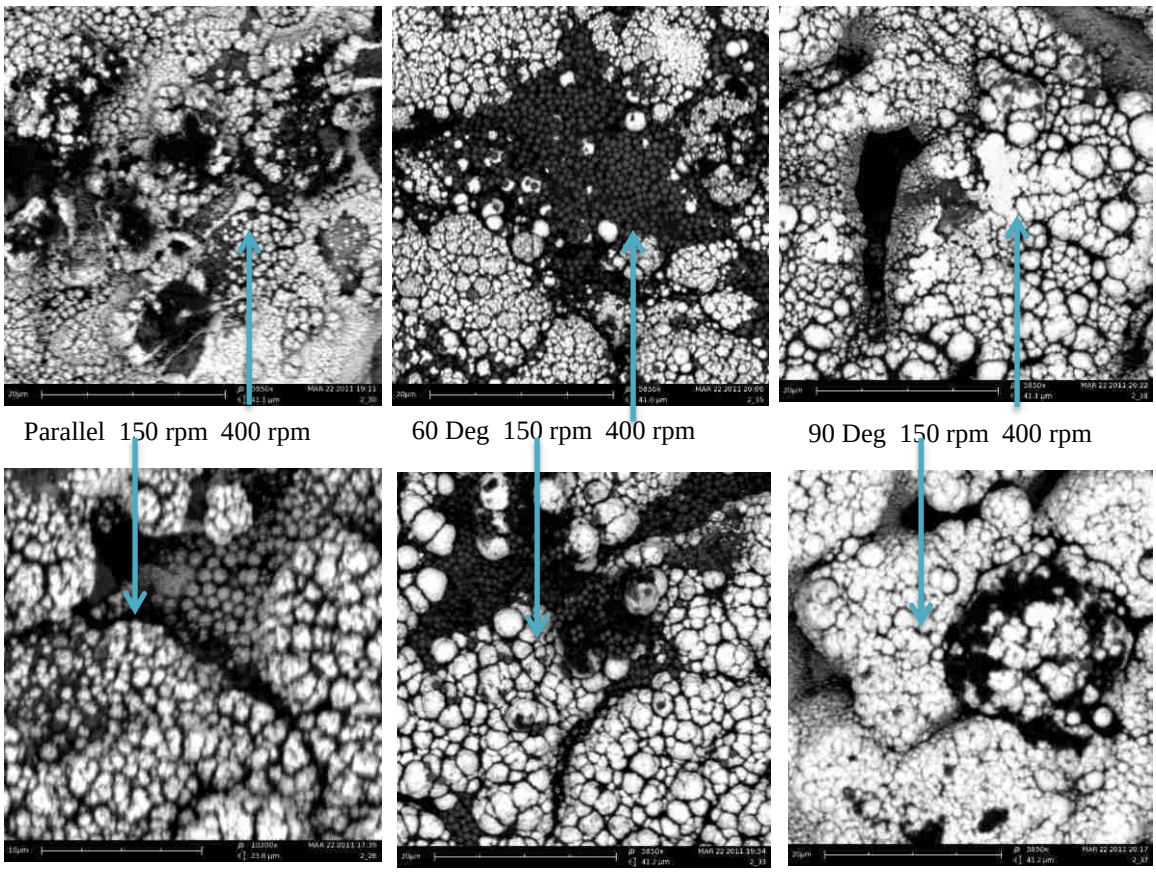

Figure 4.1.2.4: Effects of the different plating solution stir speeds and plating angle.

Zirconia particle behavior is shown in figure 4.1.2.5. The surface is essentially palladium plated stainless steel. See too that even though the literature suggests 400 rpm [Error! Bookmark not defined.,Error! Bookmark not defined.] as optimal for the full use of the palladium salt in the solution, variation of the plating speed allows control of the amount of nodular or coral like deposition and secondary fill.

The differing oxide treatments, plating angles and stir speeds revealed some interesting trends (see figure 4.1.2.6).

- Plating, and stirring at 400 rpm and plating parallel to the direction of flow allowed some secondary fill, but forced the formation of large palladium nodules in mostly primary coverage.

These nodules are a waste of palladium as some areas were not subjected to the secondary fill needed for complete membrane coverage. These nodules also seem to be weakly anchored.

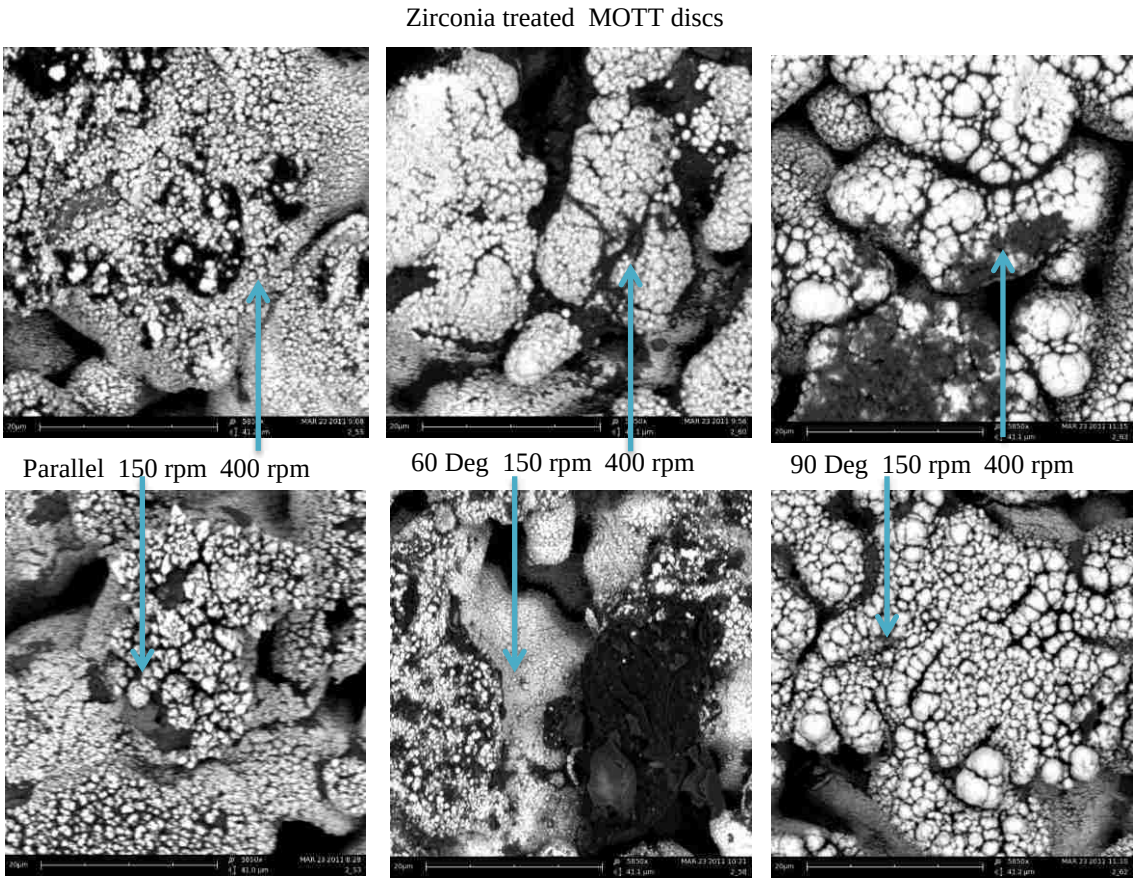

Figure 4.1.2.5: Effects of the different plating solution stir speeds and plating angle.

- Plating, and stirring at 400 rpm and plating 60 deg to the direction of flow allowed for a more controlled deposition, limiting the presence of palladium nodules, enhancing secondary palladium fill over and around the oxide particle treatment in a branching coral like formation with palladium fill.
- Plating, and stirring at 150 rpm and plating parallel to the direction of flow allowed some secondary fill and sharply decreased the nodule formation.

- Plating twice, stirring at 150 rpm and plating 60 deg to the direction of flow allowed more secondary fill and optimized the primary branching seen earlier between the particle/substrate and particle/ particle interactions.
- The silica particle seemed to have the better palladium fill in and around the grains creating a more comprehensive coverage.
- Slowing down the stir rate seemed to stimulate the palladium secondary fill and limit the primary substrate/palladium deposits.

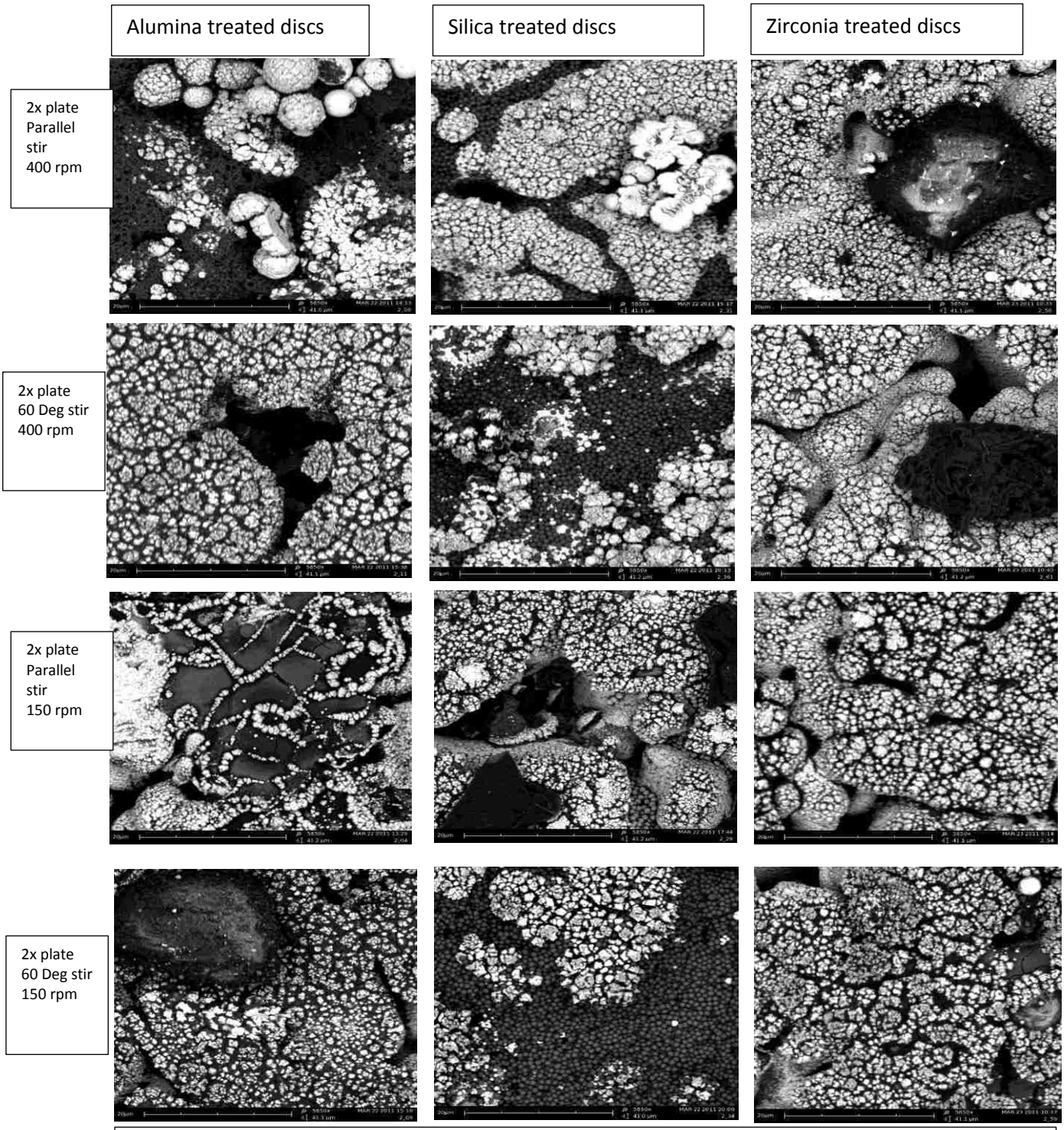

Figure 4.1.2.6: Comparison of the differing oxide treatments, plating angles and stir speeds.

Examining alternative palladium plating solutions provided some insight on possible plating applications. All of these discs were activated and seeded as described in experiment 1.

The alumina particle treated discs (see figure 4.1.2.7 a-c) followed the earlier observed trends of good primary formations with dendritic coral like formations and some secondary fill using $PdCl_2$.The palladium acetate deposited a thin, crust-like primary coating that was not well anchored and allowed limited secondary fill. The palladium nitrate had limited solubility and was unstable in solution. It deposited a thin crust that was not well anchored to the substrate very well.

a. MOTT disc plated by $PdCl_2$ and NH_4OH/hydrazine

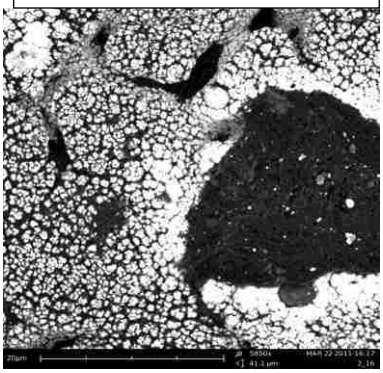

b. MOTT disc plated by $Pd(Oac)_2$ and NH_4OH/hydrazine

c. MOTT disc plated by $Pd(No_3)_2$ and NH_4OH/hydrazine

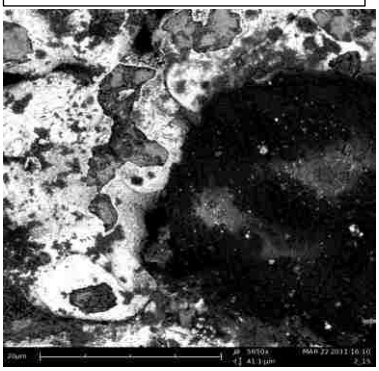

Figure 4.1.2.7: Alumina particle treated alternative solution plated MOTT discs.

The silica particle treated discs (see figure 4.1.2.8 a-c) followed the trend of good primary formations with dendritic coral like formations and some secondary fill using $PdCl_2$The palladium acetate allowed mostly primary formations with limited dendritic coral like formations and some secondary fill. The palladium acetate deposited mostly primary coating that allowed some secondary fill in and around the silica particles. The palladium nitrate deposited a thin crust that was not well anchored to the substrate.

a. MOTT disc plated by $PdCl_2$ and NH_4OH/hydrazine

b. MOTT disc plated by $Pd(Oac)_2$ and NH_4OH/hydrazine

c. MOTT disc plated by $Pd(No_3)_2$ and NH_4OH/hydrazine

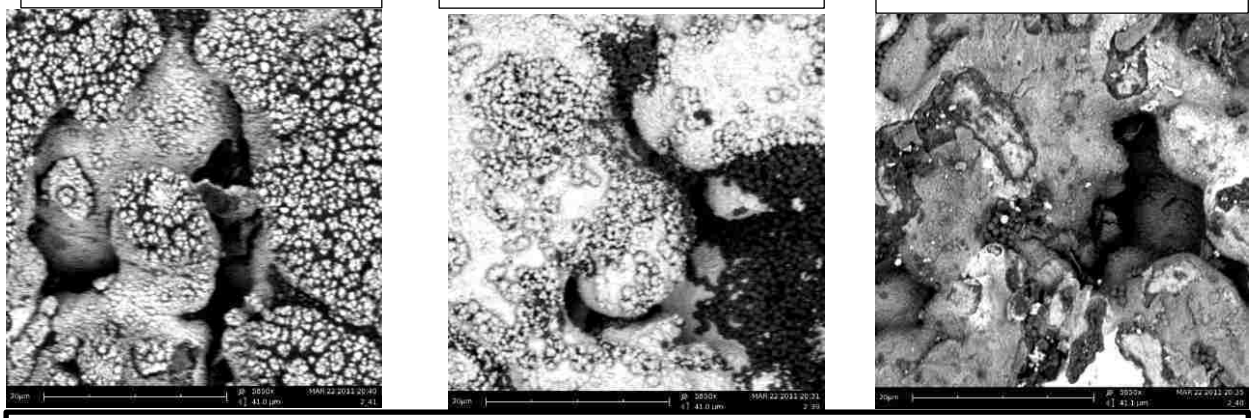

Figure 4.1.2.8: Silica particle treated alternative solution plated MOTT discs.

The zirconia particle treated discs (see figure 4.1.2.9 a-c) followed the same observed trends of dendritic coral-like formations. These show large nodules that were actually coming off when using $PdCl_2$.The palladium acetate deposited dendritic coral-like formations with limited secondary fill. The palladium nitrate had limited solubility was unstable in solution. It deposited a thin crust that was not well anchored to the substrate.

a. MOTT disc plated by $PdCl_2$ and NH_4OH/hydrazine

b. MOTT disc plated by $Pd(Oac)_2$ and NH_4OH/hydrazine

c. MOTT disc plated by $Pd(No_3)_2$ and NH_4OH/hydrazine

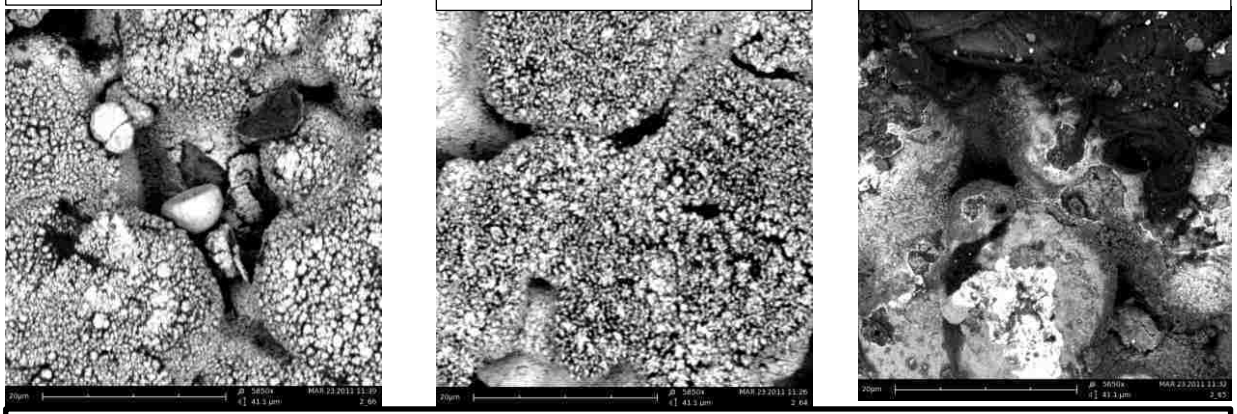

Figure 4.1.2.9: Zirconia particle treated alternative solution plated MOTT discs.

4.1.2.2 Summary of results in experiment 2

The alumina and silica treated media produced good results when seeded and plated once or multiple times. The plating angle experiments suggest that the depositional morphology is a function of fluid flow dynamics with 60^0 being optimum for the morphology desired in this application. The fluid stir speed experiments suggest that depositional morphology is also a function of mass transfer of the dissolved Pd^{2+} and surface availability of the reduced palladium catalyzing the unreduced palladium/hydrazine/ hydroxide couples. A stir speed of 150 rpm allowed a more controlled depositional morphology, in contrast to the established procedure of 400 rpm which was optimized for best plating kinetics[4]. The zirconium treatment left much of the PSS substrate unmodified. The different palladium salts affected thickness and depositional morphology. Based on the differences of the Si-O and the Al-O bond the silica substrate is a better particle treatment that can withstand the operating conditions of elevated temperatures and a reducing atmosphere pressures. The silica particles offered good particle-to-particle nucleation, good primary, and good secondary palladium fill characteristics.

4.1.3 Experiment series 3

Experiment 3 was subdivided into three sections. Once the MOTT discs were seeded and coated with palladium, the variables of deposition were selected for the new substrate. A micro fabricated 420 PSS disc manufactured at the CAMP facility in Butte Mt was given provided. This was to apply knowledge of deposition parameters onto a new and novel substrate.

Figure 4.1.3 shows a comparison of the MOTT disc and the CAMP discs after preliminary disc prep, before surface modification. The new CAMP substrate has flow-through characteristics that are almost 8X greater than the MOTT discs (see Appendix A supplemental N_2 flow data in experiment 1 for the MOTT disc average flow rate of 2.206 standard liters per minute (SLPM) and supplemental N_2 flow

data in experiment 5-4 for the CAMP disc flow rate of 17 SLPM). Note that the flow-through characteristics displayed by the MOTT discs varied substantially from lot to lot. This variability led to inconsistent results in the oxide particle coating process. This performance variation from lot to lot of the MOTT substrate was also proposed to have a huge effect on the performance of the membrane. Note that the limited channels formed in between the large stainless steel particles in the MOTT disc allowed for the easy formation of small membranes that spanned the large pore sizes. All of the small palladium particles deposited on the huge stainless steel particles seen in the picture of the MOTT disc (see figure 4.1.3 a-b) are wasted and membrane based on EDX studies allow for unimpeded metallic diffusion of iron and chromium into the palladium membrane. The hydrogen generated from the diffusion through the palladium membrane has to go either through the interface of the palladium/stainless steel juncture into the stainless steel itself or find a path of least resistance to an open channel.

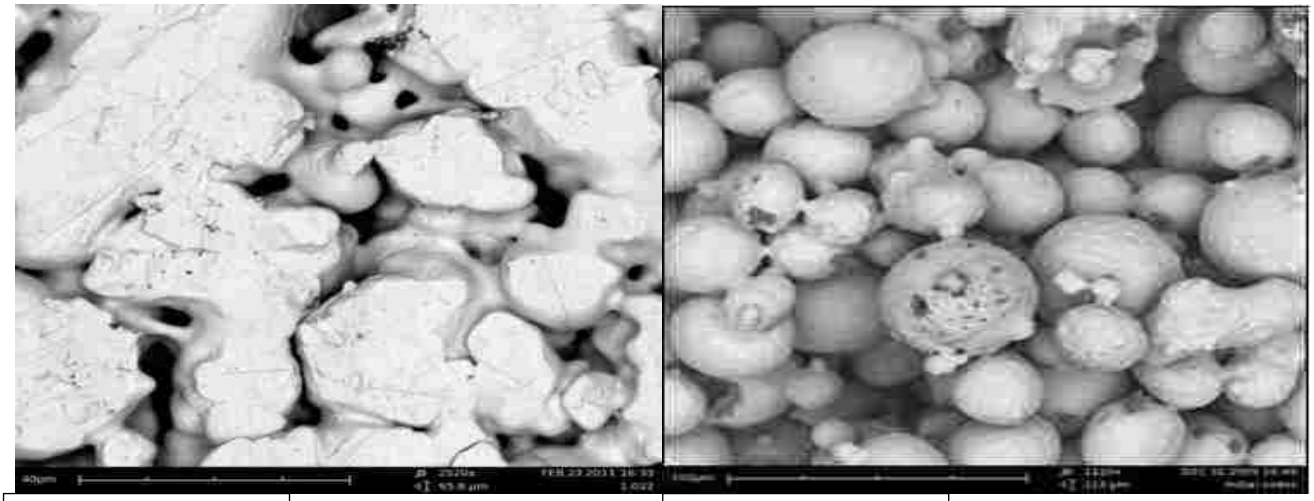

a. MOTT disc b. CAMP disc

Figure 4.1.3: Side by side comparison of the MOTT and CAMP discs used as a PSS substrate

4.1.3.1 Experiment 3-1

Fifteen CAMP discs were treated with silica gel particles and sintered[36] as listed in the experimental matrix 3-1. Disk 3-16 was a MOTT disc that was treated as a control for result comparison.

What is not shown in experimental matrix 3-1 is that there were different amounts of silica particles (light, medium and heavy applications) used in the fill and infiltration methods. The sinter at 950^0C was not needed, as the 900^0C sinter worked just as well. The object of varying sintering temperature was to find a sintering temperature and time that allowed partial necking but not total vitrification of silica beads into a solid glass membrane.

One trend that was observed was that the PSS CAMP discs were so porous (see figure 4.1.3) that the silica beads fell through. The vacuum infiltration method practiced on the MOTT discs did not work at all. A new method was needed. Instead of placing the disc and septum (see figure 3.4.1) under vacuum into a solution that was being sonicated, the septa and disc were inverted (see figure 4.1.3.1.1). Acetone was used to wet the disc under vacuum. A small amount of silica powder was added to the top of the surface of the disc and then acetone was added to help pull the powder into the PSS matrix. The excess powder was trowelled off with a spatula and the disc allowed to dry under vacuum. The excess dry powder was removed with a stiff toothbrush with the safety precaution of using a dust mask to keep the 0.1µm beads from being respired. The silica powder is an irritant and long term exposure could lead to silicosis. Various combinations were tried, with discs 10, 11, 13 showing the best coverage (see figure4.1.3.1.2)

Figure 4.1.3.1.1 CAMP disc silica application apparatus

a. CAMP disk 3-1-10 silica treated

b. CAMP disk 3-1-11 silica treated

c. CAMP disk 3-1-13 silica treated

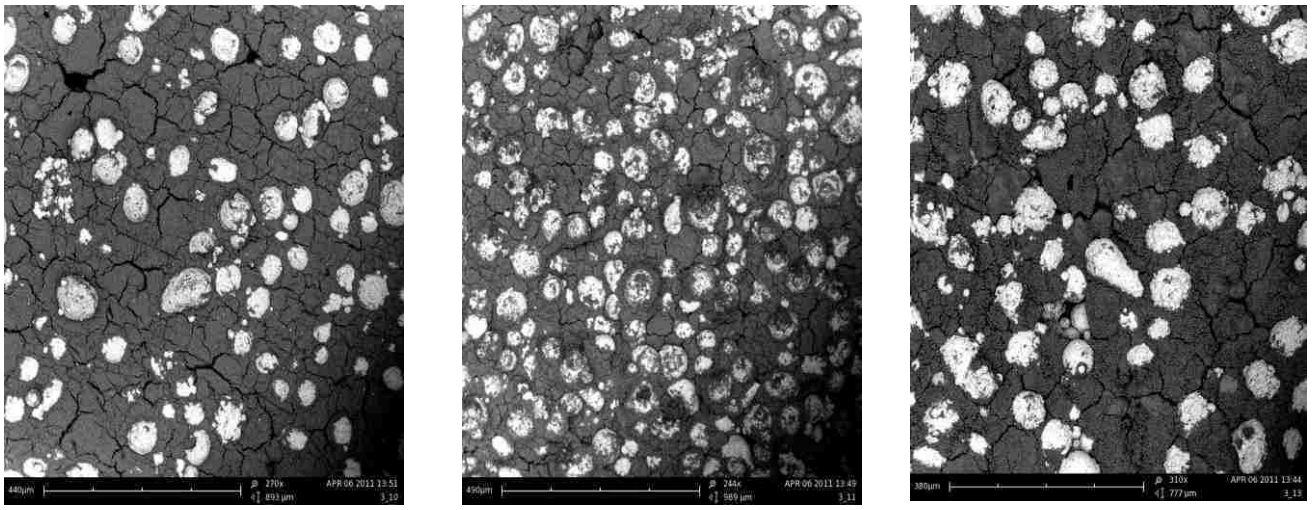

Figure 4.1.3.1.2: silica particle treated CAMP discs

4.1.3.2 Experiment 3-2

Twenty four CAMP discs were treated with silica particles, a combination of solvents, vacuum and hand application according to the experimental matrix 3-2. These discs were then sintered under N_2 at 900^0C (see figure 4.1.3.2.1). Note that an older tube furnace was used for the sintering. Unanticipated altering of the nitrogen gas flow through the tube furnace in this experiment produced some interesting results: some of the silica beads formed into fine needles that covered the PSS substrate. (See figure 4.1.3.2.2).

CAMP discs that were silica treated under vacuum and then sintered treated face up

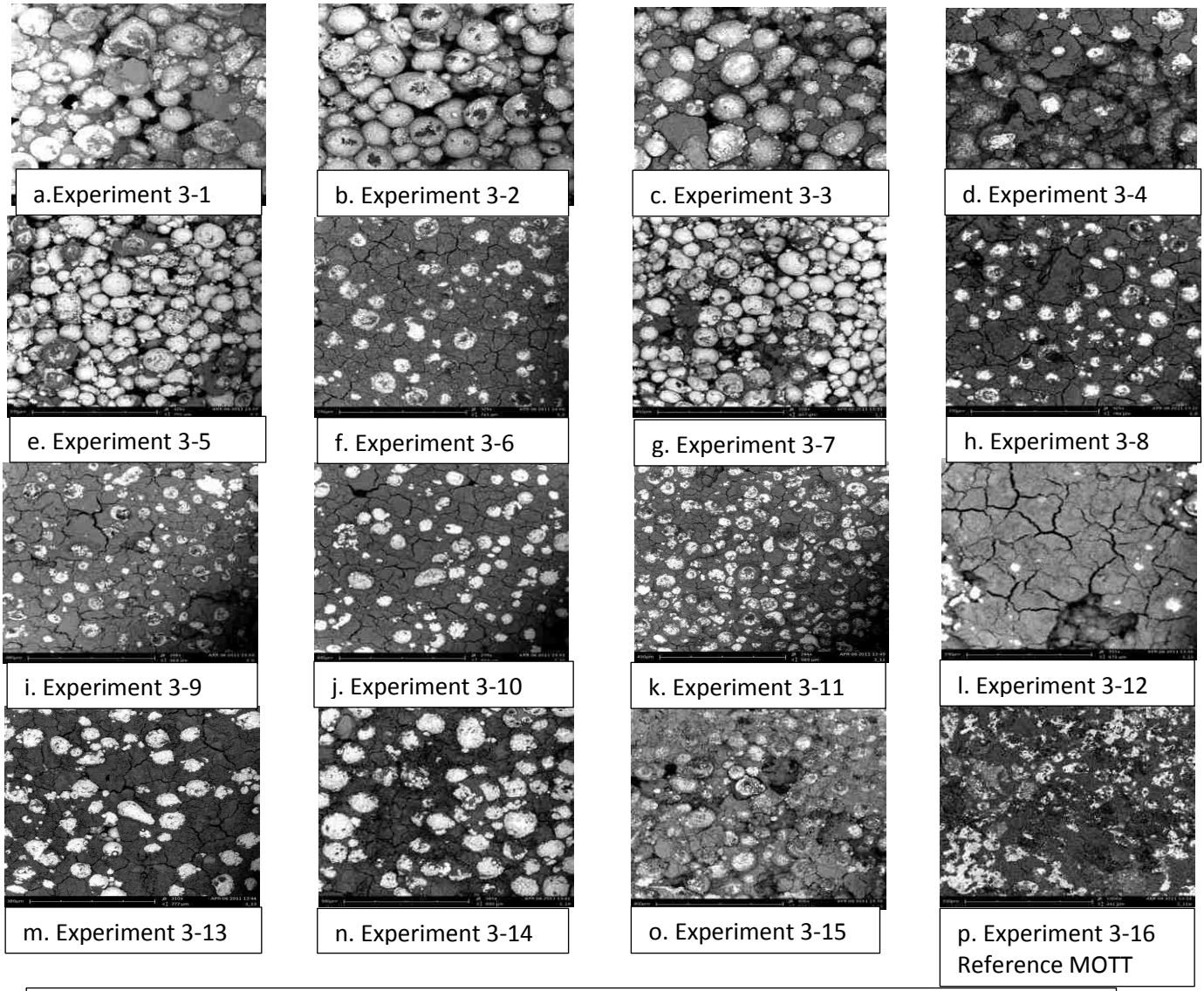

Figure 4.1.3.2.1: CAMP discs with silica particles treated with various combinations of solvents, vacuum and hand application.

a. Experiment 3-2-18

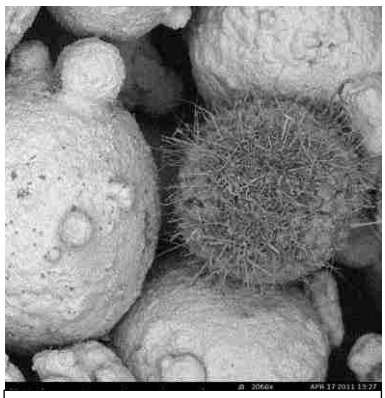

b. Experiment 3-2-20

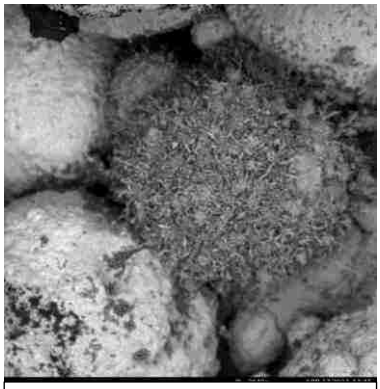

c. Experiment 3-2-23

Figure 4.1.3.2.2: Filaments formed from the silica beads during sinter.

The filaments formed from the silica beads were an unexpected result of gas flow and temperature. This could have a large effect on the final epitaxial morphology of the palladium membrane and needs to be monitored closely.

Experiment 3-2-(figure 4.1.3.2.3 a-c) shows a good representation of the discs that were successfully treated. The most successful treatment was described earlier in experiment 3-1.

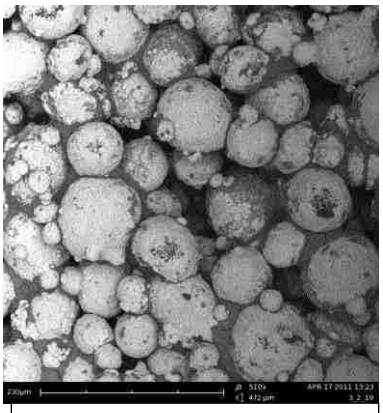

a. Experiment 3-2-19

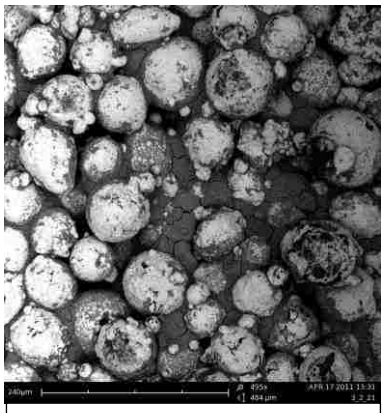

b. Experiment 3-2-21

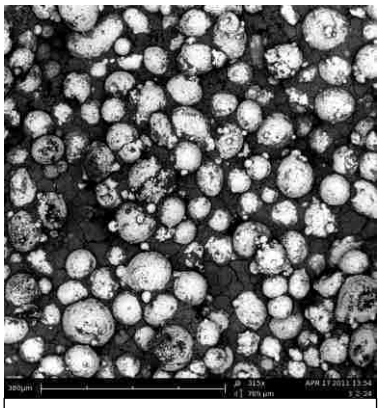

c. Experiment 3-2-24

Figure 4.1.3.2.3: Discs that were successfully treated.

4.1.3.3 Experiment 3-3

Experiment 3-2 disk numbers (19, 21) were sensitized and plated using techniques gained from earlier experiments. These discs examined under SEM (see figure 4.1.3.3.1 a-f) are shown below.

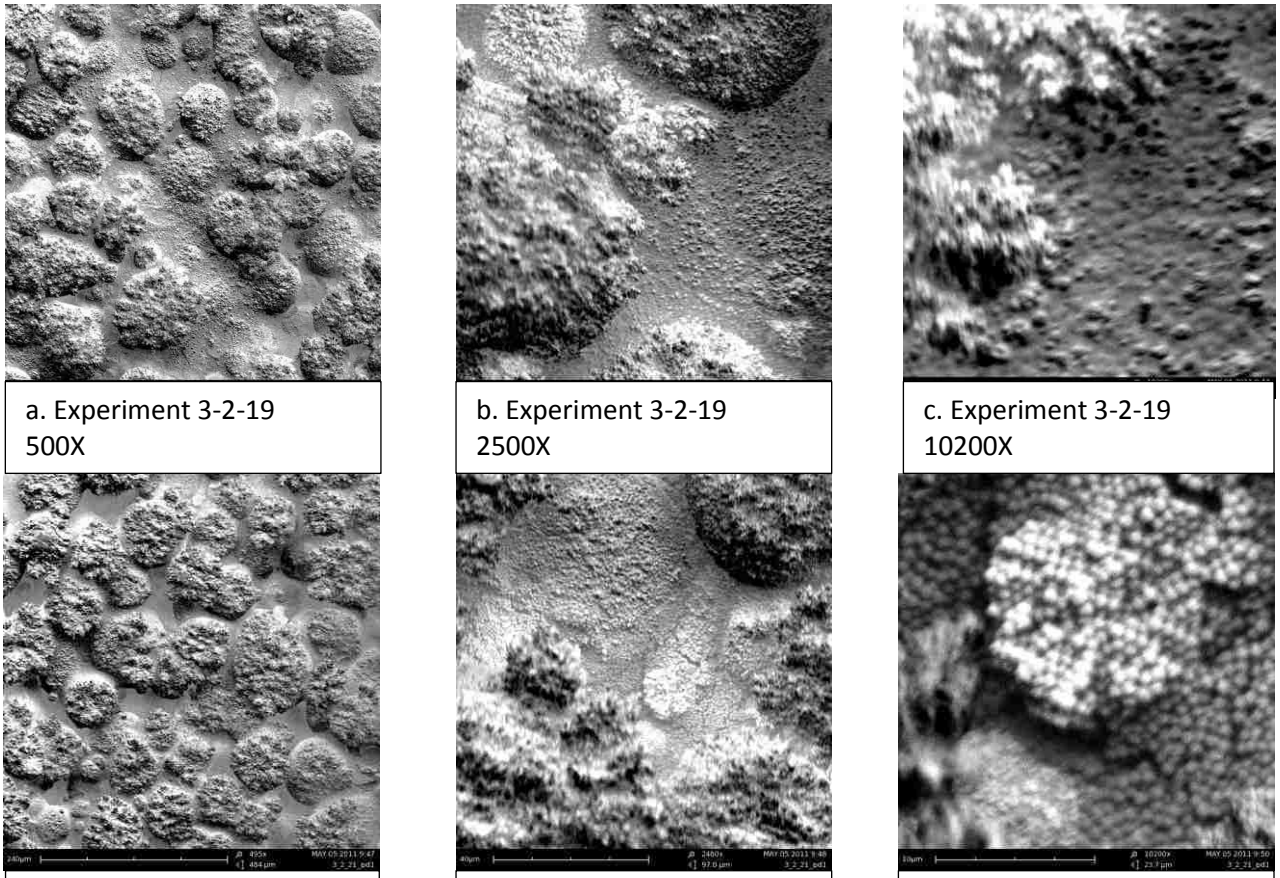

a. Experiment 3-2-19 500X

b. Experiment 3-2-19 2500X

c. Experiment 3-2-19 10200X

d. Experiment 3-2-21 495X

e. Experiment 3-2-21 2480X

f. Experiment 3-2-21 10200X

Figure 4.1.3.3.1 : Discs (19, 21) that were successfully $SnCl_2/PdCl_2$, sensitized and plated using $Pd(NH_3)_4Cl_2$/hydrazine.

As seen in figure 4.1.3.3.1 above there is excellent primary covering and secondary fill in and around the silica beads and the PSS support matrix.

To validate the reproducibility of the results, a new matrix was designed (see experimental matrix 3-3-2a) to apply the knowledge gained earlier. Both palladium and copper were plated on the

treated discs, in multiple layers, and different palladium salts were used to maximize the best epitaxial morphology.

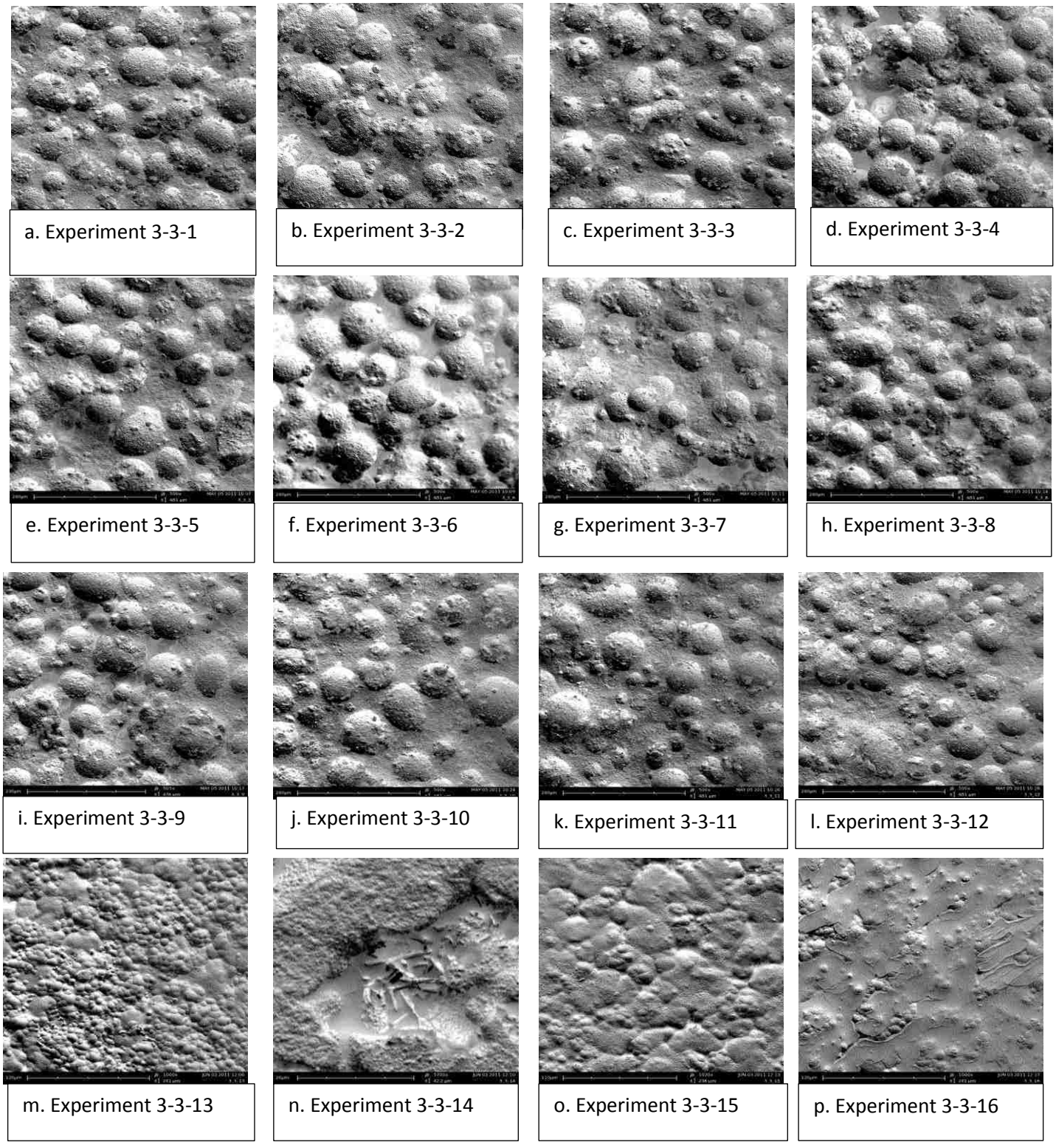

a. Experiment 3-3-1
b. Experiment 3-3-2
c. Experiment 3-3-3
d. Experiment 3-3-4
e. Experiment 3-3-5
f. Experiment 3-3-6
g. Experiment 3-3-7
h. Experiment 3-3-8
i. Experiment 3-3-9
j. Experiment 3-3-10
k. Experiment 3-3-11
l. Experiment 3-3-12
m. Experiment 3-3-13
n. Experiment 3-3-14
o. Experiment 3-3-15
p. Experiment 3-3-16

Figure 4.1.3.3.2: Experiment 3-3-2a discs that were Pd/Cu treated.

The comparison of the original results, which forced the abandonment of the CAMP substrate as a support matrix, and the application of the system of fundamental depositional variation to that substrate, make a startling contrast (see figure4.1.3.3.3).

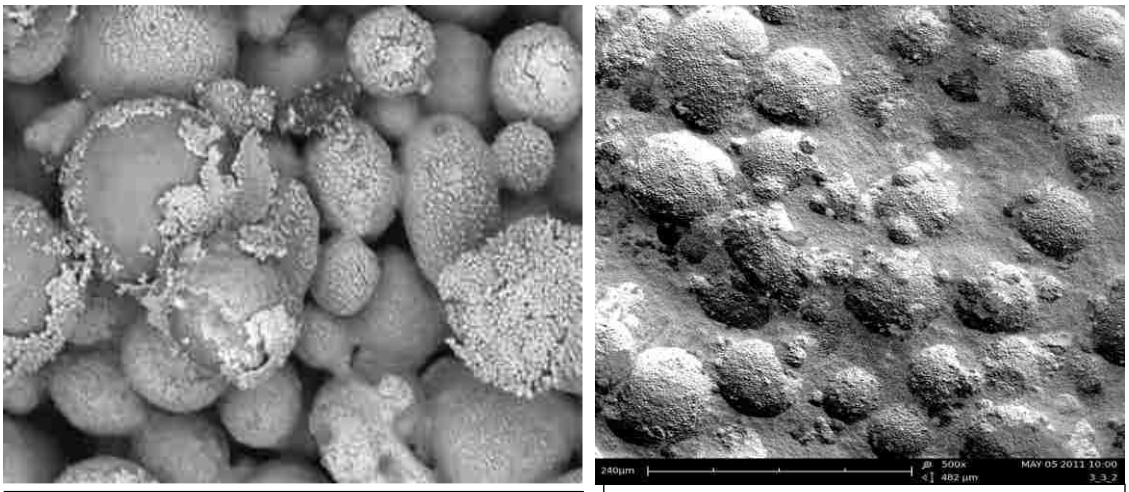

a. Initial Pd plating attempt 5-19-2010

b. New plating system applied on 5-20-2011

Figure 4.1.3.3.3: Comparison of original and final plating system.

There were some very interesting trends noticed in this series of experiments. The palladium plating step worked well, and subsequent copper plating also worked well. Plating over the copper with palladium was unsuccessful, as the palladium deposited poorly, if at all, onto the copper coated palladium layer on the MOTT disks and poorly on the like-plated CAMP disks. It was postulated that palladium particles need to be exposed on the surface to act as a depositional catalyst. The palladium/ copper layers need to be annealed to form the alloy and expose more palladium reduction catalytic sites and then replated. Multiple plating layering seemed to work poorly on the CAMP discs due to the rough surface area exposing small areas of palladium particles as catalytic reduction sites. That implies the incomplete coverage of the copper onto the palladium membrane.

The plated discs were then pressure tested for pinhole leaks pre-and post-anneal. This was done using a manometer apparatus (see figure 3.6.3.2), prior to sending the discs to the Montana Tech

campus for in depth gas and pressure differential testing. This testing was done using a special in-house apparatus designed with NETL guidelines and blueprints. All CAMP discs had pressure leaks pre- and post-anneal, and the plated MOTT discs (3-3-13- through 15 see figure 4.1.3.3.2 a-p) all held pressure pre- and post-anneal. These results were not totally surprising.

The nature of the spherical substrate, the interlocking crystal deposition and the subsequent fill was postulated to hold pinhole leaks. The testing done at the CAMP center confirmed this hypothesis (see experimental results table 4.1.3.3).

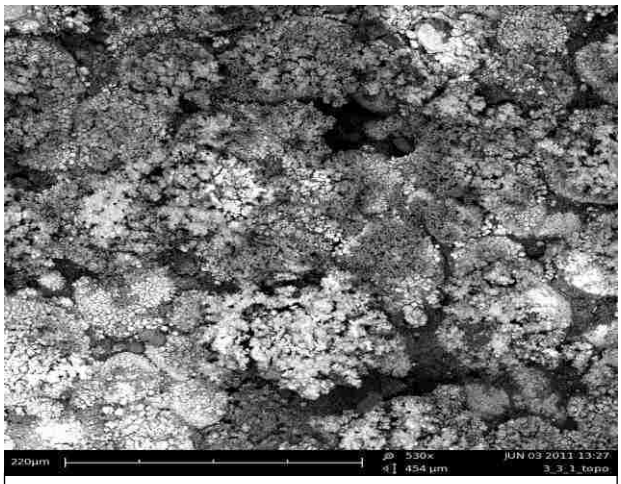

a. Experiment 3-3-1 Full view 530X

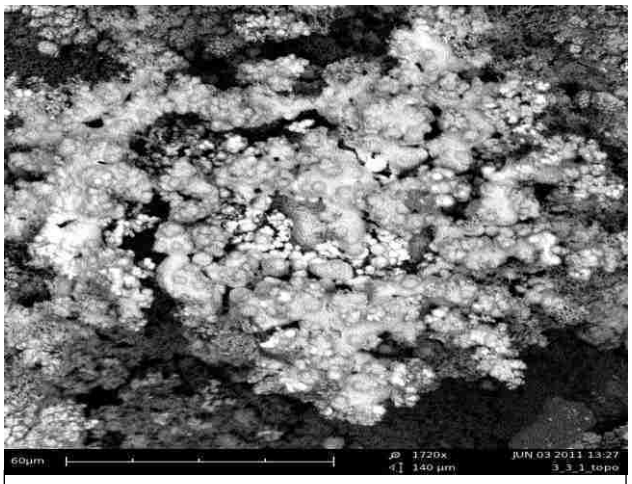

b. Experiment 3-3-1 Full view 1720X

Figure 4.1.3.3.4: Full view at high magnification showing the nature of the Pd/Cu depositional layers on the CAMP substrate

When examined above at under high magnification, the nature of the multiple depositional layers and substrate becomes clearer. There are copper deposits covering most of the palladium, but not all (see figure 4.1.3.3.4 a-b). It was judged that the copper/palladium layers need to be annealed into an alloy. This homgenation might allow the flow of high energy surface areas to lower energy surface areas and allow the intercalation of copper into the palladium crystal lattice.

Table 4.1.3.3 N_2 experimental results

Sample ID	Pressure (PSI)	Flow Rate (SLPM)	Comments
3-3-1	60	16.8	For CAMP discs, the substrate will pass roughly 17 SLPM
3-3-2	60	16.75	CAMP disc Pd/Pd layer
3-3-3	N/A	N/A	Broken
3-3-4	60	16.75	CAMP disc Pd/Cu Pd/Cu Pd layers
3-3-5	60	16.75	CAMP disc Pd/Cu layer
3-3-6	60	16.73	CAMP disc Pd/ Pd layer
3-3-7	N/A	N/A	Broken
3-3-8	60	16.74	CAMP disc Pd/Cu Pd/Cu Pd layers
3-3-9	60	16.75	CAMP disc Pd/Cu layer
3-3-10	60	16.8	CAMP disc Pd/ Pd layer
3-3-11	N/A	N/A	Broken
3-3-12	60	16.73	CAMP disc Pd/Cu Pd/Cu Pd layers
3-3-13	60	.09	MOTT disc 1 Pd/Cu layer
3-3-14	60	.04	MOTT disc Pd/Pd layer
3-3-15	60	0	MOTT disc 1 Pd/Cu/Pd layer
3-3-16	60	.05	MOTT disc Pd/Cu Pd/Cu Pd layers

All discs in experiment 3-3 were annealed for 120 hours at 500^0C under 3/97% H_2/N_2 gas mixture in an atmospherically and temperature controlled tube furnace (See appendix A for pre- and post-anneal XRD data). The annealing of the discs was judged to be successful.

There were some interesting trends noticed with regard to the migration of iron and chromium, see discs 3-3-(8, 10, 11, 13) (see Figures 4.1.3.3.5-8). For informational XRD data on disks 8 and 11 (see Figure 4.1.3.3.5). All showed the presence of iron post anneal(for more information see Appendix A XRD data experiment 3-3 pre- and post-anneal). Discs 1,2,9,10,12,and 15 showed no iron at all (see figure 4.1.3.3.6 a-c for XRD, SEM, and EDX data on disc 3-3-10 post anneal

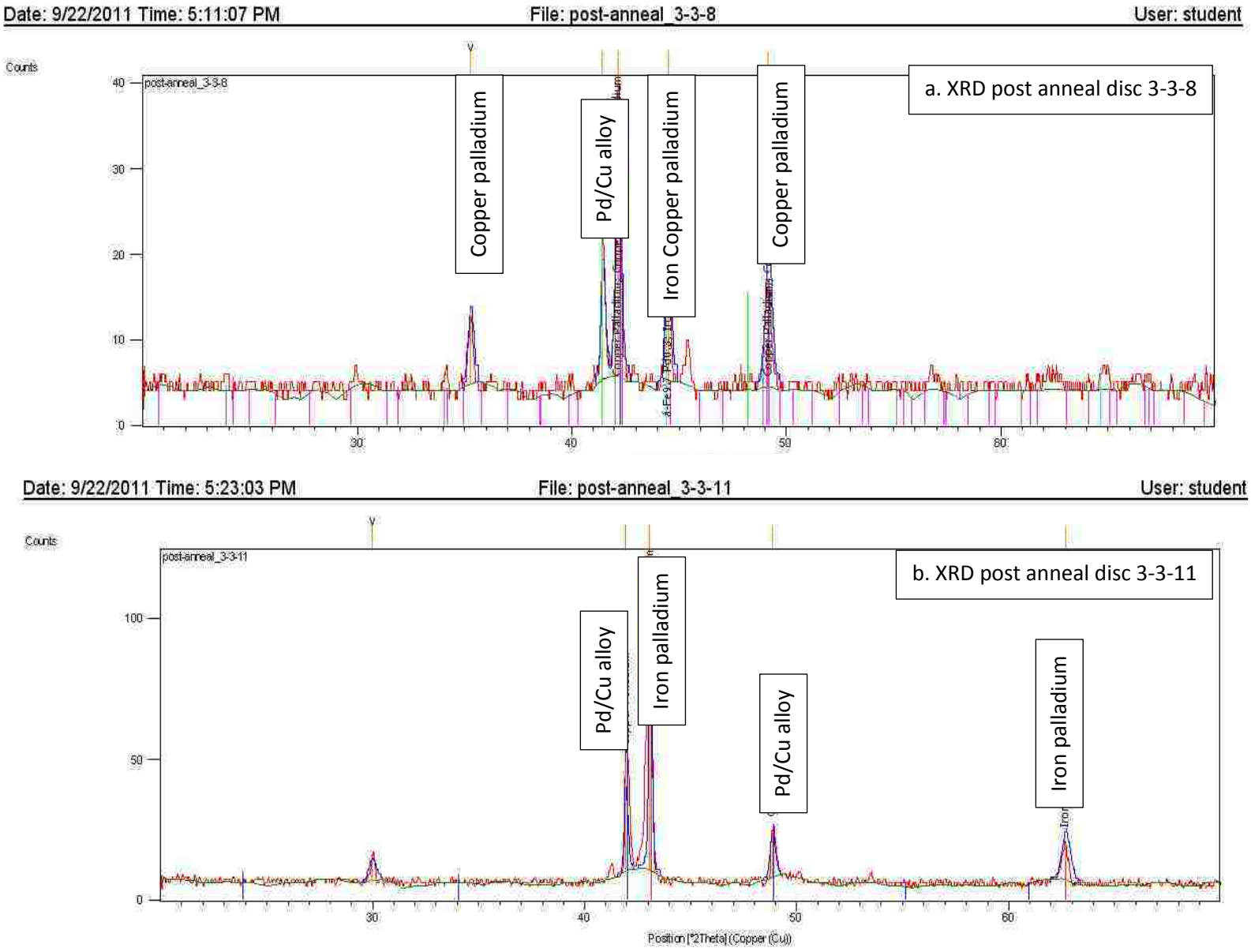

Figure 4.1.3.3.5 XRD post anneal disks 3-3-8 and 3-3-11

Another explanation for the trend of decreasing iron concentration post anneal could be iron contamination due to the plating rinse of HCL solubilizing small amounts of surface iron from the PSS substrate. That surface contamination could be absorbed into the alloy during the anneal period, and due to the low concentration, the iron signal could get masked by the higher concentration of the alloy The HCL rinse could also mobilize more iron due to the higher surface area of the spherical substrate,

and allow diffusion into the alloy during the anneal step, creating the iron contamination observed earlier. Note that there is no presence of chromium. Note too, that there is no set guideline on how much iron it takes to weaken the integrity of the membrane and how much iron can diffuse into the working membrane before function is degraded. At this point, the discs produced from this matrix were moved over to the CAMP center at Montana Tech for permeance testing.

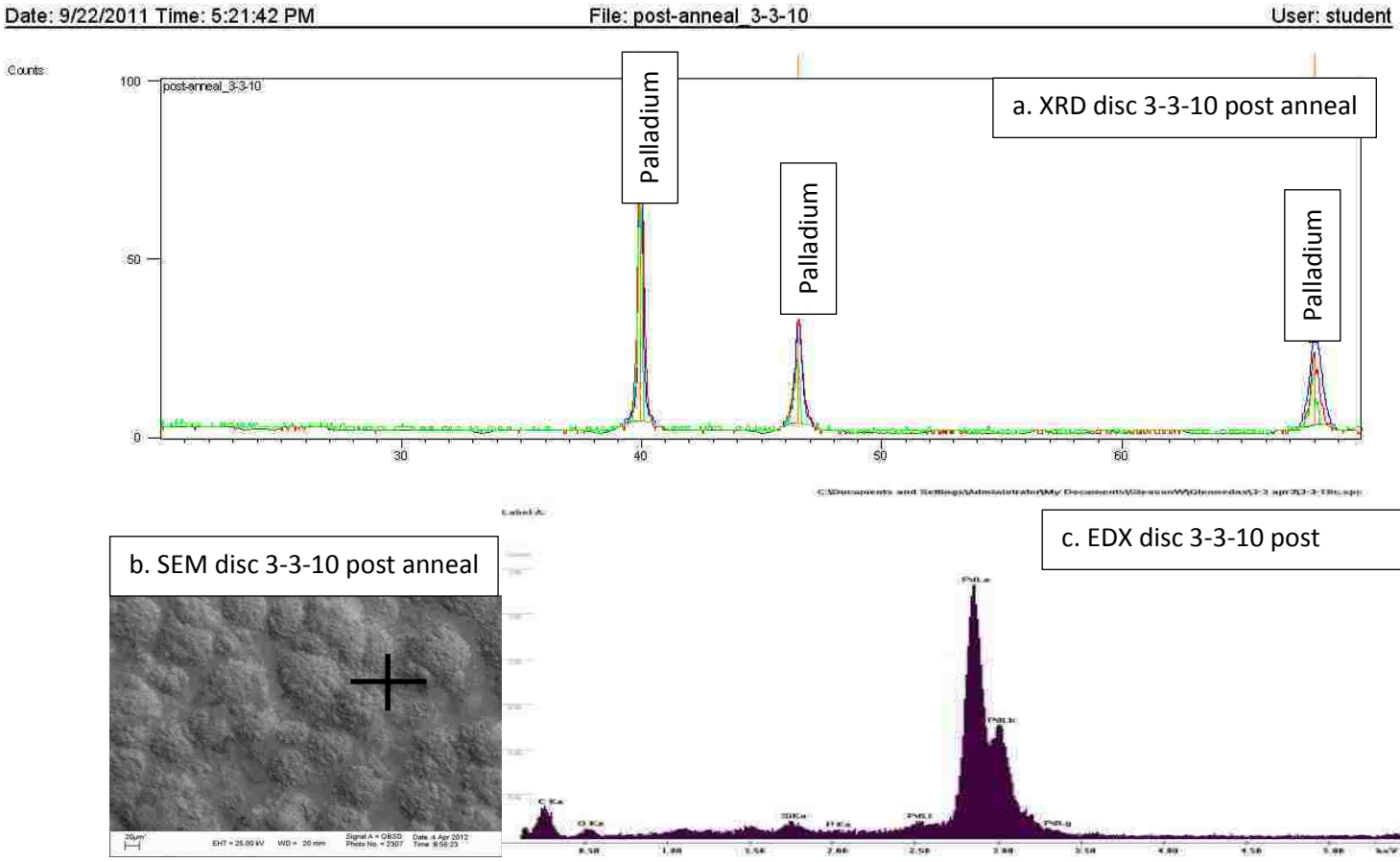

Figure 4.1.3.3.6 XRD, SEM, EDX disc 3-3-10 post anneal

According to the XRD data (see Figure 4.1.3.3.7 a-b), discs 3-13 showed an iron presence (a)pre-anneal and none(b) post-anneal. This could be explained by the anneal forcing the flow of alloy onto previously exposed PSS matrix , removing the iron signal in the case of disc 13. Notice there is no chromium present post anneal, except in (disc 6) shown by XRD of the membranes (see Appendix A XRD experiments 3-3). Disc 6 shows no chromium pre anneal, this might be evidence of metal flow exposing previously unexposed PSS substrate. Figure 4.1.3.3.8 a-c shows pre- (a) and post-anneal (b) SEM and (c) post-anneal EDX. There are some obvious changes during the annealing process. The post-anneal presence of pinholes was unexpected. The post-anneal EDX(c) shows the presence of iron while the XRD does not. This is due to the deeper penetration of the electrons with the technique EDX that go all the way through the palladium into the PSS substrate. The XRD measures the surface crystal structure.

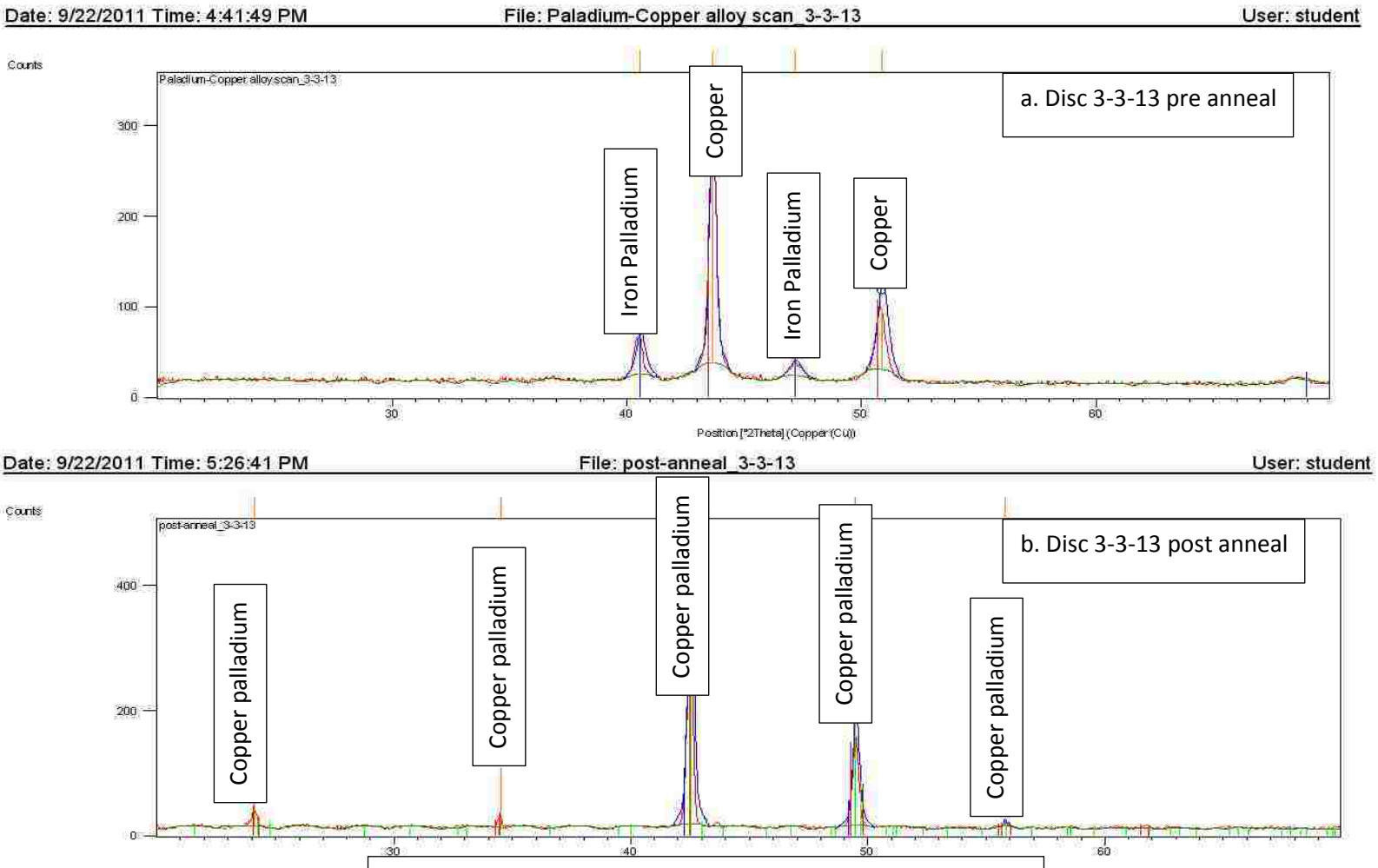

Figure 4.1.3.3.7 Pre and post anneal XRD on CAMP disc 3-3-13

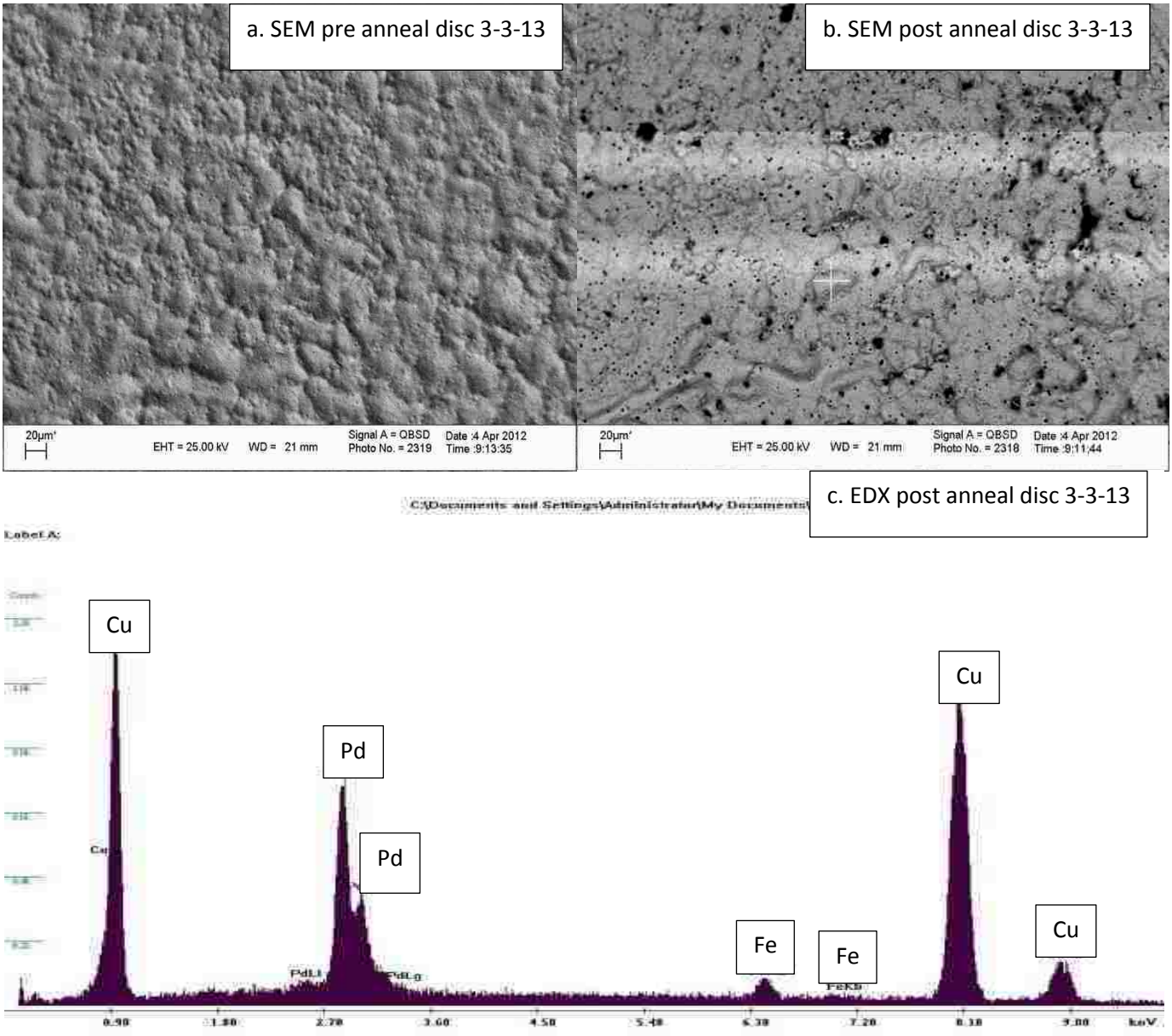

Figure 4.1.3.3.8 Pre and post SEM and post anneal EDX on CAMP disc 3-3-13

4.1.3.3.1 Summary of results experiment 3

Sintering the silica particles locked the particles into the voids and spaces of the PSS substrate(both CAMP and MOTT). This silica particle fill was effective in both Pd seeding, cross branching and secondary

Pd to Pd particle fill. The smaller spherical nature of both the CAMP and the silica substrate created an interlocking lattice when plated with Pd or Pd/CU. This interlocking metal lattice showed pinholes when measured pre- and post-anneal. In some of the experiments iron migrated into the metallic membrane from the PSS substrate through intermetallic diffusion. When the alloy was not annealed, the Pd coverage was poor to nonexistent over the Cu layer. It appears as though the annealing step is crucial to multiple Pd/Cu layer deposition. When the Pd/Cu was annealed, the evidence showed an alloy formed and flowed over the exposed PSS substrate.

4.1.4 Summary of initial goal experiments

Experiment series 1 showed that reducing the pore size by applying an oxide coating tends to produce 1^0 deposition with a nice filling layer of 2^0 Pd deposits. Seeding multiple times and then plating tends to produce almost exclusively 1^0 Pd covering with almost no filling layer of 2^0 Pd deposits. The oxide particles need to be better controlled during the seeding and plating steps. If certain conditions are present, a palladium layer can be laid down without the need for activation and seeding.

Experiment series 2 showed that plating angle affects the depositional morphology as a function of fluid flows with 60^0 being optimum for the morphology desired. Fluid stir speed affects depositional morphology as a function of mass transfer, and surface availability of the reduced palladium catalyzing the unreduced $Pd^{2+/}$hydrazine/ hydroxide couples. Using our experimental geometry a lower stir speed of 150 rpm allowed a more controlled depositional morphology, contrary to the established procedure of 400 rpm which was optimized for best plating kinetics[4]. Silica beads produced a uniform substrate and worked well for Pd nucleation, branching, and particle to particle palladium fill characteristics. The type of Pd salt had an effect on thickness and depositional morphology. Silica beads demonstrated a need to be sintered to maintain cohesion during the plating process.

Experiment series 3 applied the knowledge gained in the previous experiments to the CAMP substrate. Utilizing sintering to lock in silica particles was successful. The silica particles acted as good nucleation, branching, and secondary Pd to Pd fill sites. Using preliminary pre-and post-flow data, it was observed that the electroless Pd of Pd/Cu plating left pinholes in the membrane. The Pd or Pd/Cu layers need to be annealed to create the alloy. The process of annealing left pinholes in the Pd/Cu membrane. The annealing step is critical to the re deposition of Pd over the Cu layer. Annealing allowed iron migration into the metal crystal lattice in some of the experiments and not in others. In some of the experiments the presence of the iron pre anneal was covered up post-anneal. This is evidence that the annealing of the alloy allowed metal flow over previously exposed PSS substrate.

4.2 Project secondary goals

The secondary goal for this project was to study the effect of using the silica sol-gel method to coat the silica-bead-treated, micro-fabricated, stainless steel substrates; to be explored were the effect it has on palladium membrane deposition and, ultimately, the membrane service lifetime.

The sub goals of this area of investigation are:

- To investigate how well different silica sol-gel mixtures mitigate chromium and iron migration from the stainless steel substrate into the palladium membrane.
- To investigate the effect of oxidation on different treated stainless steel substrates.
- To investigate the effect of substrate oxidation on the mechanical and chemical stability of the silica coatings.
- To examine the effect of the silica sol-gel on the efficiency of the electroless palladium alloy membrane deposition.
- To investigate the efficiency of the palladium alloy membrane to selectively filter hydrogen
- To study the effect that the sol-gel coating method has on the service lifetime.

4.2.1 Experiment 4-1 and Experiment 4-2

Due to faulty lab tech stoichiometry calculations, experiments 4-1 and experiment 4-2 were discarded. Preliminary flow data suggest flow constriction, but the results are suspect. For experimental SEM and EDX data see Appendix A section 4-1 through 4-2.

Table 4.2.1 N_2 flow at 60 PSI for experiment 4-1 discs 1-6 and 4-2 discs 1-4					
Sample ID	Flow Rate (SLPM)	Pressure (PSI)	Sample ID	Flow Rate (SLPM)	Pressure (PSI)
4-1-1	11.14	60	4-2-1	16.5	60
4-1-2	6.8	60	4-2-2	13.97	60
4-1-3	8.72	60	4-2-3	3.67	60
4-1-4	4.48	60	4-2-4	6.88	60
4-1-5	6.21	60			
4-1-6	5.6	60			

4.2.2 Experiment 5

A new batch of discs was provided by the CAMP team. Differences in appearances were immediately seen. They had an uneven layer of what appeared to be a reddish/brown coating of iron oxide. This might be a byproduct of mass sintering the 420 stainless steel discs in a large lot. The new disks stuck together magnetically and attracted the magnetic stir bar in solution.

4.2.2.1 Experiment 5-1

Experiment 5-1 uses a modified sol-gel coating previously used on 316 stainless steel[28]. Pure TEOS was used as described in experimental section 3.8, no nitric acid wash was used to remove surface iron deposits. Note that the high surface area and porosity seemed to hold a lot of residual acid. 24 hours after oxidation and multiple rinses in DI water, initial test disks prepped prior to the matrix 5-1 showed continued degradation of the stainless steel and chromium.

16 CAMP disks were prepped and sol-gel treated as per experimental matrix 5-1. Some interesting trends were noted. For supplemental experimental SEM and EDX data see the appendix section for experiments 5-1 discs 1-16.

In experiment 5-1 disks 1-4 suggest that the oxidation of the sintered and sol-gel dipped discs had no apparent effect and was not needed (see figures 4.2.2.1.(1-8) and appendix for supplemental SEM/EDX data). Figures 4.2.2.1.1(a, b) and Figures 4.2.2.1.2(a, b) show evidence of a sol-gel coating over the stainless steel and are supported by SEM(a) and EDX(b) data of disc 5-1 and 5-2. Figure 4.2.2.1.3(a,

b) shows intermittent palladium deposition and is supported by the SEM (a) and the EDX(b) data of disc 5-3. Figure 4.2.2.1.4(a, b) suggests comprehensive copper coverage of the palladium deposition and sol-gel coating.

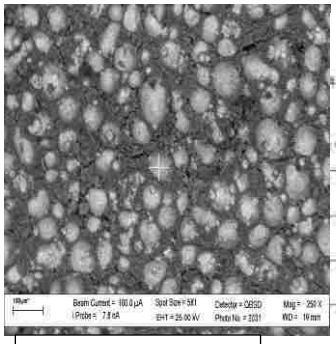

a. SEM Disc 5-1-1

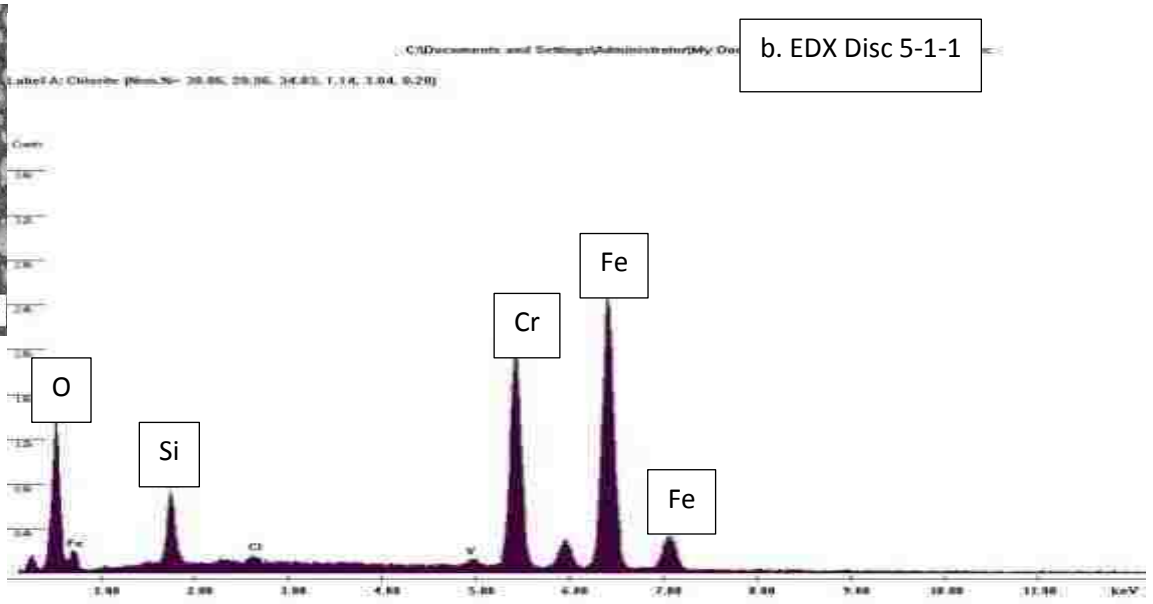

Figure 4.2.2.1.1: SEM and EDX of disc 5-1-1

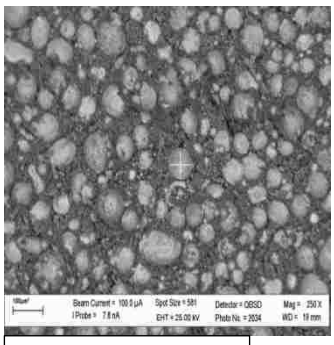

a. SEM Disc 5-1-2

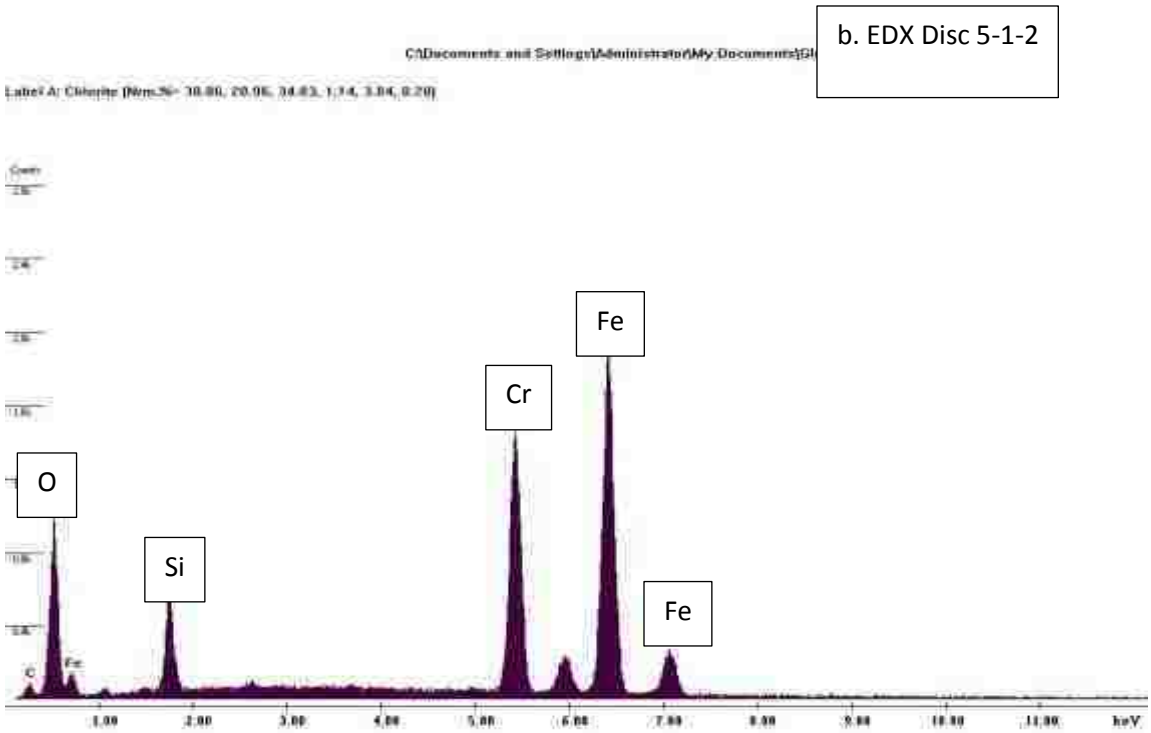

Figure 4.2.2.1.2: SEM and EDX of disc 5-1-2

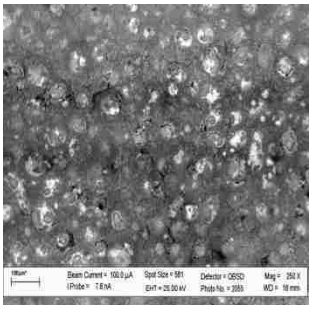

a. SEM Disc 5-1-3

b. SEM Disc 5-1-3

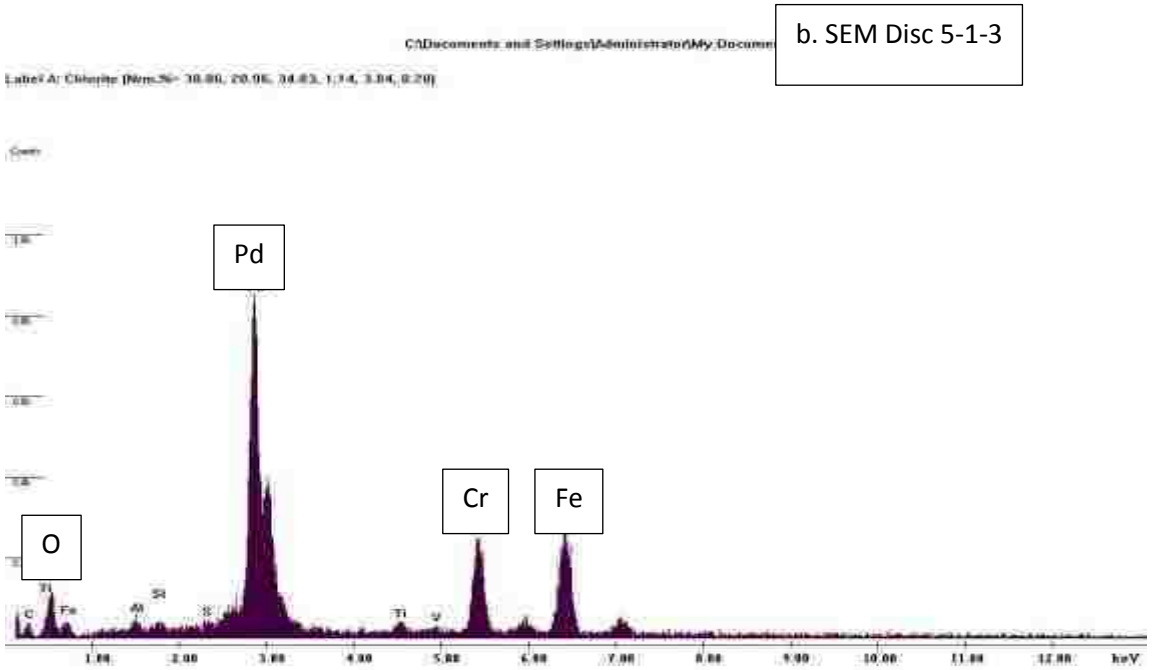

Figure 4.2.2.1.3: SEM and EDX of disc 5-1-3

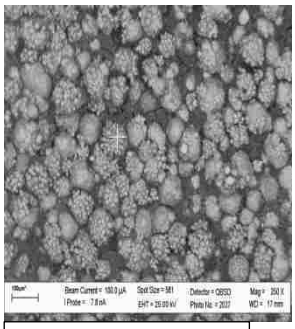

a. SEM Disc 5-1-4

b. EDX Disc 5-1-4

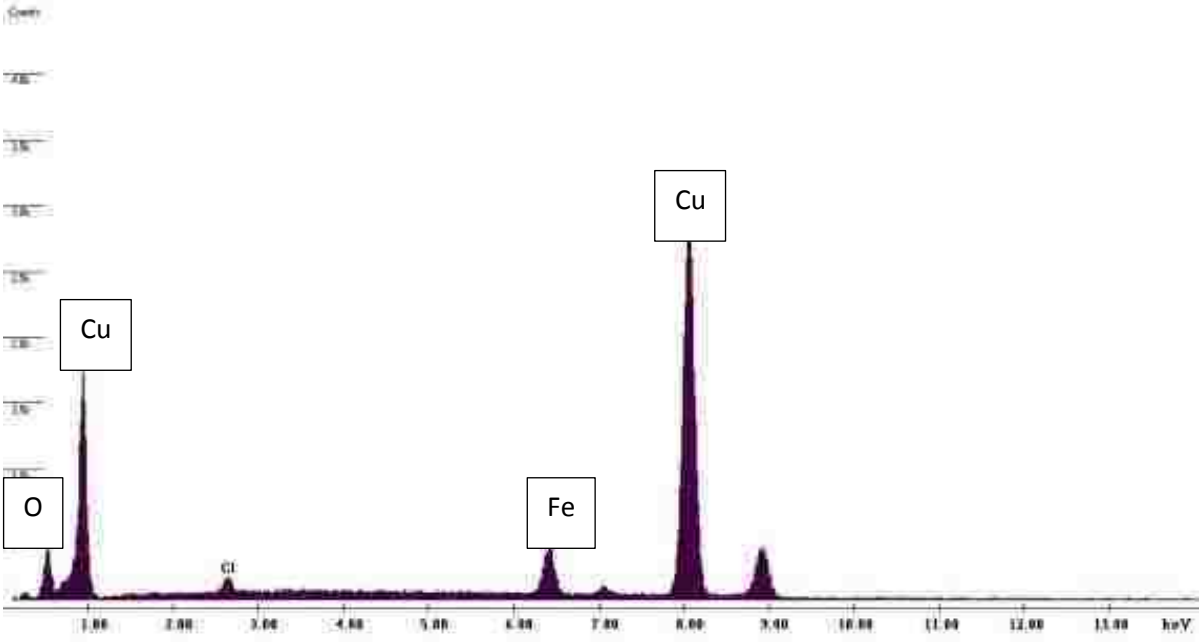

Figure 4.2.2.1.4: SEM and EDX of disc 5-1-4

Figure 4.2.2.1.5(a, b) demonstrates that the viscosity and surface tension of the silica sol-gel coating step was not enough to create a bridging coating. EDX (b) data suggest a thin coating of silica over the CAMP substrate. No fill was observed. Subsequent palladium sensitizing and plating showed no signs of working (see figure 4.2.2.1.7(a, b0)).

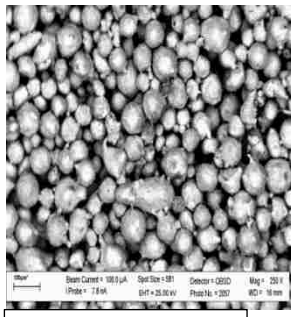

a. SEM disc 5-1-5

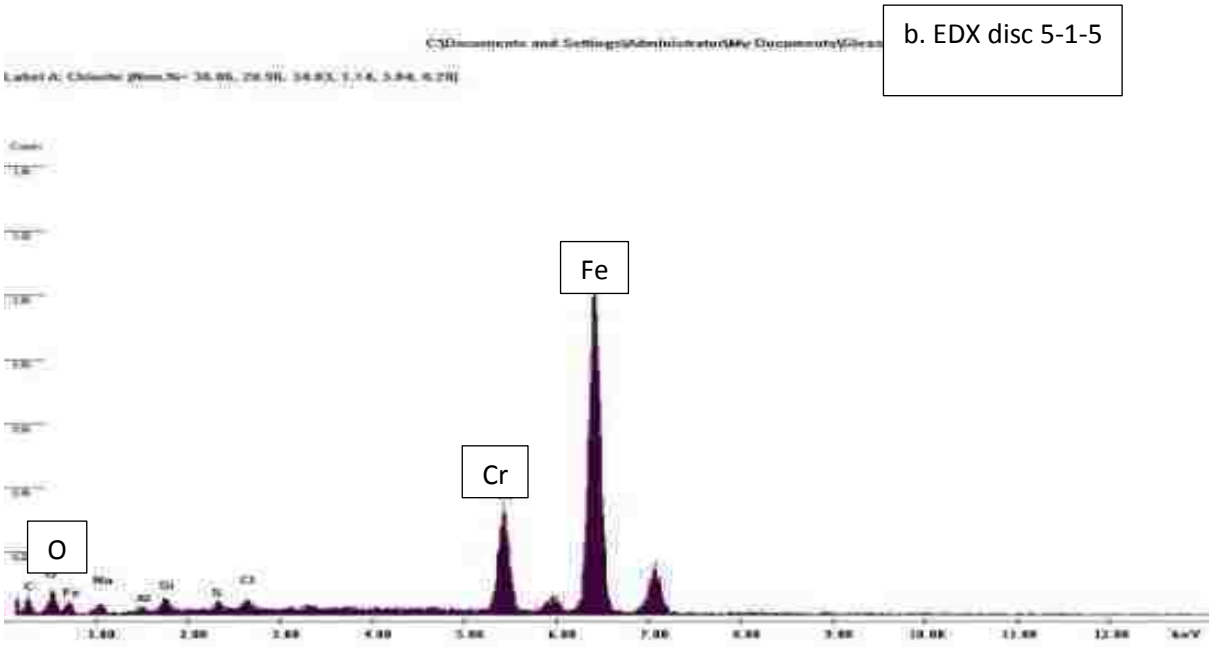

Figure 4.2.2.1.5: SEM and EDX of disc 5-1-5

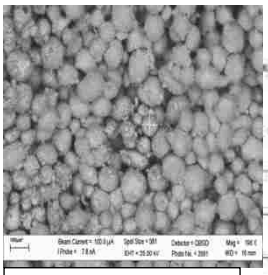

a.SEM disc 5-1-6

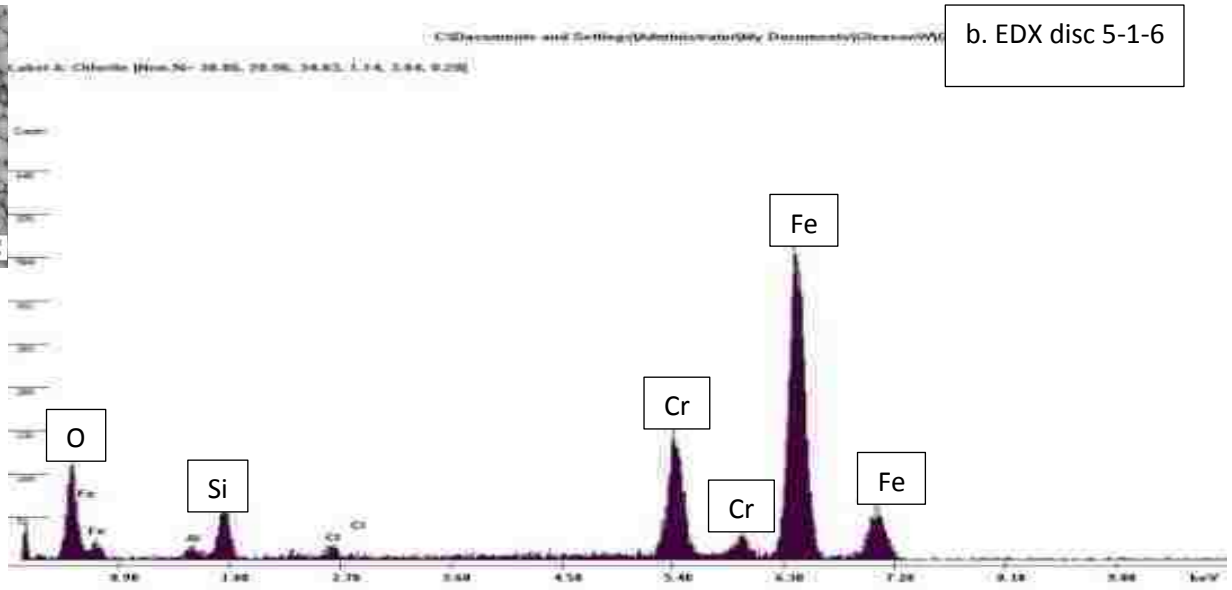

Figure 4.2.2.1.6: SEM and EDX of disc 5-1-6

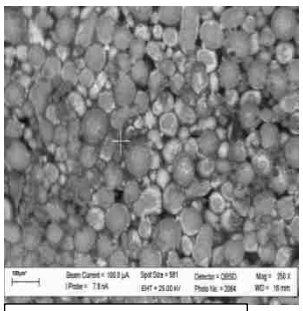

a. SEM disc 5-1-7

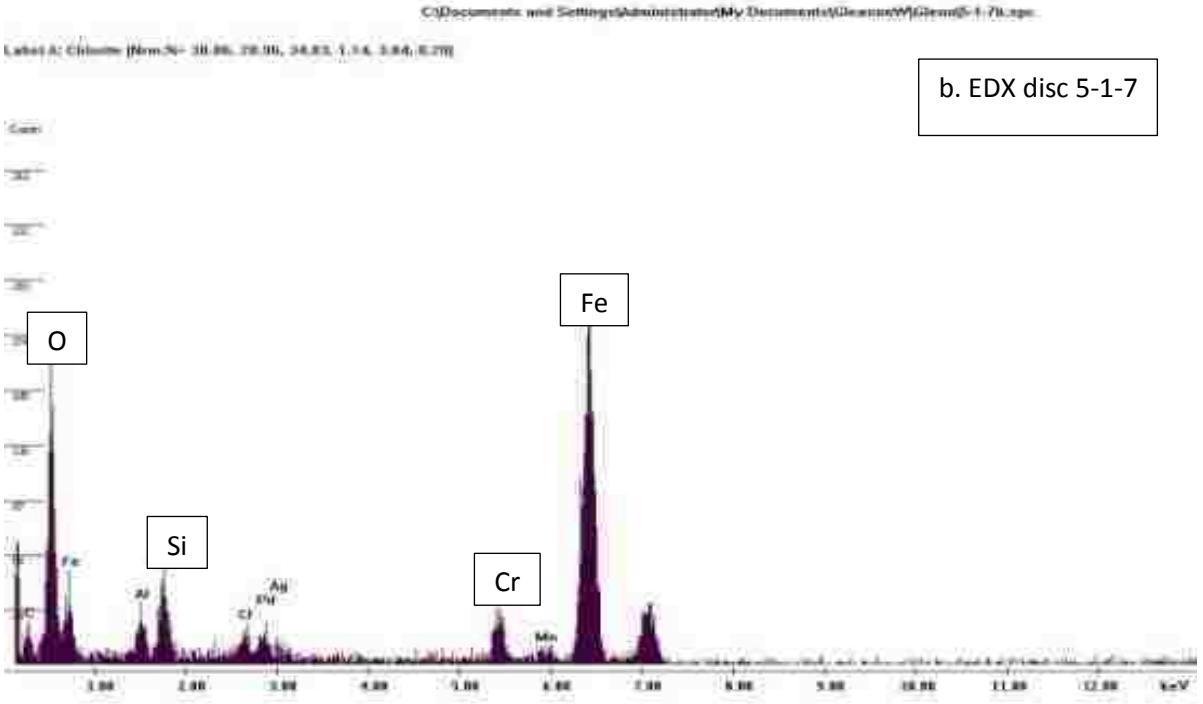

Figure 4.2.2.1.7: SEM and EDX of disc 5-1-7

Figure 4.2.2.1.8(a, b) showed some interesting dendritic copper morphology of disc 5-1-8. Upon later examination of the lab notebook and the copper plating recipe, it became apparent that disc 5-1-8 was also an anomaly because of a lab tech stoichiometry calculation error.

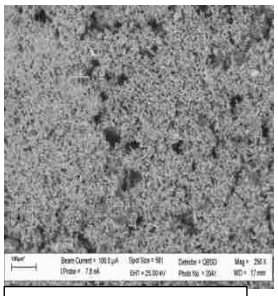

a. SEM disc 5-1-8

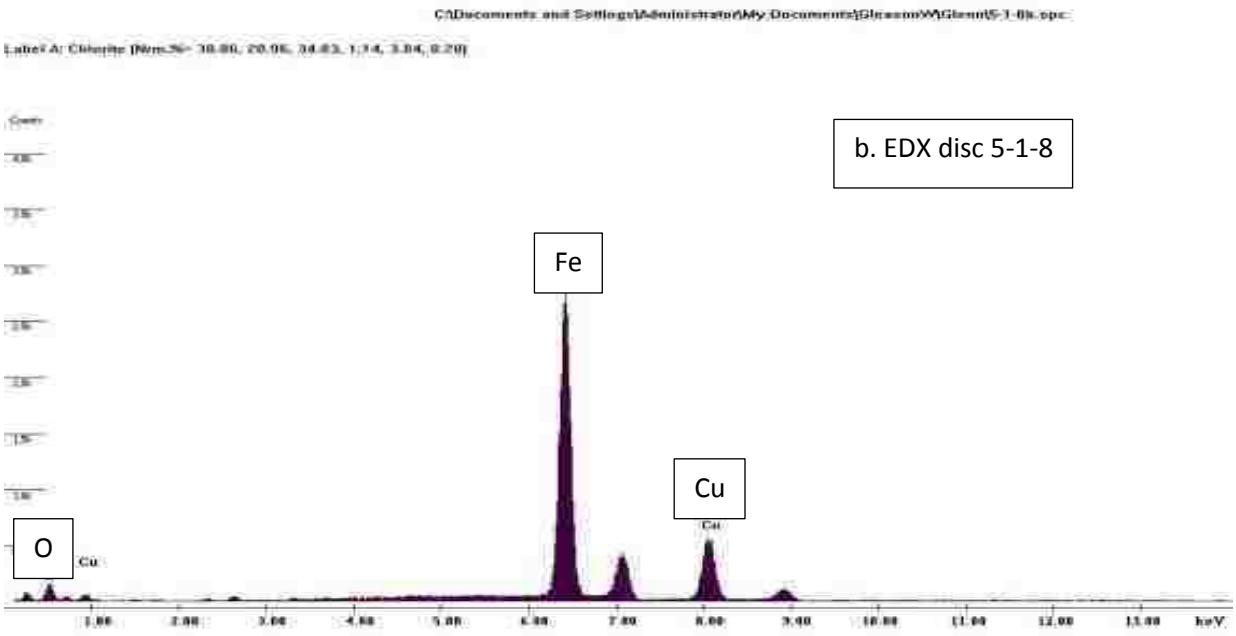

Figure 4.2.2.1.8: SEM and EDX of disc 5-1-8

Experiment 5-1 disc series 9-16 showed the same earlier observed trends: the oxidation before silica bead and sol-gel application seemed to have no effect, the palladium seeding showed no results, and the copper plating seemed to work well (see supplementary information experiments 9-16),with the exception of a small palladium peak in the SEM(a) and EDX(b) of disc 16 (see figure 4.2.2.1.9(a, b)).

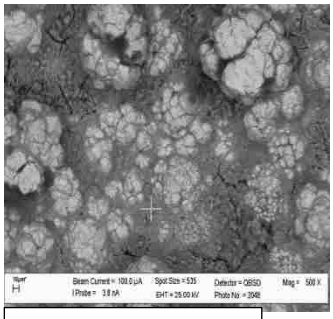

a. SEM disc 5-1-16

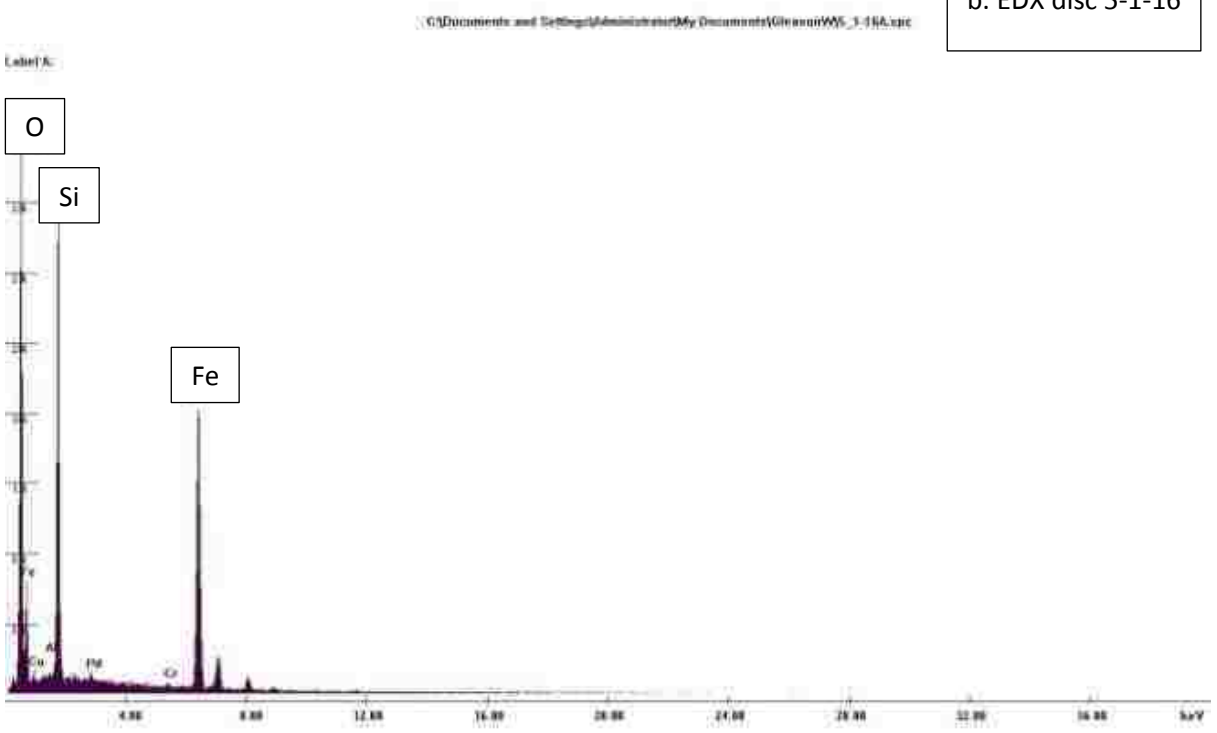

b. EDX disc 5-1-16

Figure 4.2.2.1.9: SEM and EDX of disc 5-1-16

In figure 4.2.2.1.9 (a, b) the SEM(a) shows extensive SiO coverage. This supports the experimental N_2 flow data that show differences in flow rates due to possible extensive silica sol-gel coverage. Experiment 5-1 results suggest that another method of seeding needs to be explored. Without good substrate palladium seeding, further palladium deposition is severely restricted. The copper deposition seems to work well, even without a reducing agent.

Table 4.2.2.1 N_2 flow at 60 PSI for experiment 5-1 discs 1-16			
Sample ID	Flow Rate (SLPM)	Pressure (PSI)	Comments
5-1-1	5.91	60	
5-1-2	8.64	60	
5-1-3	N/A	N/A	Broken
5-1-4	1.58	60	
5-1-5	N/A	N/A	Broken
5-1-6	N/A	N/A	Broken
5-1-7	16.73	60	
5-1-8	16.72	60	
5-1-9	13.96	60	Broke at 60 PSI, Possible O-ring size issue
5-1-10	16.72	60	Broke at 60 PSI, Possible O-ring size issue
5-1-11	15.17	60	Broke at 60 PSI, Possible O-ring size issue
5-1-12	12.7	60	Broke at 60 PSI, Possible O-ring size issue
5-1-13	7.45	60	
5-1-14	12.77	60	
5-1-15	8.23	60	
5-1-16	5.66	60	

4.2.2.2 Experiment 5-2 and 5-3

Upon examination of the lab notebook and questioning of the lab tech, the results of experiments 5-2 and 5-3 were subject to faulty stoichiometry calculations.

4.2.2.3 Experiment 5-4

Taking into consideration trends noticed in experiment 5-1, we chose two new seeding techniques[25,26](see experimental conditions , experimental matrix 5-4). Using the earlier work done, the plating angle chosen was 60 deg, the solution temp 60^0C, the stir rate to be 150 rpm in order to better control the deposition rate. The silica sol-gel formula was still pure TEOS, and the coating and disc prep procedures were as described in section 4.2.2.1 experiment 5-1.

Disc four shows an excellent covering by the silica sol-gel and a palladium coating (see figure 4.2.2.3.1 (a, b)).

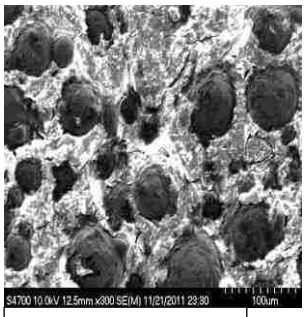

a. SEM disc 5-4-4

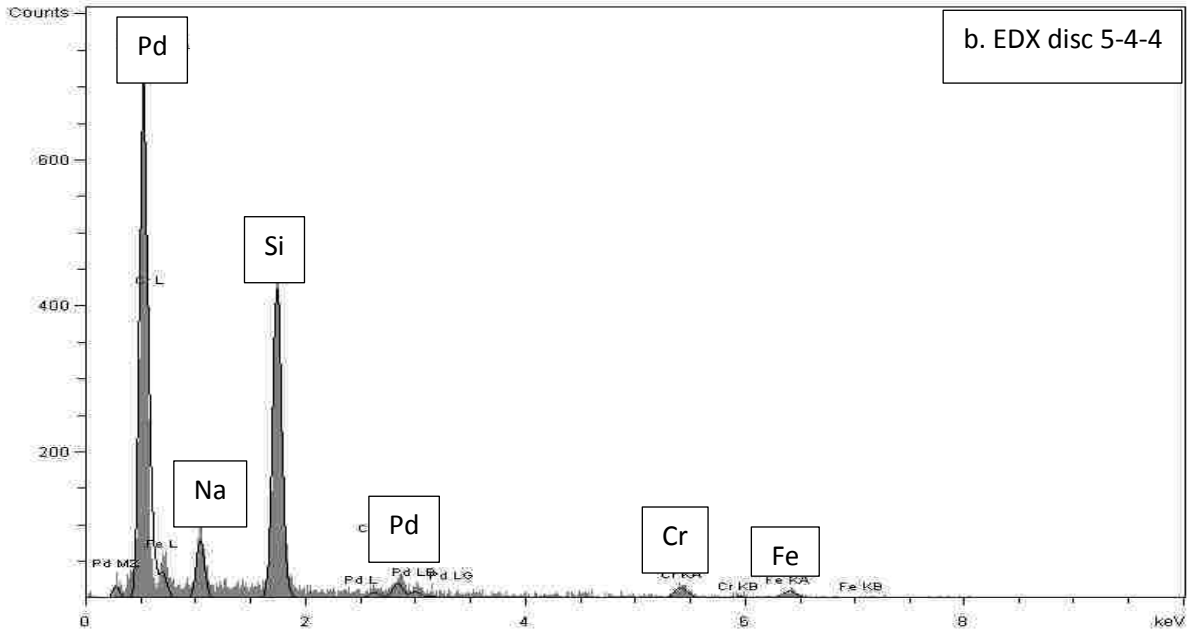

Figure 4.2.2.3.1: SEM and EDX of disc 5-4-4

The Figure 4.2.2.3.2 (a, b) SEM(a) shows a good silica sol-gel layer that is fractured and subsequently palladium plated on the sol-gel coat and PSS substrate. The EDX(b) gives evidence of the Pd coating. This fracturing was thought to be either the result of the hydrogen pressure in the reactor upon the substrate or the effect of surface tension during the curing process. The seeding and plating using the palladium acetate/chloroform mixture seemed to be successful. Figure 4.2.2.3.3 (a, b) shows the same trends as disc 7 with a larger fracture pattern that might be due to an impact by a stir bar during plating.

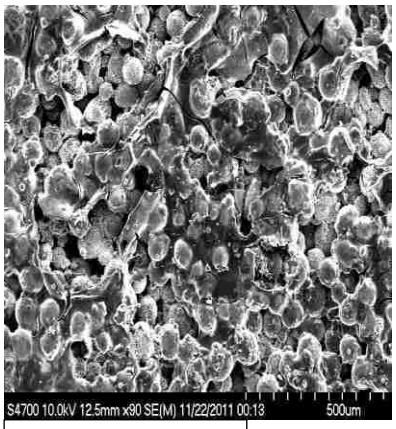

a. SEM disc 5-4-7

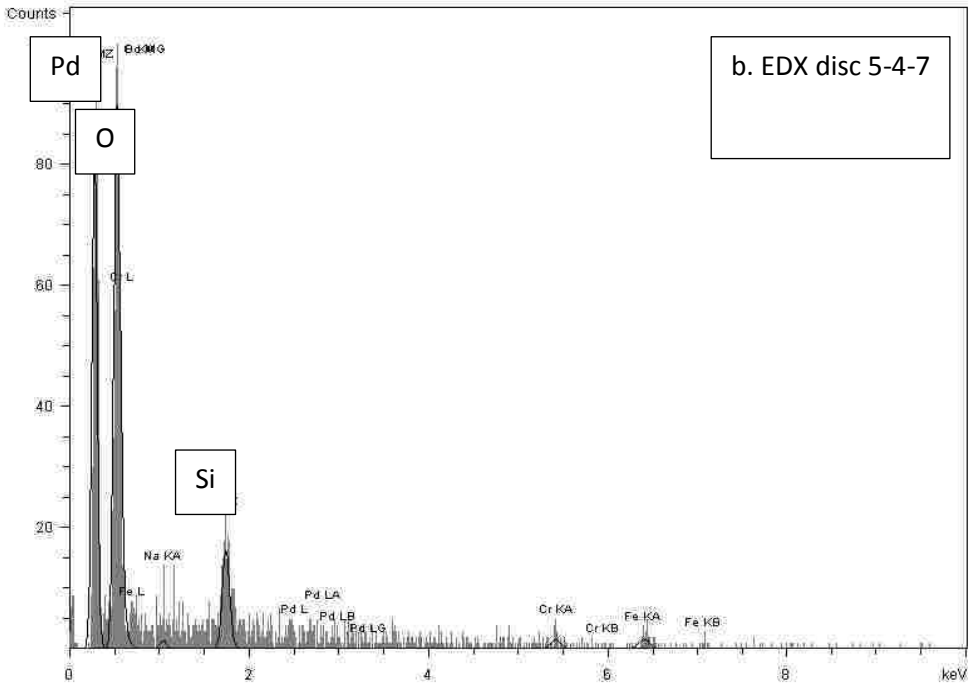

Figure 4.2.2.3.2: SEM and EDX of disc 5-4-7

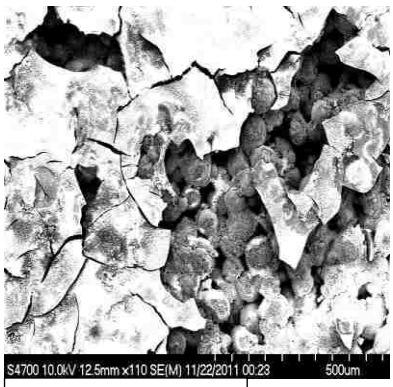

a. SEM disc 5-4-8

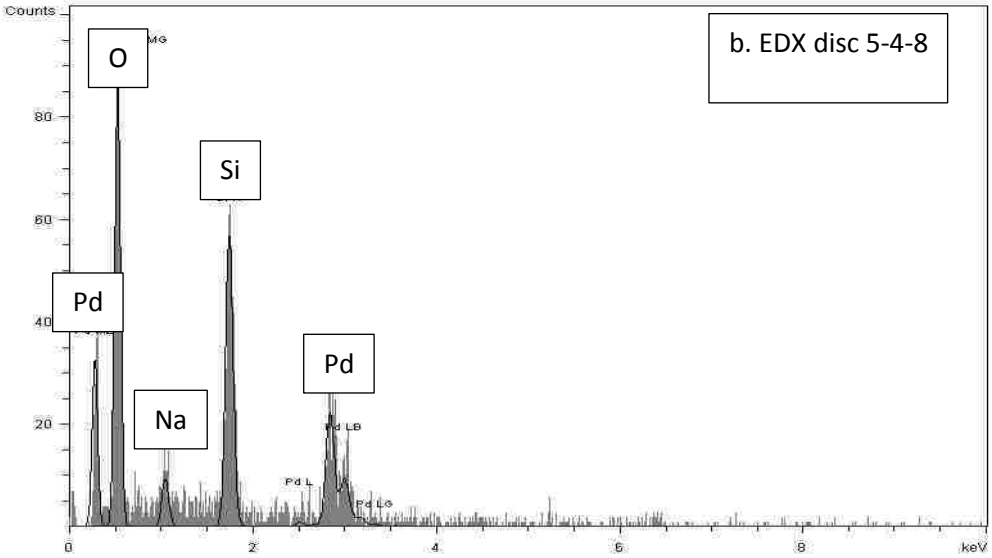

Figure 4.2.2.3.3: SEM and EDX of disc 5-4-8

Experiment 5-4 results suggest good seeding and plating using palladium acetate/chloroform and hydrogen peroxide (H_2O_2) to oxidize the organic acetate groups and reduce the seeded palladium with ammonium hydroxide and hydrazine. Experiment 5-4 also suggests good coverage by the sol-gel. For more information on experiment 5-4 see the appendix for supplemental experiment 5-4 SEM/EDX and experimental data.

4.2.2.4 Experiment 5-5

Figure 4.2.2.4.1 SEM(a) data for disc 5-5-1 and EDX(b) data suggest the seeding and plating worked well. The annealing of the alloy allowed the flow of palladium across the silica surface. The membrane needs more metal plated to allow a better and more comprehensive coating once annealed. The data also suggest the new anneal profile works. Figure 4.2.2.4.2 (a, b) SEM and EDX data for CAMP disc 5-5-2 suggest good Pd coverage and flow over membrane post anneal. Discs 5-5-3 through 5-5-8 follow the same trend (see Appendix A supplemental experiment 5-5 SEM/EDX data).

b. EDX disc 5-5-2 post anneal

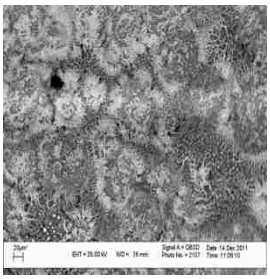

a. SEM disc 5-5-1 post anneal

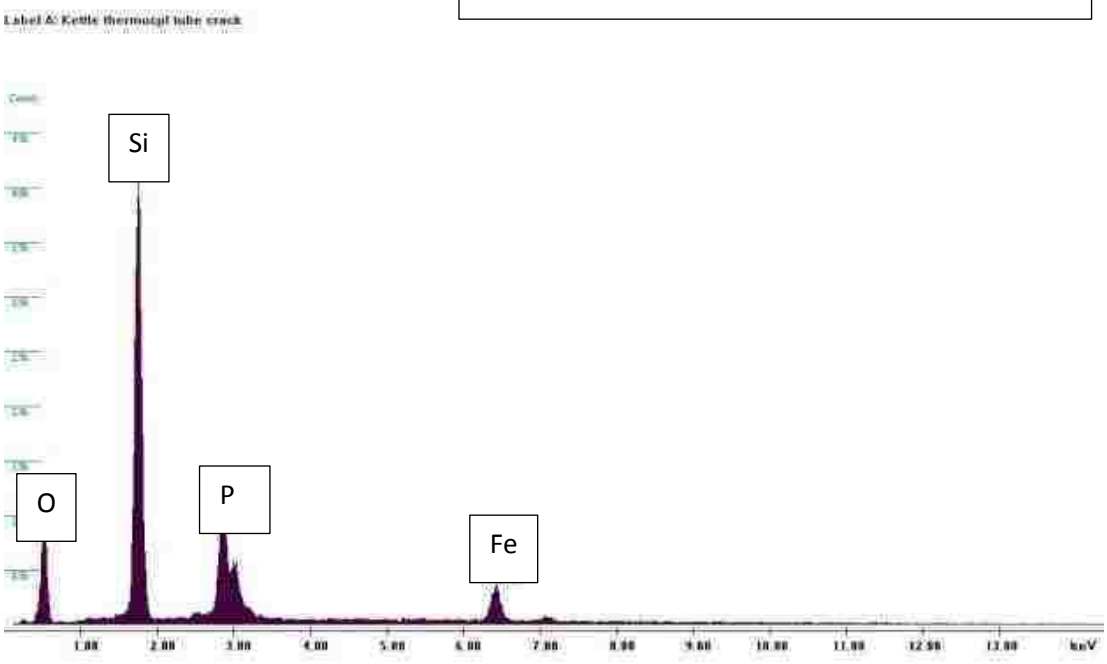

Figure 4.2.2.4.1: SEM and EDX of disc 5-5-1

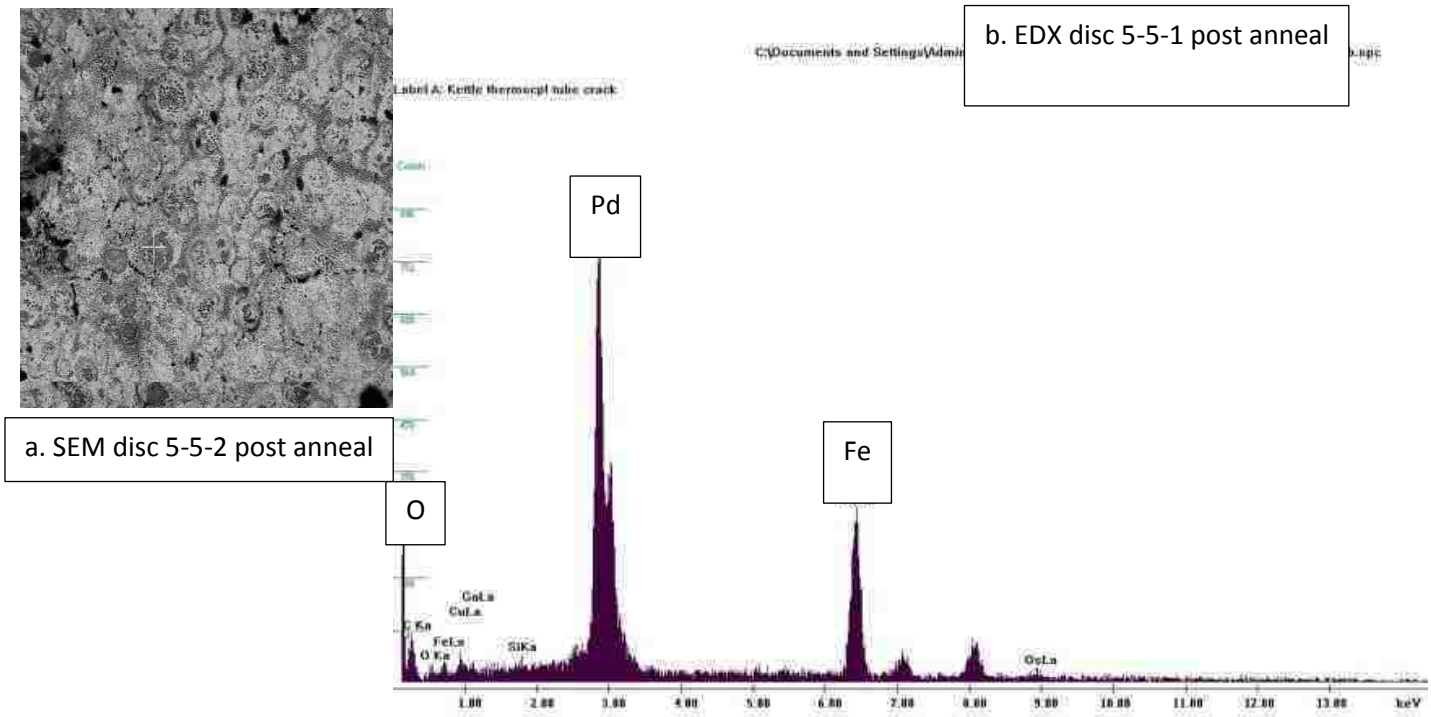

Figure 4.2.2.4.2: SEM and EDX of disc 5-5-2

The N_2 flow data suggest some trends. The sol-gel coated controls all showed more flow constriction than the plated experiments. This suggests that there is an initial sol-gel membrane coverage that is significantly altered during the plating and annealing steps. Experiment 5-5-2 (see figure 4.2.2.4.2(a, b) also showed constriction of flow. The SEM(a) of experiment 5-5-2 shows considerable metal coverage, which is corroborated by the EDX(b). The evidence suggests that there is incomplete coverage of the surface and that more plating steps need to be added to complete the coverage.

Table 4.2.2.4 N_2 flow at 60 PSI for experiment 5-5 discs 1-8

Sample ID	Flow Rate (SLPM)	Pressure (PSI)	For CAMP discs, the substrate will pass roughly 17 SLPM
5-5-1	10.35	60	1 coat silica sol-gel 1 Pd layer
5-5-2	5	60	1 coat silica sol-gel 1Pd/Cu/Pd layer
5-5-3	10.46	60	1 coat silica sol-gel Pd/Cu Pd/Cu Pd layers
5-5-4	16.73	60	1 coat silica sol-gel Pd/Cu Pd/Cu Pd/Cu Pd layers
5-5-5	16.8	60	3 coats silica sol-gel 1 Pd layer
5-5-6	16.77	60	3 coats silica sol-gel 1Pd/Cu/Pd layer
5-5-7	12.02	60	3 coats silica sol-gel Pd/Cu Pd/Cu Pd layers
5-5-8	9.96	60	3 coats silica sol-gel Pd/Cu Pd/Cu Pd/Cu Pd layers
5-5 (XC)	3.08	60	1 coat silica sol-gel
	5.57	60	1 coat silica sol-gel
5-5 (3XC)	1.51	60	3 coats silica sol-gel
	4.28	60	3 coats silica sol-gel

4.2.2.5 Experiment 5-6

Experiment 5-6 was designed to apply the knowledge gained in experiment 3 that showed the copper coated palladium needed to be annealed and to re-expose the palladium to continue the cycle. Experiment 5-6 was basically experiment 5-5 expanded (see matrix 5-6) to study the effects of :

- multiple Pd/Cu plating cycles,
- the effectiveness of the new anneal profile,
- the repeatability of the surface prep,
- The effect of the anneal on the deposited palladium and copper layers.

Experiment 5-6 was also designed to give annealed and partially annealed discs to the CAMP Center to use in calorimetry experiments that would determine the conditions required to maximize the alloy formation from single or multiple plating steps.

Experiment 5-6, disc series one (see figure 4.2.2.5.1) shows that there is a good base for particle nucleation. The silica sol-gel coating seemed to anchor the silica particles quite well, without over coating.

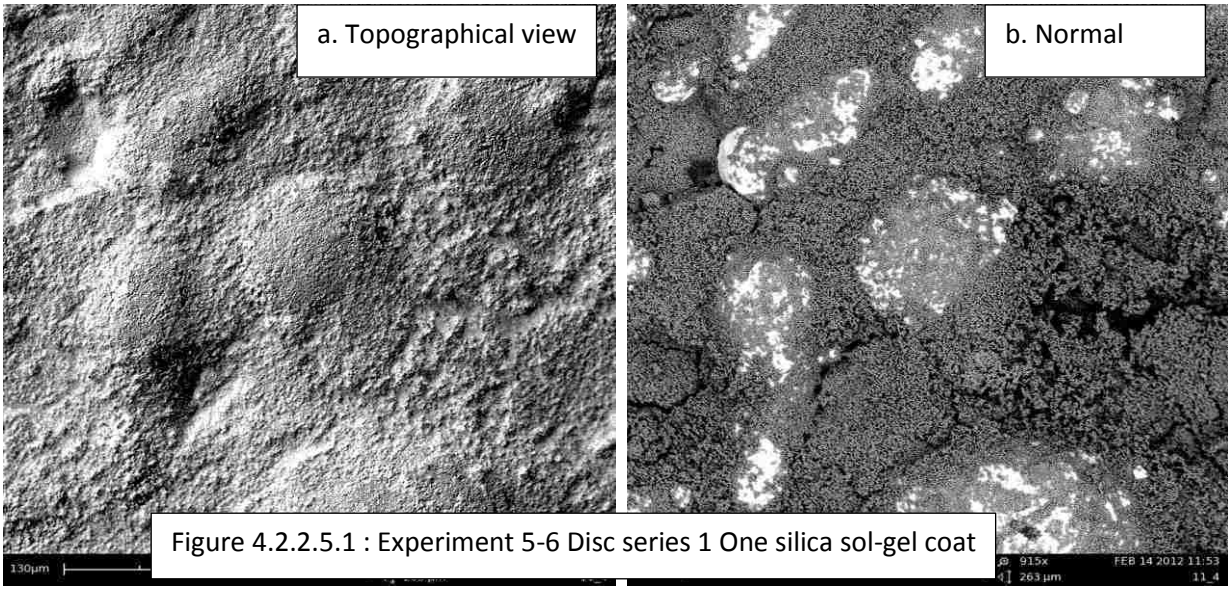

Figure 4.2.2.5.1 : Experiment 5-6 Disc series 1 One silica sol-gel coat

Experiment 5-6 disc series two (see figure 4.2.2.5.2) shows a good base for particle nucleation. It seems as though some of the silica beads either popped out from thermal expansion or were dissolved in the multiple sol-gel applications. It appears to be an effective coating method to introduce a thicker diffusion barrier between the PSS and the palladium membrane.

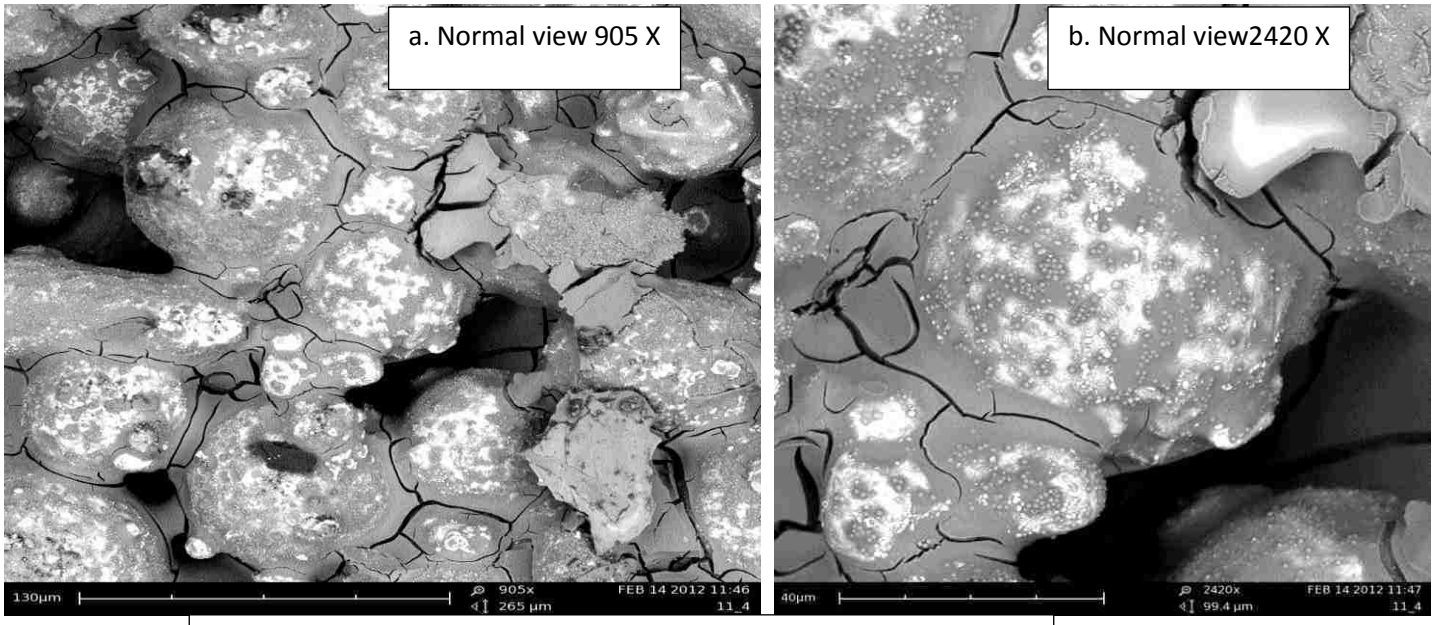

Figure 4.2.2.5.2: Experiment 5-6 Disc series 2 three silica sol-gel coats

It was also observed that there was good nucleation of the metals on the smaller gap sizes initially, without the nodular palladium formations seen in earlier experiments. As each layer is annealed there is an exposure of the Pd^0 catalytic site that allows the re-deposition of the palladium and then the copper coating. As each Pd/Cu layer is deposited and annealed, the re-exposure of Pd^0 allows the reduction of the aqueous Pd^{2+} to happen at select sites. These exposed catalytic sites then become nucleation sites for more Pd^{2+}reduction, forming Pd nodules.

When examining the cross section of a disc from the 5-6-6 series (see Figure 4.2.2.5.3 a, b) one can see the fill of the first two layers of the micro fabricated CAMP disc using the 0.1 µm silica beads. One can also see the anchoring effect of the sol gel coating. It is also apparent that the annealed Pd/Cu alloy is limited to the surface layer of sol-gel treated silica beads, with minimal plating through the membrane. There is minimal Pd/Cu under the sol-gel-treated surface layer. This data supports the earlier concept of creating a surface layer of silica particles and leaving increased flow channels for the filtered H_2 to flow through.(see Figure 1.3.4). The EDX b in Figure4.2.2.5.3 supports decreased iron and chromium diffusion into the annealed alloy membrane.

When comparing the annealed versus the non-annealed palladium copper coated discs (see figure 4.2.2.5.4 a-f), one can see that this trend is supported by SEM (a-f) evidence. Upon annealing of the large Pd nodules, there is metal flow across the silica sol-gel layer (see SEM f).

Examining Table 4.2.2.5 showing the N_2 flow at 60 PSI for experiment 5-6 disc series 1-8 does not reveal any solid trends. This is due to insufficient alloy covering the surface, creating an incomplete membrane.

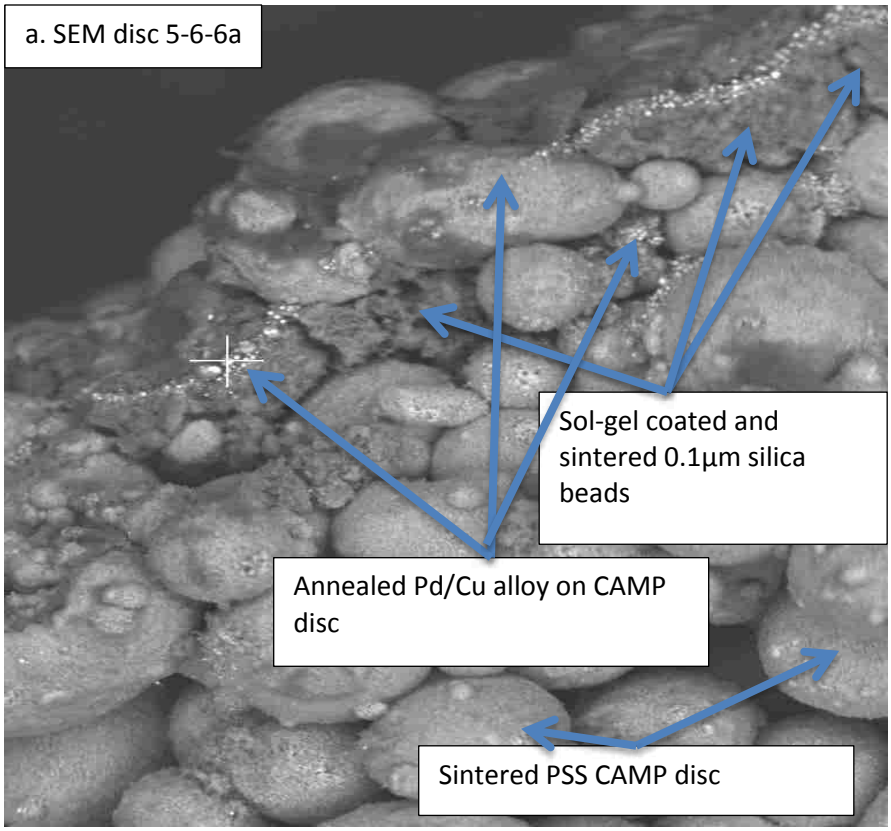

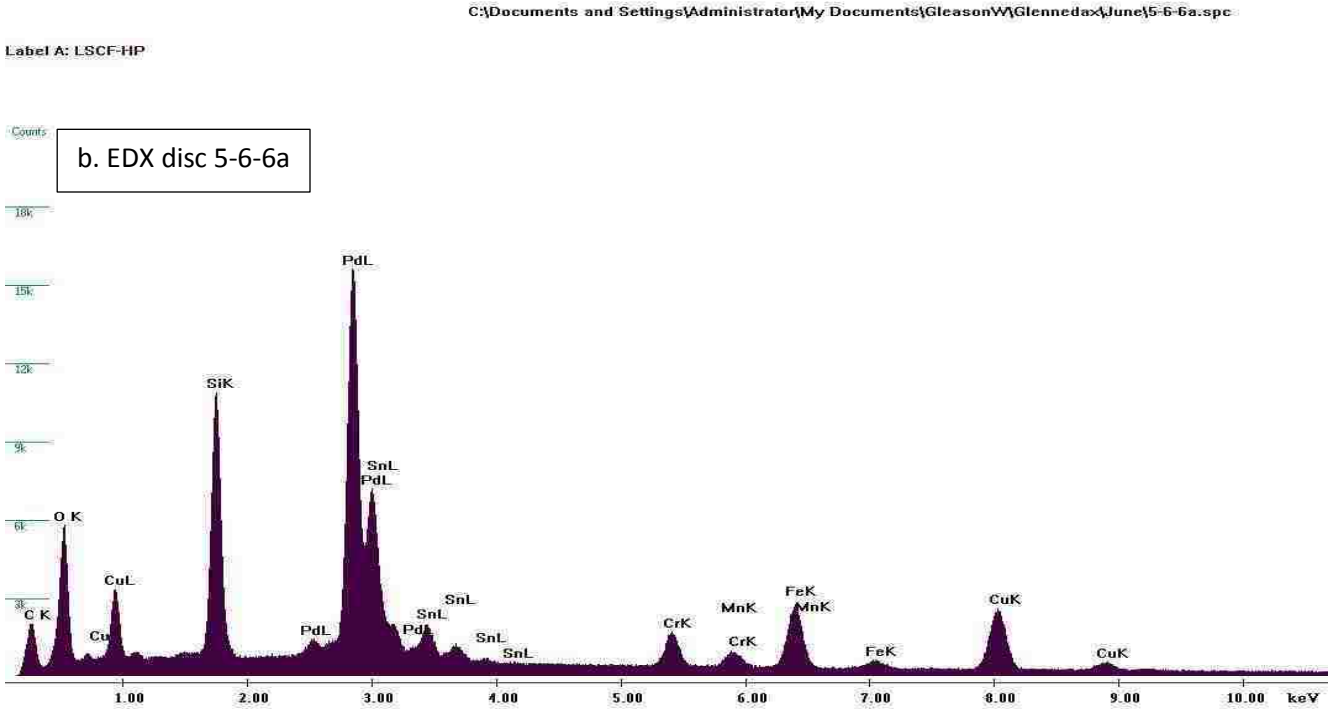

Figure 4.2.2.5.3 Side profile SEM and EDX of Pd/Cu plated silica sol-gel treated CAMP disc, crosshairs indicates location of EDX for this sample, and multiple spots were examined

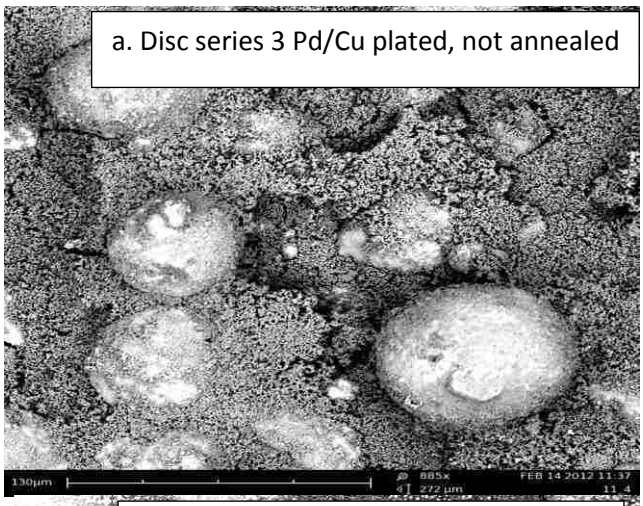

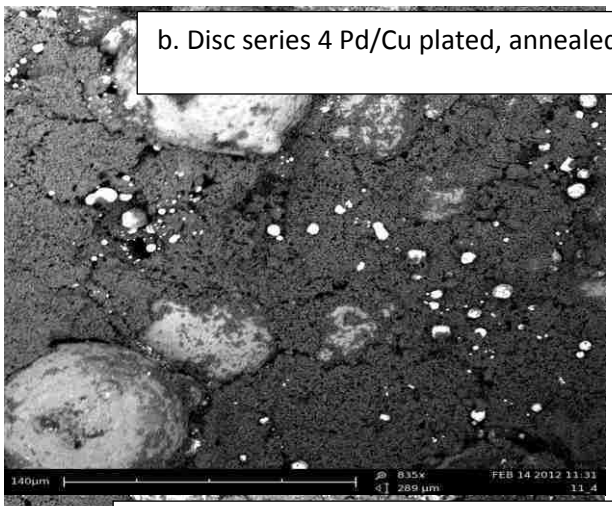

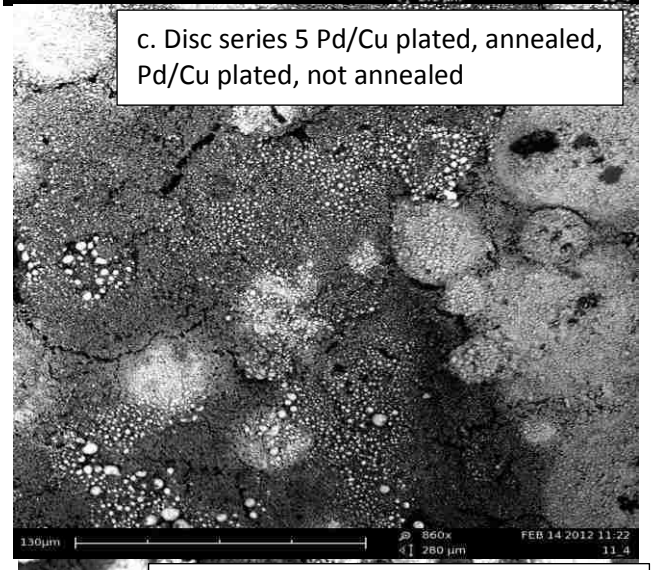

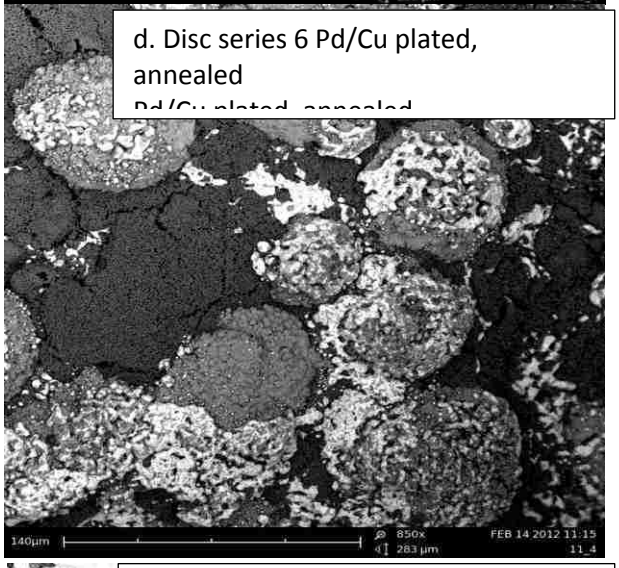

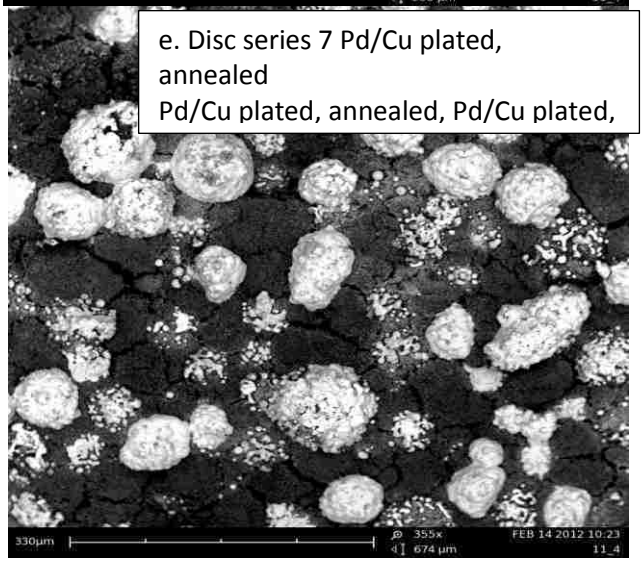

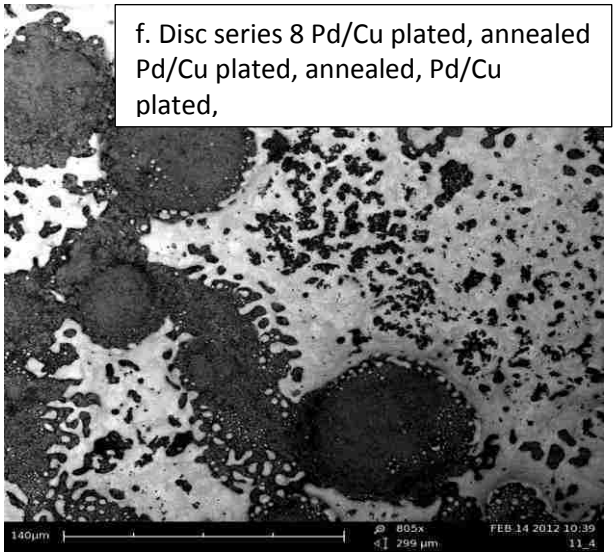

Figure 4.2.2.5.4: Comparison of annealing, Pd/Cu re-deposition, and alloy formation and flow

Table 4.2.2.5 N_2 flow at 60 PSI experiment 5-6 disc series 1-8			
Sample ID	Pressure (PSI)	Flow Rate (SLPM)	Comments
5-6-1	60	13.38	For CAMP discs, the substrate will pass roughly 17 SLPM
	60	10.81	1 Sol-gel coat
	60	12.08	1 Sol-gel coat
	60	15.19	1 Sol-gel coat
	60	5.85	1 Sol-gel coat
5-6-2	60	16.78	3 Sol-gel coats
	60	10.83	3 Sol-gel coats
	60	5.95	3 Sol-gel coats
	60	7.37	3 Sol-gel coats
	60	12.75	3 Sol-gel coats
5-6-3	N/A	N/A	Broken
	60	9.31	1 Sol-gel coat 1 Pd/Cu plating cycle, no anneal
	60	11.53	1 Sol-gel coat 1 Pd/Cu plating cycle, no anneal
	60	12.34	1 Sol-gel coat 1 Pd/Cu plating cycle, no anneal
	60	16.73	1 Sol-gel coat 1 Pd/Cu plating cycle, no anneal
5-6-4	60	16.78	1 Sol-gel coat 1 Pd/Cu plating cycle, anneal
	60	16.77	1 Sol-gel coat 1 Pd/Cu plating cycle, anneal
	60	16.8	1 Sol-gel coat 1 Pd/Cu plating cycle, anneal
	60	16.8	1 Sol-gel coat 1 Pd/Cu plating cycle, anneal
	60	10.22	1 Sol-gel coat 1 Pd/Cu plating cycle, anneal
	60	16.8	1 Sol-gel coat 1 Pd/Cu plating cycle, anneal
	60	16.8	1 Sol-gel coat 1 Pd/Cu plating cycle, anneal
5-6-5	60	16.8	1 Sol-gel coat 1 Pd/Cu plating anneal cycle,1 Pd/Cu plating cycle no anneal
5-6-6	60	16.78	1 Sol-gel coat 2 Pd/Cu plating anneal cycles
	60	16.8	1 Sol-gel coat 2 Pd/Cu plating anneal cycles
	60	16.8	1 Sol-gel coat 2 Pd/Cu plating anneal cycles
	60	16.78	1 Sol-gel coat 2 Pd/Cu plating anneal cycles
	60	16.8	1 Sol-gel coat 2 Pd/Cu plating anneal cycles
5-6-7	60	16.78	1 Sol-gel coat 2 Pd/Cu plating anneal cycles,1 Pd/Cu plating no anneal
5-6-8	60	16.78	1 Sol-gel coat 3 Pd/Cu plating anneal cycles
	60	9.16	1 Sol-gel coat 3 Pd/Cu plating anneal cycles
	60	16.8	1 Sol-gel coat 3 Pd/Cu plating anneal cycles
	60	16.78	1 Sol-gel coat 3 Pd/Cu plating anneal cycles
	60	16.8	1 Sol-gel coat 3 Pd/Cu plating anneal cycles

Chapter 5 Conclusions

To electroless plate Pd or Pd/Cu alloys onto different substrates, an in depth study was performed to determine the variables that could be manipulated to achieve consistent and reliable results. Experiments 1 and 2 identified the use of different sizes and types of oxide particles, stir speed, different palladium salts, and plating angles as variables of interest. Experiment 3 applied those variables to a new micro fabricated porous stainless steel (PSS) substrate produced at CAMP . Experiments 4 and 5 investigated silica sol-gel treating PSS CAMP discs, and manipulating variables of interest to achieve a Pd/Cu alloy membrane over the treated disc. Experiments 3, 4, and 5 established the use of silica and silica sol-gel treated particles as a pore modifier, Pd nucleation site, and barrier to diffusion of iron and chromium into the annealed metal membrane.

Experiment 1 demonstrated the relationship between cavity size and oxide packing on a known substrate produced the MOTT Corporation. When different combinations of oxide treatments were applied to that substrate and then Pd seeded once or multiple times, different palladium epitaxial morphology was observed. Experiment 1-15 showed Pd seeding is not needed to form a palladium membrane under certain conditions.

Experiment series 2 showed that fluid flow dynamics and mass transfer influence the epitaxial deposition of nodular and coral like formations (see figures 4.1.2.4 through 4.1.2.6). Experiment 2 used only the 0.2µm MOTT filter discs, allowing a comparison of the experimental results to the established procedures and published results[Error! Bookmark not defined.,Error! Bookmark not defined.,Error! Bookmark not defined.,Error! Bookmark not defined.]. Experiment 2 examined some of the preliminary findings in Experiment 1 in greater depth and detail. It demonstrated the need for sintering of the oxide coating and showed that 0.1 µm silica particles worked out well as nucleation sites for the Pd seeding and plating of the PSS substrate. The silica particles showed better palladium fill in and around the particles, creating a more comprehensive primary and secondary coverage. Varying the plating speed and plating angle resulted in different

depositional morphologies. The experiments that varied the plating angle showed depositional morphology as a function of fluid-flow dynamics with 60^0 being optimum for the primary Pd coverage of the substrate and secondary Pd-to-Pd particle fill. Slowing down the stir rate seemed to stimulate the palladium secondary fill and limit the primary substrate/palladium deposits, under these experimental conditions. A stir speed of 150 rpm allowed a more controlled depositional morphology, contrary to the previously reported procedure of 400 rpm which was optimized for best plating kinetics[21].

In experiment 2, examining alternative palladium plating solutions provided some insight into possible plating applications. On the alumina and silica treated MOTT discs, the $PdCl_2$ followed the observed trends of good primary formations with dendritic coral like formations and some secondary fill. Palladium acetate deposited a thin crust-like primary coating that was not anchored down well and allowed secondary fill. The palladium nitrate had limited solubility and was really unstable in solution. It deposited a thin crust that was not well anchored to the substrate. The zirconia treated discs plated much the same as a nontreated discs.

Experiment 3 showed that selectively varying the experimental conditions allowed Pd and Pd/Cu plating on a substrate that was initially thought to be incapable of forming a continuous surface (see figure 4.1.3.3.3).). Experiment 3 showed the plating of Pd and Cu onto CAMP and MOTT discs, permitting a comparison of electroless plating (Pd or Pd/Cu) onto a known substrate to an unknown substrate. Figure 4.1.3.3.4 shows the interlocking nature of Pd and Cu metal crystals on the spherical substrate. The metal crystals needed to be annealed in order to form a continuous surface membrane. XRD data shows the successful formation of a palladium copper alloy under anneal conditions for single and multiple Pd/Cu plating cycles (see figures 4.1.3.3.(5-8)).

Discs in experiment 3 showed limited iron, but no chromium, diffusion migration into the metal membrane from the PSS substrate (see figure 4.1.3.3.5 a, b). Figure 4.2.2.5.3 presents SEM data that

suggest the need to anneal after the Pd/Cu plating step in order to re-expose Pd to catalyze further Pd reduction.

Experiment 4 and plating portions of experiments 5-1 through 5-4 were subject to stoichiometry calculation errors and the results were judged unreliable.

Experiment 5 series 5 made scientific advances in silica sol-gel treating, electroless plating (Pd or Pd/Cu) onto the CAMP substrate, and annealing the alloy and observing metal flow over the sol-gel coated surface. Evidence of a sol-gel coating over the stainless steel is supported by SEM and EDX data (See Appendix A, Supplemental information SEM EDX data experiment series 5-1). Two new seeding techniques[25,26] were chosen. Using earlier work done, we chose the plating angle of 60 deg, the solution temp at 60^0C, and the stir rate at 150 rpm to control the deposition rate and morphology. Experiment 5-4 results suggest good seeding and plating using palladium acetate/chloroform and hydrogen peroxide (H_2O_2) to oxidize the organic acetate groups and reduce the seeded palladium with ammonium hydroxide and hydrazine. Experiment 5-4 also suggests good coverage by the sol-gel prior to plating.

Experiment 5-5 SEM data suggest the seeding and plating worked well before the anneal. The anneal allowed the flow of palladium and copper onto the silica surface. The preliminary data also suggest the new anneal profile works(1000^0C for 8 hours, then step down of 2 hours to 800^0C, hold for 16 hours, then step down of 2 hours to 600^0C ,hold for 44 hours under 97/3% N_2/H_2) .

Experiment 5-6 showed good nucleation of the Pd upon the silica spheres and Pd filling in the reduced pores sizes, without the initial large nodular palladium formations seen in earlier experiments. A cross section of a disc from the 5-6-6 series (see Figure 4.2.2.5.3 a, b) shows fill of the first two layers of the micro fabricated CAMP disc using sol-gel coated 0.1 μm silica beads and the anchoring effect of the sol-gel coating. Note that in the cross sectional view of there was excellent silica coverage of the first two layers with a Pd/Cu layer limited to the surface. This demonstrates the annealed Pd/Cu alloy is limited to the surface layer of sol-gel treated silica beads, with minimal plating through the membrane.

There is minimal Pd/Cu under the sol-gel-treated surface layer. Note the increased flow channels beneath the sol-gel coated silica beads filling the first two layers of the disc. This data supports the earlier concept of creating a surface layer of silica particles and leaving increased flow channels for the filtered H_2 to flow through.(see Figure 1.3.4). The EDX b in Figure4.2.2.5.3 supports decreased iron and chromium diffusion into the annealed alloy membrane. Experiment 5-6 shows the alloy flow across the less accessible part of the disc, the bridging particles and sol-gel coating, increasing the membrane coverage as the layers or amount of Pd/Cu alloy increases (demonstrated in figure 4.2.2.5.3 a-f). Note that annealing (see figure 4.2.2.5.3 f) has redistributed the palladium coating as well as forming the Pd/Cu alloy. By creating a bridge between silica particles, the sol-gel coating decreases the available surface area for deposition, increasing the efficiency of the plating operation. By bridging the silica particles, the distance the Pd and Pd/Cu have to move is reduced (both vertically and horizontally), enhancing the flow characteristics of the Pd metal or metal alloy under anneal conditions.

Experiments 3-3 and 5-6 demonstrate that a way has been found to inhibit, slow down or completely stop the migration of iron and chromium into the Pd/Cu or Pd membrane. Note the total lack of a chromium peaks in figures 5.1.2 (a, b) through 5.1.3(a, b). Note, too, the high intensity of the Fe peak in the Pd/Cu alloy on the MOTT disc in experiment 3-3-16 (see figure 5.1.2 b). It needs to be noted that the Pd exposed surface area of the stainless steel MOTT disc is greater than the CAMP disc (see figure1.3.1 a, b), especially after silica particle and silica sol-gel coating. Looking at the intensity and purity of the SEM peaks in figures 5.1.1 through 5.1.3, reveals a trend of better plating and coverage of the Pd/Cu alloy in the silica sol-gel coated discs. The iron migration peak (see figure 5.1.3, b) is the same amplitude as the noise level. It shows considerable improvement over the silica particle treated and plated MOTT disc (seen in figure5.1.1, b).

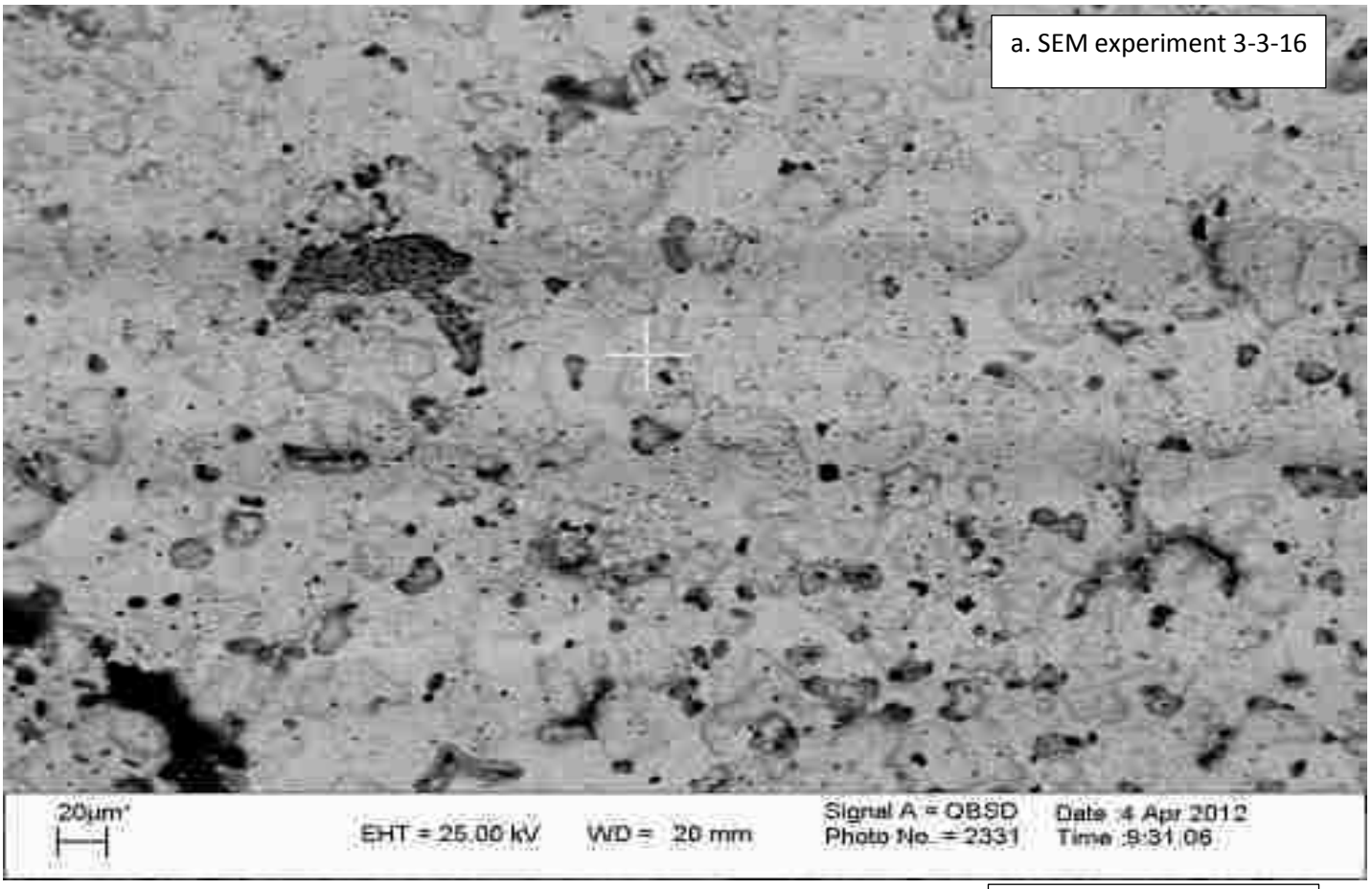

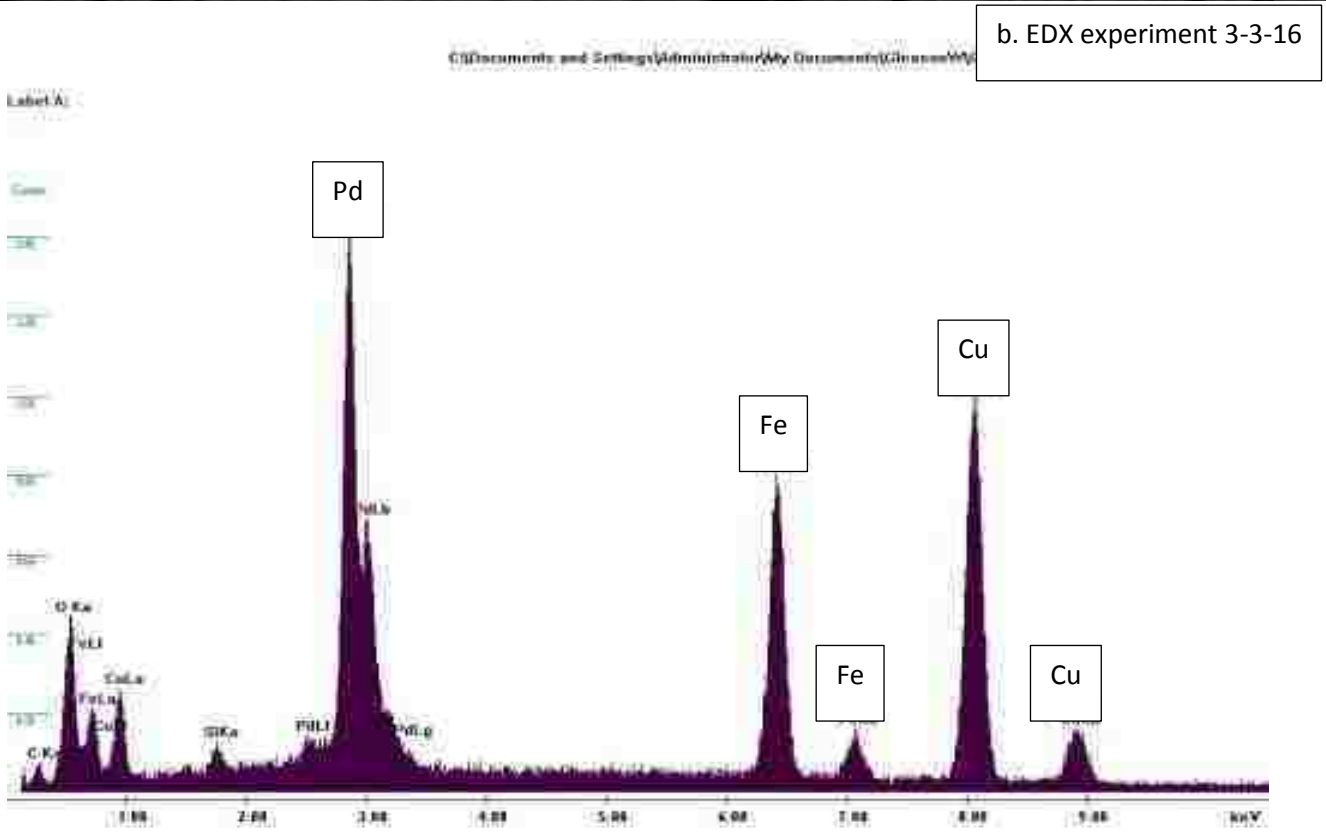

Figure 5.1.1 Experiment 3-3-16,MOTT disc, 0.1µm silica bead treated,3 Pd and 2Cu platings, annealed

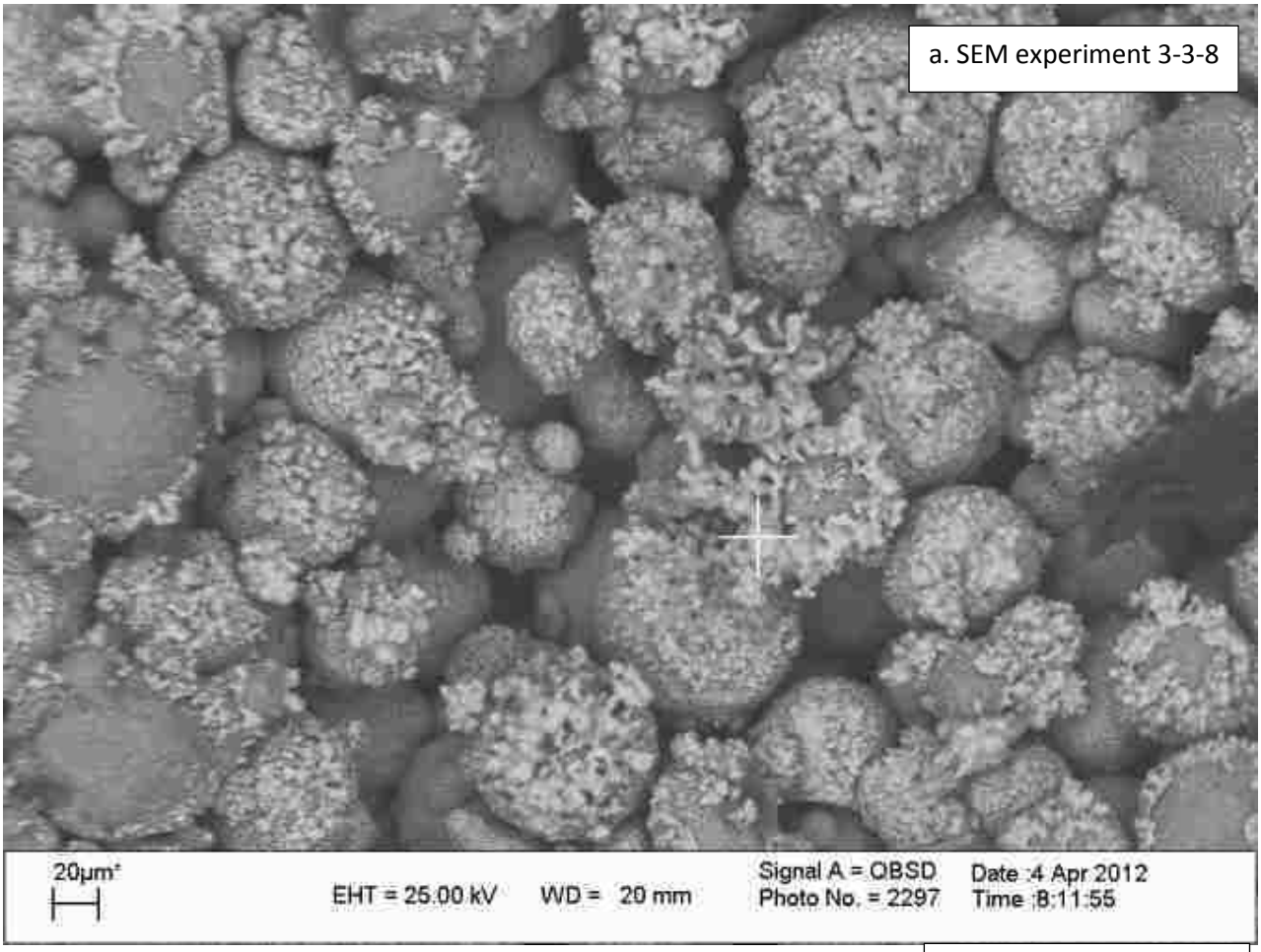

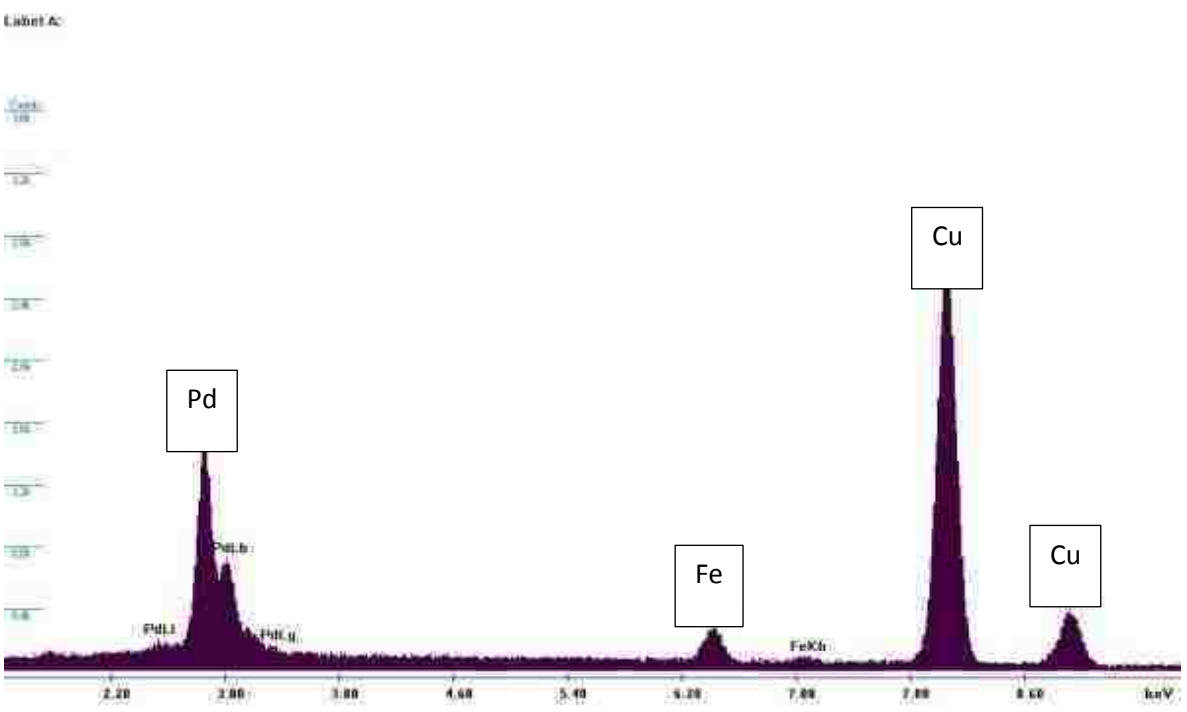

Figure 5.1.2 Experiment 3-3-8, CAMP disc, 0.1µm silica bead treated,3 Pd and 2 Cu platings, annealed

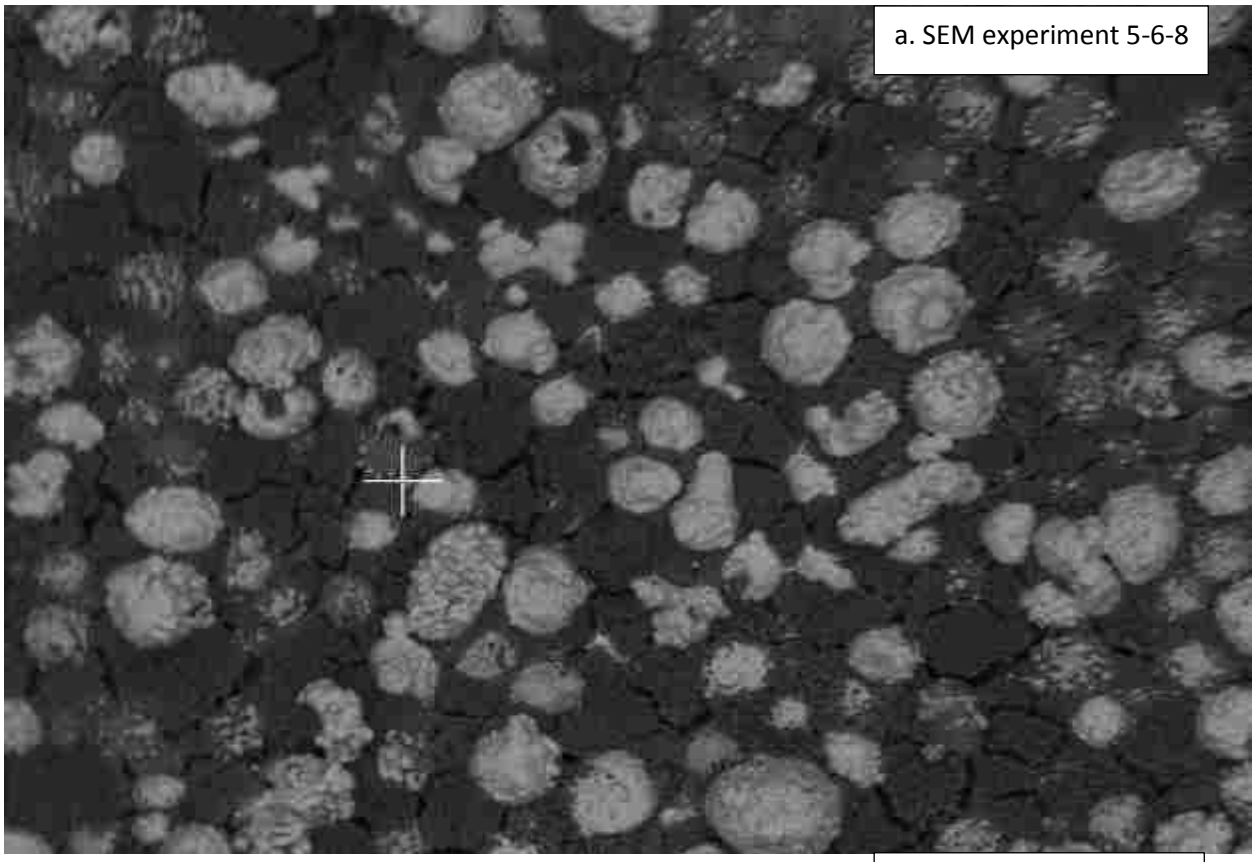

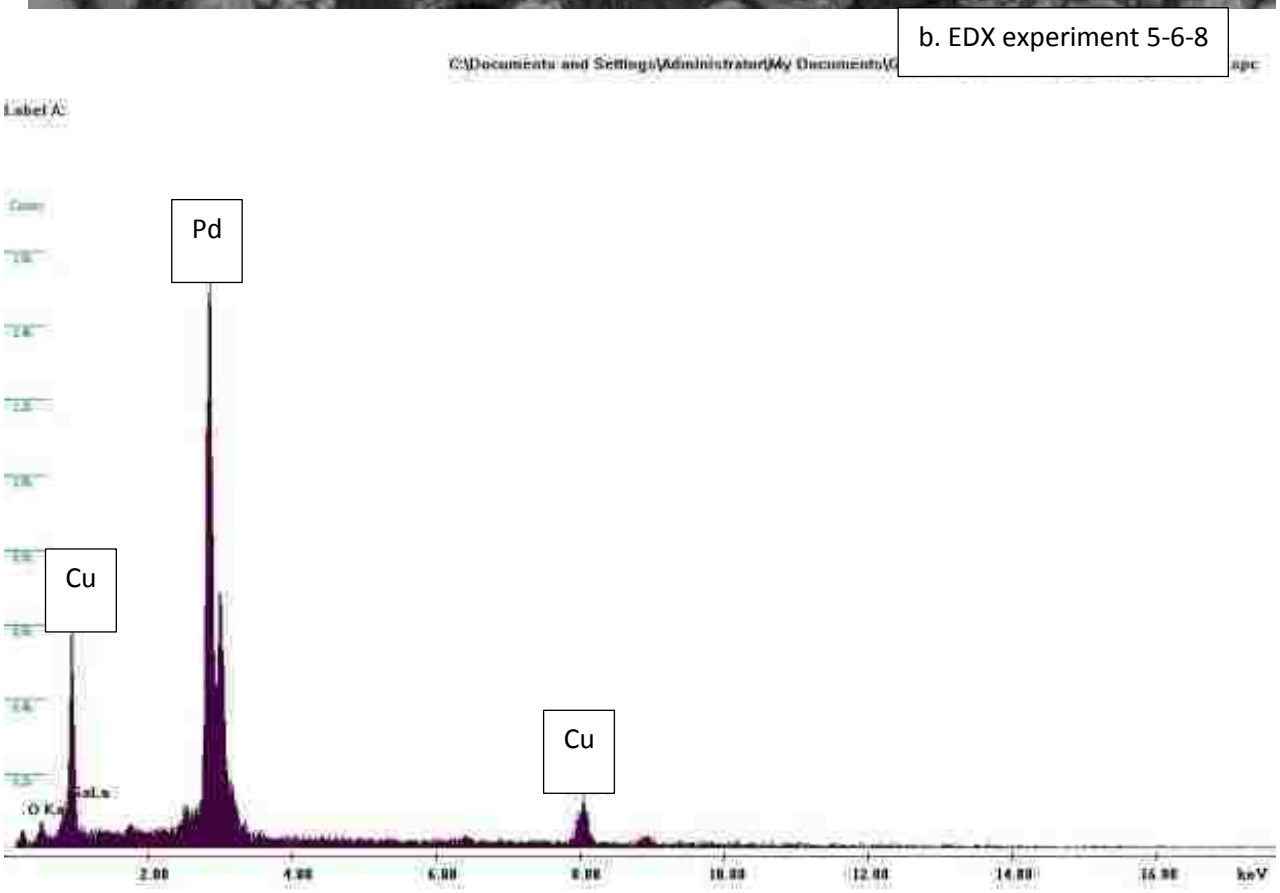

Figure 5.1.3 Experiment 5-6-8, CAMP disc, 0.1µm silica bead sol-gel treated, 3 Pd and 3 Cu platings, annealed

Chapter 6 Future studies

Future studies will look at how to optimize the plating process using multiple Pd plating layers and then plating layers of Cu. Initial attempts have focused on limiting the number of coatings to gain a solid understanding of the underlying mechanisms involved. This is in contrast to methods currently in use that simply plate until the desired results are obtained[Error! Bookmark not defined.]. While this produces a suitable membrane, it does not optimize results nor minimize metal use. More coatings need to be applied in order to obtain the perfect seal

Future work will also investigate coating the CAMP discs with a sol-gel treatment of silica /polyamine, or imine composite. This is aimed at using the nitrogen of these groups to chemically anchor down the Pd and form nitrides and carbides during at working conditions (300-750^{o}C and reducing atmosphere pressures). These nitrides and carbides offer another way to chemically and mechanically anchor the alloy membrane to the PSS substrate. Work needs to be done to study the carbide and nitride formation using the silica polyamine composite followed by Pd/Cu plating under the previously established plating conditions working conditions using XRD to study metal atom diffusion. This needs to be done to compare the migration of iron and chromium using the polyamine composite with the sol-gel coating procedure reported here.

Future work will investigate how flow can be used to control the coating, even between annealing steps so that bridging is maximized on the silica surface

Future work must include permeance testing at operating temperatures and reducing atmosphere pressures. This needs to be done in order to evaluate the true effectiveness of these experimental results. Operation at these conditions is a critical factor in investigating lifetime studies, as well as XRD monitoring the metal crystallography of the membrane for iron and chromium diffusion. Comparison of known plated PSS substrates can provide insights into the effectiveness of the surface treatments, the different sol-gel coatings, and subsequent Pd/Cu alloy coatings. Studying these membranes at operating

conditions can also illuminate potentially more effective methods of anchoring and tethering the Pd. This could make for a more robust membrane and a longer lived one.

Bibliography for palladium membranes

Ahmad 2007 *Sol–gel synthesized of Nano composite palladium–alumina ceramic membrane for H2 permeability Preparation and characterization*, International Journal of Hydrogen Energy 32 (2007) 2010 – 2021

Ahmad, A.L., N.N.N. Mustafa, 2007. *Sol-Gel Synthesized of Nano composite Palladium-Alumina Ceramic Membrane for H2 Permeability: Preparation and Characterization*, Int. J. Hydrogen Energy, 32, 2010-2021.

Akis, B.C., E.E. Engwall, I.P. Mardilovich, Y.H. Ma, 2003. *Effect of the in situ Formation of an Intermetallic Diffusion Barrier Layer on the Properties of Composite Palladium Membranes*, ACS Fuel Chem. Div. Preprints, 48(1), 337.

Alqasmi, R.A., S. Paasch, H.-J. Schaller, 1999. *Thermodynamic Properties of Pd-Y and Pd-Gd Intermetallic Phases, J. Alloys and Compounds*, 283, 173-177.

Amandusson, H., L.-G. Ekedahl, H. Dannetun, 2001. *Hydrogen Permeation through Surface Modified Pd and PdAg Membranes*, J. Membrane Science, 193, 35-47.

Armor, J.N., 1998. *Applications of Catalytic Inorganic Membrane Reactors to Refinery Products*, J. Membrane Science, 147, 217-233.

Arturk, M.E., Yi Hua Ma, 2009. *Electroless Pd and Ag Deposition Kinetics of the Composite Pd and Pd/Ag Membranes Synthesized from Agitated Plating Baths*, J. Membrane Science, 330, 233-45.

Arturk, M.E., E.A. Payzant, S.S. Speakman, Y.H. Ma, 2008. *Isothermal Nucleation and Growth Kinetics of Pd/Ag Alloy Phase via in situ Time-Resolved High-Temperature X-ray Diffraction* (HTXRD) Analysis, J. Membrane Science, 316, 97-111.

Ayturk, M. Engin, Ivan P. Mardilovich, Erik E. Engwall, Yi Hua Ma, 2006. *Synthesis of Composite Pd-Porous Stainless Steel (PSS) Membranes with a Pd/Ag Intermetallic Diffusion Barrier,* J. Membrane Science, 285, (1-2), 385-394.

Ayturk, M.E., E.E. Engwall, Y.H. Ma, 2007. *Microstructure Analysis of the Intermetallic Diffusion Induced Alloy Phases in Composite Pd/Ag/Porous Stainless Steel (PSS) Membranes*, Ind. Eng. Chem. Res., 46 (12), 4295-4306.

Ayturk, M.E., I.P. Mardilovich, E.E. Engwall, Y.H. Ma, 2006. *Synthesis of Composite Pd-Porous Stainless Steel (PSS) Membranes with a Pd/Ag Intermetallic Diffusion Barrier,* J. Membrane Science, 285(1-2), 385.

Bhandari, R., Yi Hua Ma, 2009. *Pd-Ag Membrane Synthesis: The Electroless and Electro-plating Conditions and their Effect on the Deposits Morphology*, J. Membrane Science, 334, 50-63.

Bosko, M.L., F. Ojeda, E.A. Lombardo, L.M. Cornaglia, 2009. *NaA Zeolite as an Effective Diffusion Barrier in Composite Pd/PSS Membranes,* J. Membrane Science, 331, 57-65.

Bosko, María L., David Yepes, Silvia Irusta, Pierre Eloy, Patricio Ruiz, Eduardo A. Lombardo, Laura M. Cornaglia, 2007. *Characterization of Pd-Ag Membranes after Exposure to Hydrogen Flux at High Temperatures*, J. Membrane Science, 306, 56-65.

Cai, Q., 1997. *Non-Cyanide Electroless Gold Plating, Applicable Technology* Market, 4, 7-8.

Castelli, S., L. Bimbi, M. De Grancesco, A. Iasonna, S. Tosti, V. Violante, 1998. *Deposition of a Pd-Ag Film Alloy on Macroporous Ceramic Supports*, Proceedings of the 20th SOFT, Marseille, Fusion Tech., 2, 993-996.

Chang, Hsin-Fu, Wen-Ju Pai, Ying-Ju Chen, Wen-Hsiung Lin, 2010. *Autothermal Reforming of Methane for Producing High-Purity Hydrogen in a Pd/Ag Membrane* Reactor, Int. J. Hydrogen Energy, 35, 12986-92.

Chen, Chao-Huang, Yi Hua Ma, 2010. *The Effect of H2S on the Performance of Pd and Pd/Au Composite Membrane*, J. Membrane Science, 363, 535-44.

Chen, Weidong, Xiaojuan Hu, Rongxia Wang, Yan Huang, 2010. *On the Assembling of Pd/Ceramic Composite Membranes for Hydrogen Separation*, Separation and Purification Tech., 72, 92-97.

Cheng, Y.S., K.L. Yeung, 1999. *Palladium-Silver Composite Membranes by Electroless Plating Technique*, J. Membrane Science, 158, 127-141.

Cheng, Y.S., K.L. Yeung, 2001. *Effects of Electroless Plating Chemistry on the Synthesis of Palladium Membranes*, J. Membrane Science, 182, 195-203.

Cheng, Y.S., M.A. Peña, J.L. Fierro, D.C.W. Hui, K.L. Yeung, 2002. *Performance of Alumina, Zeolite, Palladium, Pd-Ag Alloy Membranes for Hydrogen Separation from Towngas Mixture*, J. Membrane Science, 204, 329-340.

Chi, Yen-Hsun, Pei-Shan Yen, Ming-Shan Jeng, Shu-Ting Ko, Tai-Chou Lee, 2010. *Preparation of Thin Pd Membrane on Porous Stainless Steel Tubes Modified by a Two-Step Method*, Int. J. Hydrogen Energy, 35, 6303-6310.

Collins, J.P., J.D. Way, 1993. *Preparation and Characterization of a Composite Palladium-Ceramic Membrane*, Ind. Eng. Chem. Res., 32, 3006-3013.

Foletto, E.L., J.V. Wirbitzki Da Silverira, S.L. Jahn, 2008. *Preparation of Palladium-Silver Alloy Membranes for Hydrogen Permeation*, Lat. Am. Appl. Res, 38 (1) 8 p.

Gade, S.K., E.A. Payzant, H.J. Park, P.M. Thoen, J.D. Way, 2009. *The Effects of Fabrication and Annealing on the Structure and Hydrogen Permeation of Pd-Au Binary Alloy Membranes,* J. Membrane Science, 340, 227-233.

Gade, Sabina K., Matthew K. Keeling, Alexander P. Davidson, Oyvind Hatlevik, J. Douglas Way, 2009. P*alladium-Ruthenium Membranes for Hydrogen Separation Fabricated by Electroless Co-Deposition*, Int. J. Hydrogen Energy, 34, 6484-6491.

Gade, Sabina K., Paul M. Thoen, J. Douglas Way, 2008. *Unsupported Palladium Alloy Foil Membranes Fabricated by Electroless Plating*, J. Membrane Science, 316, 112-118.

Gao, H., J.Y.S. Lin, Y. Li, B. Zhang, 2005. *Electroless Plating Synthesis, Characterization and Permeation Properties of Pd-Cu Membranes Supported on ZrO2 Modified Porous Stainless Steel*, J. Membrane Science, 265, 142-152.

Goldbach, A., L. Yuan, H. Xu 2010*, Impact of the FCC/BCC Transition on the Homogeneity and Behavior of PdCu Membranes*, , Separation and Purification Tech., 73, 65-70.

Guazzone, F., 2005. *Engineering of Substrate Surface for the Synthesis of Ultra-Thin Composite Pd and Pd-Cu Membranes for Hydrogen Separation*, Ph.D. Thesis, Worcester Polytechnic Institute.

Guazzone, F., M.E. Ayturk, Y.H. Ma, 2004. *Effect of Intermetallic Diffusion Barrier on the Stability of Composite Pd/PSS Membranes at High Temperatures,* Proceedings of the 21st Annual International Pittsburgh Coal Conference Proceedings, September 13-17, Osaka, Japan.

Goo, Y., G. Lu, Y. Wang, R. Wang, 2003. *Preparation and Characterization of Pd-Ag/Ceramic Composite Membrane and Application to Enhancement of Catalytic Dehydrogenation of Isobutane*, Separation and Purification Tech., 32, 271-279.

Guo, Y., X. Zhang, H. Deng, X. Wang, Y. Wang, J. qiu, J. Wang, K.L. Yeung, 2010. *A Novel Approach for the Preparation of Highly Stable Pd Membrane on Macroporous α-Al2O3*, J. Membrane Science, doi:10.1016/j.memsci.2010.06.050, 23p.

Hatlevik, Oyvind, Sabina K. Gade, Matthew K. Keeling, Paul M. Thoen, A.P. Davidson, J. Douglas Way, 2010. *Palladium and Palladium Alloy Membranes for Hydrogen Separation and Production: History, Fabrication Strategies, and Current Performance*, *Separation and Purification Tech*, Separation and Purification Technology, 73, 59-64.

Hou, K., R. Hughes, 2003. *Preparation of Thin and Highly Stable Pd/Ag Composite Membranes and Simulative Analysis of Transfer Resistance for Hydrogen Separation*, J. Membrane Science, 214, 43-55.

Howard, B.H., R.P. Killmeyer, K.S. Rothenberger, A.V. Cugini, B.D. Morreale, R.M. Enick, F. Bustamante, 2004. *Hydrogen Permeance of Palladium-Copper Alloy Membranes over a Wide Range of Temperatures and Pressures*, J. Membrane Science, 241, 207-218.

Cheng, Y.S., K.L. Yeung, 2001. *Effects of Electroless Plating Chemistry on the Synthesis of Palladium Membranes*, J. Membrane Science, 182, 195-203.

Cheng, Y.S., M.A. Peña, J.L. Fierro, D.C.W. Hui, K.L. Yeung, 2002. *Performance of Alumina, Zeolite, Palladium, Pd-Ag Alloy Membranes for Hydrogen Separation from Towngas Mixture*, J. Membrane Science, 204, 329-340.

Chi, Yen-Hsun, Pei-Shan Yen, Ming-Shan Jeng, Shu-Ting Ko, Tai-Chou Lee, 2010. *Preparation of Thin Pd Membrane on Porous Stainless Steel Tubes Modified by a Two-Step Method*, Int. J. Hydrogen Energy, 35, 6303-6310.

Collins, J.P., J.D. Way, 1993. *Preparation and Characterization of a Composite Palladium-Ceramic Membrane*, Ind. Eng. Chem. Res., 32, 3006-3013.

Foletto, E.L., J.V. Wirbitzki Da Silverira, S.L. Jahn, 2008. *Preparation of Palladium-Silver Alloy Membranes for Hydrogen Permeation*, Lat. Am. Appl. Res, 38 (1) 8 p.

Gade, S.K., E.A. Payzant, H.J. Park, P.M. Thoen, J.D. Way, 2009. *The Effects of Fabrication and Annealing on the Structure and Hydrogen Permeation of Pd-Au Binary Alloy Membranes*, J. Membrane Science, 340, 227-233.

Gade, Sabina K., Matthew K. Keeling, Alexander P. Davidson, Oyvind Hatlevik, J. Douglas Way, 2009. *Palladium-Ruthenium Membranes for Hydrogen Separation Fabricated by Electroless Co-Deposition*, Int. J. Hydrogen Energy, 34, 6484-6491.

Gade, Sabina K., Paul M. Thoen, J. Douglas Way, 2008. *Unsupported Palladium Alloy Foil Membranes Fabricated by Electroless Plating*, J. Membrane Science, 316, 112-118.

Gao, H., J.Y.S. Lin, Y. Li, B. Zhang, 2005. *Electroless Plating Synthesis, Characterization and Permeation Properties of Pd-Cu Membranes Supported on ZrO2 Modified Porous Stainless Steel*, J. Membrane Science, 265, 142-152.

Goldbach, A., L. Yuan, H. Xu 2010, *Impact of the FCC/BCC Trasition on the Homogeneity and Behavior of PdCu Membranes, ,* Separation and Purification Tech., 73, 65-70.

Guazzone, F., 2005. *Engineering of Substrate Surface for the Synthesis of Ultra-Thin Composite Pd and Pd-Cu Membranes for Hydrogen Separation*, Ph.D. Thesis, Worcester Polytechnic Institute.

Guazzone, F., M.E. Ayturk, Y.H. Ma, 2004. *Effect of Intermetallic Diffusion Barrier on the Stability of Composite Pd/PSS Membranes at High Temperatures*, Proceedings of the 21st Annual International Pittsburgh Coal Conference Proceedings, September 13-17, Osaka, Japan.

Guo, Y., G. Lu, Y. Wang, R. Wang, 2003. *Preparation and Characterization of Pd-Ag/Ceramic Composite Membrane and Application to Enhancement of Catalytic Dehydrogenation of Isobutane, Separation* and Purification Tech., 32, 271-279.

Guo, Y., X. Zhang, H. Deng, X. Wang, Y. Wang, J. qiu, J. Wang, K.L. Yeung, 2010. *A Novel Approach for the Preparation of Highly Stable Pd Membrane on Macroporous α-Al2O3*, J. Membrane Science, doi:10.1016/j.memsci.2010.06.050, 23p.

Hatlevik, Oyvind, Sabina K. Gade, Matthew K. Keeling, Paul M. Thoen, A.P. Davidson, J. Douglas Way, 2010. *Palladium and Palladium Alloy Membranes for Hydrogen Separation and Production: History, Fabrication Strategies, and Current Performance*, *Separation and Purification Tech*, Separation and Purification Technology, 73, 59-64.

Hou, K., R. Hughes, 2003. *Preparation of Thin and Highly Stable Pd/Ag Composite Membranes and Simulative Analysis of Transfer Resistance for Hydrogen Separation*, J. Membrane Science, 214, 43-55.

Howard, B.H., R.P. Killmeyer, K.S. Rothenberger, A.V. Cugini, B.D. Morreale, R.M. Enick, F. Bustamante, 2004. *Hydrogen Permeance of Palladium-Copper Alloy Membranes over a Wide Range of Temperatures and Pressures*, J. Membrane Science, 241, 207-218.

Hu, Xiaojuan, Weidong Chen, Yan Huang, 2010. *Fabrication of Pd/Ceramic Membranes for Hydrogen Separation based on Low-Cost Macroporous Ceramics with Pencil Coating*, Int. J. Hydrogen Energy, 1-6.

Hu, Xiaojuan, Yan Huang, Shili Shu, Yiqun Fan, Nanping Xu, 2008. *Toward Effective Membranes for Hydrogen Separation: Multichannel Composite Palladium Membranes*, J. Power Sources, 181, 135-139.

Huang, Ting-Chia, Ming-Chi Wei, Huey-Ing Chen, 2003. *Preparation of Hydrogen-Permselective Palladium-Silver Composite Membranes by Electroless Co-Deposition*, Separation and Purification Tech., 32, 239-245.

Huang, Y., R. Dittmeyer, 2006. *Preparation and Characterization of Composite Palladium Membranes on Sinter-Metal Supports with a Ceramic Barrier against Intermetallic Diffusion*, J. Membrane Science, 282, 286-310.

Huang, Y., R. Dittmeyer, 2007. *Preparation of Thin Palladium Membranes on a Porous Support with Rough Surface*, J. Membrane Science, 302, 160-170.

Keuler, J., L. Lorenzen, S. Miachon, 2002. *Preparing and Testing Pd Films of Thickness 1-2 Micrometer with High Selectivity and High Hydrogen Permeance*, Separation Science Tech., 37, 379-401.

Kim, Daejin, A. Kellogg, E. Livaich, G. Wilhite, 2009. *Towards an Integrated Ceramic Micro-Membrane Network: Electroless-Plated Palladium Membranes in Cordierite Supports*, J. Membrane Science, 340, 109-16.

Kulprathipanja, Ames, Gökhan O. Alptekin, John L. Falconer, J. Douglas Way, 2005. *Pd and Pd-Cu Membranes: Inhibition of H2 Permeation by H2S, J. Membrane Science*, 254, 49-62.

Li, A., J.R. Grace, C.J. Lim, 2007a. *Preparation of Thin Pd-Based Composite Membrane on Planar Metallic Substrate, Part I: Pretreatment of Porous Stainless Steel Substrate*, J. Membrane Science, 298, 175-181.

Li, A., J.R. Grace, C.J. Lim, 2007b. *Preparation of Thin Pd-based Composite Membrane on Planar Metallic Substrate, Part II: Preparation of Membrane by Electroless Plating and Characterization*, J. Membrane Science, 306, 159-165.

Li, A., W. Liang, R. Hughes, 2000. *Fabrication of Dense Palladium Composite Membranes for Hydrogen Separation,* Catalysis Today, 56, 45-51.

Li, Anwu, Weiqiang Liang, Ronald Hughes, 1998. *Characterization and Permeation of Palladium/Stainless Steel Composite Membranes,* J. Membrane Science, 149, 259-268.

Li, Hui, Hengyong Xu, Wenzhao Li, 2008. *Study of n Value and α/β Palladium Hydride Phase Transition within the Ultra-Thin Palladium Composite Membrane,* J. Membrane Science, 324, 44-49.

Liang, Weiqiang, Ronald Hughes, 2005. *The Effect of Diffusion Direction on the Permeation Rate of Hydrogen in Palladium Composite Membranes*, Chemical Engineering J., 112, 81-86.

Lin, W.H., Chang, H.F., 2005. *Characterizations of Pd-Ag Membrane Prepared by Sequential Electroless Deposition,* Surface Coatings Tech., 194(1), 157-166.

Ma, Y.H., B.C. Akis, M.E. Ayturk, F. Guazzone, E.E. Engwall, I.P. Mardilovich, 2004. *Characterization of Intermetallic Diffusion Barrier and Alloy Formation for Pd/Cu and Pd/Ag Porous Stainless Steel Composite* Membranes. Ind. Eng. Chem. Res., 43 (12), 2936-2945.

Ma, Y.H., F. Guazzone, 2007. *Metallic Membranes for the Separation of Hydrogen at High Temperatures,* Science Materials, 32, 179-195.

Ma, Y.H., I.P. Mardilovich, E.E. Engwall, 2004. *Composite Gas Separation Modules Having Intermediate Porous Metal Layers,* U.S. Provisional Patent Application US2004.0237779 A1.

Ma, Y.H., L.P. Mardilovich, E.E. Engwall, 2007. *Composite Gas Separation Modules Having Intermediate Porous Metal Layers*, US Patent 7,175,694, 13 p.

Ma, Y.H., P.P. Mardilovich, Y. She, 2000. *Hydrogen Gas-Extraction Module and Method of Fabrication,* US Patent 6,152,987.

Ma, Yi Hua, F. Guazzone, 2007. *Metallic Membranes for the Separation of Hydrogen at High Temperatures,* Ann. Chim. Sci. Materials, 32 (2) 179-95.

Mardilovich, I.P., E. Engwall, Y.H. Ma, 2002. *Dependence of Hydrogen Flux on the Pore Size and Plating Surface Topology of Asymmetric Pd-Porous Stainless Steel Membranes,* Desalination, 144, 85-89.

Mardilovich, I.P., E.E. Engwall, Y.H. Ma, 2006. *Thermally Stable Composite Pd Membranes Having Intermediate Porous Metal Intermetallic Diffusion Barrier Layers Formed By Bi-Metal Multi-Layer Deposition,* In Proceedings of the 9th International Conference of Inorganic Membranes (ICIM9), Lillehammer, Norway, June 25-29, 92-95.

Mardilovich, P.P., Y. She, Y.H. Ma, M.-Hon Rei, 1998. *Defect-Free Palladium Membranes on Porous Stainless Steel Support*, AlChE J., 44(2), 310-322.

Mardilovich, P.P., Y. She, Y.H. Ma, M.H. Rei, 1998. *Stability of Hydrogen Flux through Pd/Porous Stainless Steel Composite Membranes*, In Proceedings of the 5th International Conference on Inorganic Membranes (ICIM5), Nagoya, Japan, June 22-26, 246-249.

McKinley, D.L., 1967. *Metal Alloy for Hydrogen Separation and Purification,* U.S. Patent 3,350,845.

McKinley, D.L., 1969. *Method for Hydrogen Separation and Purification,* U.S. Patent 3,439,474.

Mejdell, A.L., M. Jøndahl, T.A. Peters, R. Bredesen, H.J. Venvik, 2009. *Experimental Investigation of a Microchannel Membrane Configuration with a 1.4 μm Pd/Ag 23 wt.% Membrane-Effects of Flow and Pressure,* J. Membrane Science, 327, 6-10.

Mejdell, A.L., T.A. Peters, M. Stange, H.J. Venvik, R. Bredesen, 2009. *Performance and Application of Thin Pd-Alloy Hydrogen Separation Membranes in Different Configurations*, J. Taiwan Institute of Chemical Engineers, 40, 253-259.

Mekonnen, Wakshum, Bjørnar Arstad, Hallgeir Klette, John C. Walmsley, Rune Bredesen, Hilde Venvik, Randi Holmestad, 2008. *Microstructural Characterization of Self-Supported 1.6 μm Pd/Ag Membranes*, J. Membrane Science, 310, 337-348.

Morreale, B.D., M.V. CIocco, R.M. Enick, B.I. Morsi, B.H. Howard, A.V. Cugini, K. S. Rothenberger, 2003. *The Permeability of Hydrogen in Bulk Palladium at Elevated Temperatures and Pressures*, J. Membrane Science, 212, 87.

Nair, B.K.R., J. Choi, M.P. Harold, 2007. *Electroless Plating and Permeation Features of Pd and Pd/Ag Hollow Fiber Composite Membranes*, J. Membrane Science, 288, 67-84.

Nair, Balamurali Krishna R., Michael P. Harold, 2008. *Experiments and Modeling of Transport in Composite Pd and Pd/Ag Coated Alumina Hollow Fibers*, J. Membrane Science, 311, 53-67.

Nam, Seung-Eun, Yeon-Kyung Seong, Jae Wook Lee, Kew-Ho Lee, 2009. *Preparation of Highly Stable Palladium Alloy Composite Membranes for Hydrogen Separation*, Desalination, 236, 51-55.

Nguyen, Thu Hoai, Shinsuke Mori, Masaaki Suzuki, 2009. *Hydrogen Permeance and the Effect of H2O and Co on the Permeability of Pd0.75Ag0.25 Membranes under Gas-Driven Permeation and Plasma-Driven Permeation*, Chemical Engineering Journal 155 ,55–61

O'Brian, Casey P., Bret H. Howard, James B. Miller, Bryan D. Morreale, Andrew J. Gellman, 2010. *Inhibition of Hydrogen Transport through Pd and Pd47Cu53 Membranes by H2S at 350˚C*, J. Membrane Science, 349, 380-384.

Paglieri, S.N., J.D. Way, 2002. *Innovations in Palladium Membrane Research*, Separation Purification Methods, 31, 1-169.

Paglieri, Stephen N., King Y. Foo, J. Douglas Way, John P. Collins, Daniel L. Harper-Nixon, 1999. *A New Preparation Technique for Pd/Alumina Membranes with Enhanced High-Temperature Stability*, Ind. Eng. Chem. Res., 38, 1925-1936.

Pan, X., M. Kilgus, A. Goldbach, 2005. *Low-Temperature H2 and N2 Transport Through Thin Pd66Cu34Hx Layers*, Catalysis today, 104, 225-30.

Pan, X., G. Xiong, S. Sheng, N. Stroh, H. Brunner, 2001. *Thin Defense Pd Membranes Supported on α-Al2O3 Hollow Fibers*, Chemical Communications, 24, 2536-2537.

Paturzo, L., A. Basile, 2002. *Methane Conversion to Syngas in a Composite Palladium Membrane Reactor with Increasing Number of Pd Layers*, Ind. Eng. Chem. Res., 41, 1703-1710.

Peters, T.A., W.M. Tucho, A. Ramachandran, et al. 2009. *Thin Pd-23%Ag/Stainless Steel Composite Membranes: Long-Term Stability, Life-Time Estimation and Post-Process Characterization,* J. Membrane Science, 326, 572-81.

Phair, J.W., S.P.S. Badwal, 2006. *Materials for Separation Membranes in Hydrogen and Oxygen Production and Future Power Generation*, Science and Technology of Advanced Materials, 7, 792-805.

Phair, J.W., S.P.S. Badwal, 2006. *Review of Proton Conductors for Hydrogen Separation*, Ionics, 12, 103-15.

Pizzi, Diego, Ryan Worth, Marco Giacinti Baschetti, Giulio C. Sarti, Ken-ichi Noda, 2008. *Hydrogen Permeability of 2.5 μm Palladium-Silver Membranes Deposited on Ceramic Supports*, J. Membrane Science, 325, 446-453.

Qiao, Ailing, Ke Zhang, Ye Tian, Lili Xie, Huajiang Luo, Y.S. Lin, Yongdan Li, 2010. *Hydrogen Separation through Palladium-Copper Membranes on Porous Stainless Steel with Sol-Gel Derived Ceria as Diffusion Barrier*, Fuel, 89(6), 1274-1279.

Rebelli, J., A.A. Rodriguez, S. Ma, C.T. Williams, J.R. Monnier, 2010. *Preparation and Characterization of Silica-Supported, Group 1B-Pd Bimetallic Catalysis Prepared by Electroless Deposition Methods*, Catalysis Today, doi:10.1016/j.cattod.2010.06.011, 9 p.

Rei, M.H., 2009. *A Decade's Study and Developments of Palladium Membrane in Taiwan*, J. Taiwan Institute of Chemical Engineers, 40, 238-245.

Reed, A.H., Technic Patent, 1999. *Electroless Gold Plating Bath*, US Patent 5935306, 7 p.

Roa, Fernando, J. Douglas Way, 2003. *Influence of Alloy Composition and Membrane Fabrication on the Pressure Dependence of the Hydrogen Flux of Palladium-Copper Membranes*, Ind. Eng. Chem. Research, 42, 5827-35.

Roa, Fernando, J. Douglas Way, Robert L. McCormick, Stephen N. Paglieri, 2003. *Preparation and Characterization of Pd-Cu Composite Membranes for Hydrogen Separation*, Chemical Engineering J., 93, 11-22.

Rothenberger, Kurt S., Anthony V. Cugini, Bret H. Howard, Richard P. Killmeyer, Michael V. Ciocco, Bryan D. Morreale, Robert M. Enick, Felipe Bustamante, Ivan R. Mardilovich, Yi H. Ma, 2004. *High Pressure Hydrogen Permeance of Porous Stainless Steel Coated with a Thin Palladium Film via Electroless Plating*, J. Membrane Science, 244, 55-68.

Ryi, Shin-Kun, Nong Xu, Anwu Li, C. Jim Lim, John R. Grace, 2010. *Electroless Pd Membrane Deposition on Alumina Modified Porous Hastelloy Substrate with EDTA-Free Bath*, Int. J. Hydrogen Energy, 35, 2328-2335.

Samingprai, S., S. Tantayanon, Yi H. Ma, 2010. *Chromium Oxide Intermetallic Diffusion Barrier for Palladium Membrane Supported on Porous Stainless Steel*, J. Membrane Science, 347, 8-16.

Shi, Lei., Andreas Goldbach, Gaofeng Zeng, Hengyong Xu, 2010a. *Preparation and Performance of Thin-Layered PdAu/Ceramic Composite Membranes*, Int. J. Hydrogen Energy, 35, 4201-08.

Shi, Lei., Andreas Goldbach, Gaofeng Zeng, Hengyong Xu, 2010c. *Direct H2O2 Synthesis Over Pd Membranes at Elevated Temperature*, J. Membrane Science, 348, 160-6.

Shi, Lei., Andreas Goldbach, Gaofeng Zeng, Hengyong Xu, 2010d. *H2O2 Synthesis Over PdAu Membranes*, Catalysis Today, 156, 118-23.

Shi, Lei., G. Zeng, H. Xu, 2010b. *Characterization and Performance of High Flux PdAu/Ceramic Composite Membranes*, Cuihua Xuebao/Chinesse J. of Catalysis, 31 (6), 711-15.

Shi, Z., S. Wu, J.A. Szpunar, M. Roshd, 2006. *An Observation of Palladium Membrane Formation on a Porous Stainless Steel Substrate by Electroless Deposition*, J. Membrane Science, 280, 705-711.

Shi, Zhongliang, Shanqiang Wu, Jerzy A. Szpunar, 2006. *Microstructure Transformation of Pd Membrane Deposited on a Porous Inconel Substrate in Hydrogen Permeation at Elevated Temperature,* J. Membrane Science, 284, 424-430.

Souleimanova, R.S., A.S. Mukasyan, A. Varma, 2000. *Pd Composite Membranes Synthesized by Electroless Plating Technique*, J. Membrane Science, 166, 249-57.

Souleimanova, R.S., A.S. Mukasyan, A. Varma, 2002. *Pd Membranes Formed by Electroless Plating with Osmosis: H2 Permeation Properties of Pd-Cu Membranes Supported on ZrO2 Modified Porous Stainless Steel*, J. Membrane Science, 48, 262-268.

Strukova, G.K., G.V. Strukov, I.E. Batov, M.K. Sakharov, E.A. Kudrenko, A.A. Mazilkin, 2010. *Studies of Nanocrystalline Pd Alloy Films Coated by Electroless Deposition,* Materials Chemistry and Physics, 119, 377-383.

Strukova, G.K., G.V. Strukov, V.V. Kedrov, 2005. *Method of Deposition of Palladium and its Alloys on Metal Details*, Patent RF No. 2293138.

Strukova, G.K., G.V. Strukov, V.V. Kedrov, I.K. Bdikin, S.A. Zver'kov, 2004. *Thin Metal Coatings on Metal Substrates Obtained by Electroless Deposition from Nonaqueous Solutions*, Metal Finishing, 102 (3), 20-25.

Stukova, G.K., G.V. Strukov, V.V. Kedrov, S. Hiroyuki, 2007. JP Patent, Publication Number: JP2007217751(A).

Sun, G.B., K. Hidajat, S. Kawi, 2006. *Ultra-Thin Pd Membrane on α-Al2O3 Hollow Fiber by Electroless Plating: High Permeance and Selectivity*, J. Membrane Science, 284, 110-119.

Sun, Liangliang, Yuqiang Liu, Wei Wang, Ran Ran, Yan Huang, Zongping Shao, 2010. *Methane Catalytic Decomposition Integrated with On-Line Pd Membrane Hydrogen Separation for Fuel cell Application*, Int. J. Hydrogen Energy, 35, 2958-2963.

Tanaka, David A. Pacheco, Margot A. Llosa Tanco, Shu-ichi Niwa, Yoshito Wakui, Fujio Mizukami, Takemi Namba, Toshishige M. Suzuki, 2005. *Preparation of Palladium and Silver Alloy Membrane on a Porous α-Alumina Tube via Simultaneous Electroless Plating*, J. Membrane Science, 247, 21-27.

Tarditi, Ana M., Laura M. cornaglia, 2011. *Novel PdAgCu Ternary Alloy as Promising Materials for Hydrogen Separation Membranes: Synthesis and Characterization*, Surface Science, 605, 62-71.

Thoen, P., F. Roa, J. Way, 2006. *High Flux Palladium-Based Catalytic Membrane Reactor*, Ind. Eng. Chem. Res., 36, 3369.

Thoen, Paul M., Fernando Roa, J. Douglas Way, 2006. *High Flux Palladium-Copper Composite Membranes for Hydrogen Separations*, Desalination, 193, 224-229.

Tang, J., Yu Zuo, 2008. *Study on Corrosion Resistance of Palladium Films on 316L Stainless Steel by Electroplating and Electroless Plating*, Corrosion Science, 50, 2873-78.

Tong, J., Y. Matsumura, H. Suda, K, Haraya, 2005. *Thin and Dense Pd/CeO2/MPS Composite Membrane for Hydrogen Separation and Steam Reforming of Methane*, Sep. Purif. Technol., 46, 0-10.

Tong, J.H., L.L. Su, K. Haraya, H. Suda, 2006. *Thin and Defect-Free Pd-Based Composite Membrane without any Interlayer and Substrate Penetration by a Combined Organic and Inorganic Process*, Chemical Communications, 10, 1142-1144.

Tong, Jianhua, Lingling Su, Kenji Haraya, Hiroyuki Suda, 2008. *Thin Pd Membrane on α-Al2O3 Hollow Fiber Substrate without Any Interlayer by Electroless Plating Combined with Embedding Pd Catalyst in Polymer Template*, J. Membrane Science, 310, 93-101.

Tosti, S., A. Adrover, A. Basile, V. Camilli, G. Chiappetta, V. Violante, 2003. *Characterization of Thin Wall Pd-Ag Rolled Membranes*, Int. J. Hydrogen Energy, 28, 105-112.

Tosti, S., A. Basile, L. Bettinali, F. Borgognoni, F. Chiaracalloti, F. Gallucci, 2006. *Long-Term Tests of Pd-Ag Thin Wall Permeator Tube*, J. Membrane Science, 284, 393-397.

Tosti, S., L. Bettinali, S. Castelli, F. Sarto, S. Scaglione, V. Violante, 2002. *Sputtered, Electroless, and Rolled Palladium-Ceramic Membranes*, J. Membrane Science, 196, 241-249.

Tosti, Silvano, Fabio Borgognoni, Alessia Santucci, 2010. *Electrical Resisitivity, Strain and Permeability of Pd-Ag Membrane Tubes*, Int. J. Hydrogen Energy, 1-7.

Uemiya, S., Y. Kude, K. Sugino, N. Sato, T. Matsuda, E. Kikuchi, 1988. *A Palladium/Porous-Glass Composite Membrane for Hydrogen Separation,* Chem. Lett, 1687-1690.

Violante, V., S. Tosti, A. Colombini, S. Castelli, M. De Grancesco, 1996. *Experimental Confirmation of the Theoretical Previsions for the Applicability of Catalytic Membrane Reactors for the Fusion Fuel Cycle,* Proceedings of the 19th SOFT, Lisbon, Fusion Tech., 2, 1205-1208.

Volpe, Maurizio, Rosalinda Inguanta, Salvatore Piazza, Carmelo Sunseri, 2006. *Optimized Bath for Electroless Deposition of Palladium on Amorphous Alumina Membranes,* Surface and Coatings Technology, 200, 5800-5806.

Wang, D., T.B. Flanagan, K.L. Shanahan, 2005. *Hydrogen Permeation Measurements of Partially Internally Oxidized Pd-Al Alloys in the Presence and Absence of CO,* J. Membrane Science, 253, 165-173.

Wang, Linsheng, Ryo Yoshiie, Shigeyuki Uemiya, 2007. *Fabrication of Novel Pd-Ag-Ru/Al2O3 Ternary Alloy Composite Membrane with Remarkable Enhanced H2 Permeability*, J. Membrane Science, 306, 1-7.

Wu, J.P., Ian W.M. Brown, M.E Bowden, T. Kemmitt, 2010. *Palladium Coated Porous Alumina Membranes for Gas Reforming Processes*, Solid State Sciences, 12 1912-16.

Wu, L.Q., N. Xu, J. Shi, 2000. *Preparation of a Palladium Composite Membrane by an Improved Electroless Plating Technique,* Ind. Eng. Chem. Res., 39, 342-348.

Yang, J.Y., C. Nishimura, M. Komaki, 2008. *Hydrogen Permeation of Pd60Cu40 Alloy Covered V-15Ni Composite Membrane in Mixed Gases Containing H2S*, J. Membrane Science, 309, 246-250.

Yeung, K., S. Christiansen, A. Varma, 1999. *Palladium Composite Membranes by Electroless Plating Technique, Relationship Between Plating Kinetics, Film Microstructure and Membrane Performance*, J. Membrane Science, 159, 107-122.

Yeung, K.L., J. Sebastian, A. Varma, 1995. *Novel Preparations of Pd/Vycor Composite Membranes*, Catal. Today, 25, 231-236.

Yeung, K.L., R. Aravind, J. Szegner, A. Varma, 1996. *Metal Composite Membranes: Synthesis, Characterization and Reaction Studies, Stud. Surg*. Sci. Catal, 101, 1349.

Yuan, L., A. Goldbach, H. Xu, 2008. *Real-time Monitoring of Metal Deposition and Segregation Phenomena During Preparation of PdCu Membranes*, J. Membrane Science, 322, 39-45.

Yuan, L.H., W. Chen, R.J. Hui, Y.I. Hu, X.H. Xia, 2006. Electrochimica Acta 51, 4589.

Zahedi, M., B. Afra, M. Dehghani-Mobarake, M. Bahmani, 2009. *Preparation of a Pd Membrane on a WO3 Modified Porous Stainless Steel for Hydrogen Separation,* J. Membrane Science, 333, 45-49.

Zhang, G.X., H. Yukawa, N. Watanabe, Y. Saito, H. Fukaya, M. Morinaga, T. Nambu, Y. Matsumoto, 2008. *Analysis of Hydrogen Diffusion Coefficient during Hydrogen Permeation through Pure Niobium,* Int. J. Hydrogen Energy, 33, 4419-4423.

Zhang, Ke, Huiyuan Gao, Zebao Rui, Yuesheng Lin, Yongdan Li, 2007. *Preparation of Thin Palladium Composite Membranes and Application to Hydrogen/Nitrogen Separation,* Chinese J. Chemical Engineering, 15(5), 643-647.

Zhang, Xiaoliang, Guoxing Xiong, Wieshen Yang, 2008. *A Modified Electroless Plating Technique for Thin Dense Palladium Composite Membranes with Enhanced Stability*, J. Membrane Science, 314, 226-237.

Zhang, Y., R. Maeda, M. Komaki, C. Nishimura, 2006. *Hydrogen Permeation and Diffusion of Metallic Composite Membranes,* J. Membrane Science, 269, 60-65.

Zhang, Y., T. Ozaki, M. Komaki, C. Nishimura, 2003. *Hydrogen Permeation of Pd-Ag Alloy Coated V-15Ni Composite Membrane: Effects of Overlayer Composition*, J. Membrane Science, 224, 81-91.

Zhao, H.B., K. Pflanz, J.H. Gu, A.W. Li, N. Stroh, H. Brunner, G.X. Xiong, 1998. *Preparation of Palladium Composite Membranes by Modified Electroless Plating Procedure,* J. Membrane Science, 142, 147-157.

Zhen, Gaofeng, Andreas Goldbach, Hengyoung Xu, 2009. *Impact of Mass Flow Resistance on Low-Temperature H2 Permeation Characteristics of a Pd95Ag5/Al2O3 Composite Membrane*, J. Membrane Science, 326, 681-87.

Quoted references

[1] Silvano Tosti *Overview of Pd-based membranes for producing pure hydrogen and state of art at ENEA laboratories*, International journal of hydrogen energy 35(2010) 12650-12659

[2] Andreas Goldbach Et.al. *Impact of the fcc/bcc phase transition on the homogeneity and behavior of PdCu membranes.* Separation and Purification Technology 73 (2010) 65–70

[3] Paglieri and Way, *Innovations in Palladium Membrane Research*: Separation and Purification Methods, (2002), 31(1), 1–169

[4] Li,A et al. *Preparation of Pd/ceramic composite membrane 1. Improvement of the conventional preparation technique*, Journal of Membrane Science 110(1996) 257-260

[5] Qiao,A et al. *Hydrogen separation through palladium–copper membranes on porous stainless steel with sol–gel derived ceria as diffusion barrier*, Fuel 89 (2010) 1274–1279

[6] Zhao,H.B. et al. *Preparation and characterization of palladium-based composite membranes by electroless plating and magnetron sputtering*, Catalysis Today 56 (2000) 89–96

[7] Zhao,H.B. et al *Preparation of palladium composite membranes by modified electroless plating procedure*, Journal of Membrane Science 142 (1998) 147-157

[8] Tosti, S et al. *Sputtered, electroless, and rolled palladium–ceramic membranes*, Journal of Membrane Science 196 (2002) 241–249

[9] [1]Wulfsberg, Gary, *Inorganic Chemistry,(*2000) University Science Books,(section 10.11 pgs. 513-517), (section 12.4 pgs. 617-624).

[10] Zhang, Y et al. *Hydrogen permeation and diffusion of metallic composite membranes*, Journal of Membrane Science 269 (2006) 60–65

[11] Zhang, Ke et al. *Preparation of Thin Palladium Composite Membranes and Application to Hydrogen Nitrogen Separation*, Chin. J. Chem. Eng., 15(5) 643-647 (2007)

[12] National Energy Testing Lab *Hydrogen From Coal Program, Research, Development and Demonstration Plan*, External Draft September 2010

[13] Wikipedia

[14] MOTT Corporation (formerly MOTT Metallurgical Corporation) was founded as a Connecticut corporation on July 9, 1959 by Lambert H. MOTT. The company consists of three business segments:1 OEM Parts/Products - Porous metal shapes, components, assemblies, inline filters.2 Process Filtration Systems - Large scale filter systems (gas and liquid), filter elements, and pilot scale filters for refinery, petrochemical and power generation 3 High Purity Products - Gas filters, diffusers and flow restrictors for semiconductor quality gases; spargers and filters for biopharmaceutical applications.

[15] T.Salisbury, *Fabrication and Characterization of Porous 420 Stainless Steel Substrates Produced Using Rapid Prototyping Technology and Thermally Strengthened Using Solid State Sintering*. Master's Thesis Defense 2011 , Montana Tech, Metallurgical and Materials Science Engineering

[16] Stacy Davis *Electroless Plating of Palladium on Stainless Steel Substrates in Hydrazine Solutions: A Study of the Relationships Between Bath Parameters, Deposition Mechanisms and Deposit Morphologies*, Thesis Defense April 12, 2011 Montana Tech, Metallurgical and Materials Science Engineering

[17] Michael Biehl et al. *Off-lattice Kinetic Monte Carlo Simulations of Strained Heteroepitaxial Growth* International Series of Numerical Mathematics 2005, Vol. 149, 41–57

[18] Gao, H *Characterization of zirconia modified porous stainless steel supports for Pd membranes* ,J Porous Mater (2006) 13: 419–426

[19] Yen-Hsun Chi et al. journal of hydrogen energy 35(2010) 6303-6310

[20] Mardilovich et al. ChE Journal Feb. 1998 Vol. 44, No. 2

[21] Ayturk et al. *Electroless Pd and Ag deposition kinetics of the composite Pd and Pd/Ag membranes synthesized from agitated plating baths* Journal of Membrane Science 330 (2009) 233–245

[22] Tyler Salisbury , *Montana Tech of The University of Montana 2011 Fabrication and Characterization of Porous 420 Stainless Steel Substrates Produced Using Rapid Prototyping Technology and Thermally Strengthened Using Solid State Sintering. A thesis submitted for fulfillment of the requirements for the degree of masters in Metallurgical and Mineral Processing Engineering*

[23] Roa and Way et.al *Preparation and characterization of Pd–Cu composite membranes for hydrogen separation*, Chemical Engineering Journal 93 (2003) 11–22

[24] T.P. Chou et al. *Sol-gel coating stainless steel*, Journal of Materials Science Letters 21, (2002),251-255

[25] Gade et al. *Unsupported palladium alloy foil membranes fabricated by electroless plating* ,Journal of Membrane Science 316 (2008) 112–118

[26] Paglieri, S.N. et al. *New Preparation Technique for Pd/Alumina Membranes with Enhanced High-Temperature Stability* , Ind. Eng. Chem. Res.(1999), 38, 1925-1936

[27] Gao, H., J.Y.S. Lin, Y. Li, B. Zhang,. Electroless Plating Synthesis, Characterization and Permeation Properties of Pd-Cu Membranes Supported on ZrO2 Modified Porous Stainless Steel, J. Membrane Science, 265 (2005), 142-152

[28] Chou, T. P et.al.. *Organic-inorganic sol-gel coating for corrosion protection of stainless steel*, Journal of Materials Science Letters **21**,(2002) 251– 255

[29] Twidwell, *Recipes for electroless plating of palladium alloy membranes* CAMP internal report -Lit-3 December 2010

[30] Twidwell, *A guide to palladium and palladium alloy membranes. CAMP internal report*-Lit-2 March 2011

[31] Ayturk et al. *Synthesis of composite Pd-porous stainless steel (PSS) membranes with a Pd/Ag intermetallic diffusion barrier* Journal of Membrane Science 285 (2006) 385–394

[32] Ayturk et al. *Microstructure Analysis of the Intermetallic Diffusion-Induced Alloy Phases in Composite Pd/Ag/Porous Stainless Steel Membranes*. Ind Eng. Chem. Res. 46(2007) 4295-4306

[33] Ayturk et al. *Isothermal nucleation and growth kinetics of Pd/Ag alloy phase via in situ time-resolved high-temperature X-ray diffraction (HTXRD) analysis* Journal of Membrane Science 316 (2008) 97–111

[34] Cheng,Y.S. et al. *Effects of electroless plating chemistry on the synthesis of palladium membranes* Journal of Membrane Science 182 (2001) 195–203

[35] Mardilovich et al. *Dependence of hydrogen Flux on Pore size and Plating Surface Topology of Asymmetric Pd-Porous Stainless Steel Membranes,* Desalination 144(2002),85-89

[36] Brinker et al.*Sol Gel Science, The Physics and Chemistry of Sol Gel Processing,* Academic Press (1990) 675-742